Cold atoms in optical resonators

Dissertation
zur Erlangung des Akademischen Grades
Doktor der Naturwissenschaften

an der
Naturwissenschaftlichen Fakultät
der
Leopold-Franzens-Universität Innsbruck

eingereicht von

Mag. rer. nat. Markus Gangl

im Dezember 2001

Contents

Einleitung 9

Chapter 1. Introduction 11
1.1. Overview 11
1.2. Two level atom in the field of a single laser mode 12

Part I. Two level atoms in optical resonators 13

Chapter 2. Atom cooling 15
2.1. What is cooling? 15
2.2. Cooling schemes in free space 15
2.2.1. Doppler cooling 15
2.2.2. Sisyphus cooling 18
2.2.3. Sub-Doppler cooling 21
2.2.4. VSCPT 26

Chapter 3. Single atoms in optical resonators 29
3.1. Introduction 29
3.2. Model 31
3.3. Mechanical light effects 32
3.3.1. One-sided pumping 32
3.3.2. Symmetric pumping 33
3.3.3. Comparison between Cavity cooling and Doppler cooling 35
3.4. Quantum gate 36
3.5. Publication 1: Cold atoms in a high-Q ring cavity 41
3.5.1. Introduction 42
3.5.2. Classical N-atom and M-mode model 43
3.5.3. Atoms in a ring cavity 44
3.5.4. One-sided pumping 48
3.5.5. Symmetric pumping 48
3.5.6. N atoms in a ringcavity 55
3.5.7. Conclusion 60
3.6. Publication 2: Single-atom detection in high-Q multimode cavities 62
3.6.1. Introduction 63
3.6.2. Semiclassical model 64
3.6.3. Competitive phase–locking 66
3.6.4. Limit of small phase shift effect 68

3.6.5. Numerical solution 69
3.6.6. Conclusions 72

Chapter 4. Cavity cooling of many atoms 75
4.1. Scaling laws for many atoms 75
4.2. Experimental realization of many-atom cooling 76
4.3. Tight binding regime 76
4.4. Publication 3: Collective dynamical cooling of neutral particles in a high-Q optical cavity 78
4.4.1. Introduction 79
4.4.2. Model 80
4.5. Publication 4: Cooling neutral particles in multimode cavities without spontaneous emission 87
4.5.1. Introduction 88
4.5.2. Classical model 89
4.5.3. N particles in a two mode ring cavity 90
4.5.4. Numerical simulations 96
4.5.5. Conclusions 99

Part II. Multilevel atoms in optical resonators 101

Chapter 5. Polarization gradient cooling inside optical resonators 103
5.1. Introduction 103
5.2. Publication 5: Cavity-assisted polarization gradient cooling 110
5.3. Introduction 111
5.4. Model 112
5.5. System Dynamics 113
5.5.1. $J_g = 1/2 \rightarrow J_e = 3/2$ 113
5.5.2. $J_g = 1 \rightarrow J_e = 2$ 115
5.5.3. Forces 117
5.6. Moving atom 118
5.6.1. Adiabatic following of cavity dynamics 118
5.6.2. Adiabatic following of the atomic dynamics 120
5.6.3. Full dynamics 121
5.6.4. Friction forces 122
5.6.5. Far off resonance force 126
5.6.6. Velocity dependence 127
5.7. Conclusions 129

Chapter 6. VSCPT inside a ring cavity 131
6.1. Introduction 131
6.1.1. Cooling phases 131
6.1.2. Role of the cavity for the final VSCPT cooling phase 132
6.1.3. The role of many atoms 133

6.2. Publication 6: Cavity-mediated dark-state cooling without spontaneous emission 134

Bibliography 143

Dank 149

Lebenslauf 151

Einleitung

Der Einsatz von Lasern für das Einfangen und Kühlen neutraler Atome ist in vielen Labors auf der ganzen Welt zur Routine geworden. Die wachsende Bedeutung dieses Gebiets wurde mit der Verleihung des Physiknobelpreises im Jahr 1997 an Steven Chu, Claude Cohen-Tannoudji und William D. Phillips ersichtlich. Atome mit einer Temperatur von wenigen μK stellen einen idealen Ausgangspunkt für weitere experimentelle Arbeiten auf dem Gebiet der Quantenoptik dar, wie z. B. Präzisionsmessungen atomarer Übergangsfrequenzen zur Herstellung ultragenauer Uhren. Für solche Messungen benötigt man sehr langsame Atome die sich in einem sehr kleinen Raumbereich befinden. Ein weiteres Beispiel ist die Herstellung eines neuen Aggregatzustands der Materie (Bose-Einstein-Kondensat), wofür den beteiligten Forschern (Eric A. Cornell, Wolfgang Ketterle und Carl E. Wieman) der Nobelpreis für Physik 2001 zugesprochen wurde. Noch in seinen Anfängen befindet sich das Gebiet der experimentellen Quanteninformation, das sich mit der Implementierung der zahlreichen theoretischen Vorschläge zum Bau eines Quantencomputers beschäftigt.

So groß die Fortschritte auf dem Gebiet der Laserkühlung neutraler Atome auch sind, gibt es immer noch einige ernste Probleme: Die meisten der experimentell eingesetzten Kühltechniken verwenden die spontane Emission eines angeregten atomaren Zustands als Zerfallskanal zur Abführung der mechanischen Energie des zu kühlenden Atoms. Dies erfordert aber die Existenz eines geschlossenen atomaren Übergangs, d. h. nach einem Fluoreszenzzyklus muß sich das Atom wieder im Startniveau befinden. Andernfalls kommt es zu einer Umverteilung der atomaren Population auf Energieniveaus, die für die Kühllaser nicht erreichbar sind und der Kühlzyklus wird unterbrochen. Das ist die Ursache dafür, daß keines der herkömmlichen Kühlverfahren auf Moleküle anwendbar ist, da es zwischen allen molekularen Energieniveaus Kopplungen durch Vibrations- und Rotationszustände gibt.
Hier setzt das in der Arbeitsgruppe von Prof. Helmut Ritsch in den Jahren 1996-2001 vorgeschlagene Resonatorkühlen an. Die Grundidee des Resonatorkühlens besteht darin, die zu kühlenden Teilchen (wobei es sich auch um Moleküle oder ein Bose-Einstein-Kondensat handeln kann) an das Lichtfeld eines optischen Resonators hoher Güte anzukoppeln. Dadurch gewinnt man zweierlei:

1. Man ersetzt den atomaren Zerfallskanal durch die Resonatordissipation, wodurch die Notwendigkeit eines geschlossenen atomaren Übergangs entfällt.

2. Es zeigt sich, daß in einem Resonator hoher Güte ein sisyphus-artiger Kühlmechanismus basierend auf der Resonatorreaktionszeit auftritt. Einzige Bedingung für eine höhere Effektivität dieses Kühlverfahrens im Vergleich zum Dopplerkühlen ist eine starke Kopplung zwischen Resonatorfeld und Teilchen.

Meine Doktorarbeit beschäftigt sich mit den Konsequenzen dieser beiden Effekte. Kernstück meiner Dissertation sind die sechs Publikationen, die während der drei Jahre meiner Tätigkeit als Forschungsassistent am Institut für Theoretische Physik in Innsbruck entstanden sind. Wo dies angebracht erschien, habe ich zusätzliche Kommentare in Form von Einleitungen zu den einzelnen Publikationen geschrieben.

Die vorliegende Arbeit ist wie folgt aufgebaut: Teil I umfaßt vier Publikationen und beschäftigt sich mit dem Entwickeln einfacher Modelle zur Resonatorkühlung, wobei das Arbeitspferd der theoretischen Quantenoptik, das Modell des Zwei-Niveau-Atoms verwendet wird. Ein breites Anwendungsspektrum unserer Idee ergibt sich aus der Anwendbarkeit des Kühlverfahrens auf Ensembles von sehr vielen Teilchen, wie in den letzten zwei Publikationen dieses Teils gezeigt wird.
In Teil II wird das Verfahren auf Atome mit komplizierteren Übergängen erweitert. In den beiden Publikationen dieses Teils zeige ich, daß zahlreiche Schwachstellen bereits bekannter Kühlschemata für den freien Raum (Polarisationsgradientenkühlung, VSCPT) in einem Resonator behoben werden.

CHAPTER 1

Introduction

1.1. Overview

Using lasers to cool and trap neutral atoms has become routine in laboratories all over the world in the last years. Atoms cooled to a few μK can be used as a starting point for further experimental work, e. g. precision measurements of atomic transition frequencies which is needed for the operation of ultra-precision clocks. For any such measurement atoms with very small Dopplershifts confined to a very small region of space are needed. Cold trapped atoms have also enabled experimentalists to achieve Bose-Einstein-condensation (BEC), thus opening an exciting new field for further research. This was rewarded by the Nobel prize in 1997 (Steven Chu, Claude Cohen-Tannoudji and William D. Phillips) and 2001 (Eric A. Cornell, Wolfgang Ketterle and Carl E. Wieman). Another promising field is the experimental implementation of theoretical Quantum Information schemes for which cold atoms in perturbation-free environments are needed.
Nevertheless there are processes inherent to optical cooling schemes that limit the reachable steady-state temperature and density. In most of the schemes spontaneous emission from the excited atomic states is used as a dissipation channel to get rid of the motional energy of the atoms. This directly introduces momentum diffusion via the random number and direction of the spontaneous emission events involving atomic recoil. In addition the scattered photons can be reabsorbed to further increase the diffusion. Furthermore the applicability of these cooling schemes is limited to atoms with a closed optical transition, i. e. a transition where spontaneous decay always returns the atoms to the same initial level which is essential for the ongoing of the optical cooling process. In molecules no such closed transition exists due to the existence of vibrational and rotational couplings between all of the energy levels. As an alternative one could use the dissipative dynamics of a cavity field instead of a Sisyphus effect using the internal atomic structure as has been suggested [1, 2, 3] and partly experimentally confirmed [4, 5, 6].

In this thesis I present a detailed investigation of this cavity cooling scheme resulting from the work I have done during my PhD studies in the work group of Prof. Helmut Ritsch at the Institute of Theoretical Physics in Innsbruck.
This thesis is organized as follows: It consists of two parts and a total of six chapters.

In part I, after a short qualitative overview on atom cooling I study the mechanical light effects on one (chapter 3) or many (chapter 4) neutral two-level atoms in optical resonators.

In part II, I discuss cavity cooling for atoms with several degenerate sublevels in their ground- and excited states. Chapter 5 presents a generalization of polarization gradient cooling to atoms interacting with several degenerate cavity modes. Chapter 6 discusses dark state cooling inside a cavity and shows that many of the problems connected with free space VSCPT can be overcome in a resonator.

1.2. Two level atom in the field of a single laser mode

As the interaction of a two-level atom with a single laser mode is the building block of quantum optics let us recapitulate the most important facts. In the interaction picture with respect to the laser frequency ω_P the Hamiltonian reads

$$H = \hbar\Delta_a|e\rangle\langle e| + \hbar g\sqrt{I}\left(\sigma^\dagger + \sigma^-\right) \tag{1}$$

In order to properly describe also the incoherent part of the system dynamics, we have to include a reservoir for the atomic spontaneous emission and deal with the master equation for the reduced atom-field density operator ρ. Using standard quantum optics assumptions and methods one gets:

$$\begin{aligned}\dot{\rho} &= -\frac{i}{\hbar}[H,\rho] + \mathcal{L}\rho \\ \mathcal{L}\rho &= -\Gamma\left(\sigma^\dagger\sigma^-\rho - 2\sigma^-\rho\sigma^\dagger + \rho\sigma^\dagger\sigma^-\right).\end{aligned} \tag{2}$$

$$\begin{aligned}\dot{\Pi}_e &= -2\Gamma\Pi_e + ig\sqrt{I}\left(\rho_{eg} - \rho_{ge}\right) \\ \dot{\Pi}_g &= 2\Gamma\Pi_e - ig\sqrt{I}\left(\rho_{eg} - \rho_{ge}\right) \\ \dot{\rho}_{ge} &= \left(-\Gamma + i\Delta_a\right)\rho_{ge} - ig\sqrt{I}\left(\Pi_e - \Pi_g\right)\end{aligned} \tag{3}$$

Setting the left hand side of eqs.3 to zero we obtain the steady-state values for the populations

$$\begin{aligned}\Pi_g &= \frac{1}{1+2sI} \\ \Pi_e &= \frac{sI}{1+2sI}\end{aligned} \tag{4}$$

where we have defined the saturation parameter per photon

$$s = \frac{g^2}{\Delta_a^2 + \Gamma^2}. \tag{5}$$

For very high saturation $1 \ll sI$ we see that $\Pi_e = 1/2$ and $\Pi_g = 1/2$.

Part I

Two level atoms in optical resonators

CHAPTER 2

Atom cooling

2.1. What is cooling?

Atom cooling means decreasing the phase-space volume accessible for atoms, in other words increasing the phase-space density. In laser cooling this is done by shining laser light on atoms. Why *laser* cooling? Only the development of tunable light sources that emit their photons within a very small frequency band (i. e. a laser) allowed the first experimental realization of laser cooling in 1982 by Phillips and Metcalf [7].
The cooling process consists of two parts, slowing down and trapping atoms. Slowing down an atom means to decrease its kinetic energy by a *velocity*-dependent force. In order to get rid of the kinetic energy of the atom a dissipation channel is needed. In the conventional free space cooling schemes spontaneous emission from the atomic excited states is used. Due to the random nature of the spontaneous emission events a "heating" mechanism is inevitably introduced. This restricts the achievable steady-state temperature of the cooling process.
Trapping atoms means to restrict the atomic motion to some trapping volume. For this *position*-dependent forces are needed to push/attract the atoms to a minimum of the potential energy.
In the next section we will give an overview on the most important cooling schemes in free space. As there is an extensive literature on this field in the form of research papers [8, 9], review articles [10, 11, 12, 13, 14] and monographs [15, 16, 17] we will focus on presenting a physical picture for each of the schemes. For computational details the reader is referred to one of the works cited above.

2.2. Cooling schemes in free space

2.2.1. Doppler cooling

The conceptually simplest cooling scheme is Doppler cooling. It relies on the photon recoil connected to the absorption of a photon by an atom. Fig. 1 shows the Doppler cooling cycle. A two-level atom in its ground-state absorbs a photon with momentum $\hbar k$. The atom is excited and has increased its momentum by $\hbar k$ in the direction of the absorbed photon. The kinetic atomic energy is dissipated by spontaneous emission and the atom returns to the initial ground state where the cycle starts over again. Due the to isotropic nature of the spontaneous emission process the mean momentum of the atom is not changed. As the direction of the emitted photons is random the atom experiences a random walk around its mean

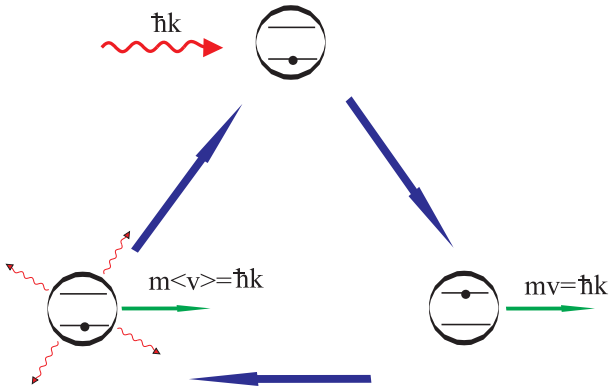

FIGURE 1. Doppler cooling cycle. In order to repeat this cycle a closed optical transition is needed.

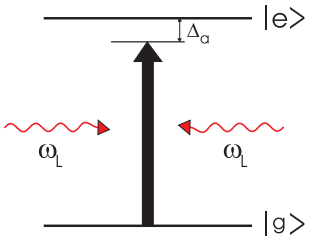

FIGURE 2. Doppler cooling in one dimension. The atom is moving in a red-detuned standing wave.

position. This leads to an increase in the mean-squared atomic momentum $\langle P^2 \rangle$ and thus to heating. The competition between cooling and heating processes leads to a steady-state temperature around $k_B T = \hbar\Gamma$, which is the so-called Doppler limit (see below).

In order to slow down an atom one has to use a setup with two counterpropagating laser beams of equal frequency ω_L (see fig. 2):

As the atomic absorption rate is frequency-dependent (see fig. 3), for resonant absorption the frequency of the incident light must match the atomic transition frequency. For red-detuned light ($\Delta_a = \omega_L - \omega_a < 0$) an atom moving to the right sees the counterpropagating light with a frequency $\omega_L + kv$ due to the Doppler shift, and the copropagating laser light with frequency $\omega_L - kv$. Thus more photons are scattered out of the counterpropagating beam leading to a decrease of atomic momentum. Optimal cooling is provided for $\Delta_a = -\Gamma$, which gives in the low saturation limit $sI \ll 1$ the maximum cooling force for a slowly moving atom, $kv \ll \Gamma$ averaged over one wavelength

$$f_{Dopp} = -\hbar k^2 I s v. \tag{6}$$

In this limit the friction coefficient $\beta = \hbar k^2 I s$ depends linearly on the saturation and thus on the intensity. The velocity capture range is given by $kv = \Gamma$.

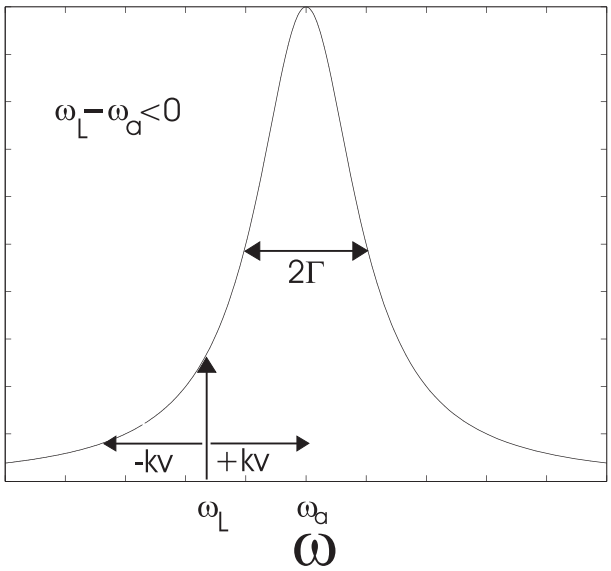

FIGURE 3. Atomic absorption rate versus ω. It can be described by a Lorentzian with full-width at half-mean of 2Γ centered at ω_a.

As mentioned above an important requirement on the sample that should be cooled is the existence of a closed optical transition. In order to achieve appreciable kinetic effects one needs to scatter lots ($\approx 10^4$) of photons. In order to stop a Na atom escaping from an oven at 600 K with a velocity around 900 m/s one needs to scatter about 30000 counterpropagating photons. (Each photon recoil corresponds to a velocity change of 0.03 m/s.) If the transition is not closed, population is transferred to states not accessible to the cooling lasers. This excludes molecules from Doppler cooling due to the existence of rotational and vibrational couplings between all of the energy levels.

The stochastic nature of photon absorption and emission gives rise to an increase in $\langle E_{kin}^2 \rangle$. Hence there is a competition between heating and cooling processes that limits the achievable steady-state temperature. Defining the diffusion coefficient as

$$2D = \frac{d}{dt}\Delta P^2(t) \tag{7}$$

where $\Delta P^2(t) = \langle [P(t) - \langle P(t) \rangle]^2 \rangle$ and defining the friction coefficient β by

$$f = -\beta v$$

we see that

$$\frac{dP}{dt} = -\frac{\beta}{m}P$$
$$\frac{dP^2}{dt} = -\frac{2\beta}{m}P^2,$$

and from the definition of the diffusion

$$\frac{dP^2}{dt} = 2D.$$

Heating and cooling processes cancel in steady state so that

$$\frac{\beta}{m}P^2 = D.$$

Accordingly we obtain for the final steady-state temperature

$$\frac{k_B T}{2} = \frac{P^2}{2m} = \frac{D}{2\beta}. \tag{8}$$

For Doppler cooling this becomes $k_B T = \hbar\Gamma$, the so called Doppler limit. For Rb^{85} we get $T \approx 141\mu$K.

2.2.2. Sisyphus cooling

We have seen in the previous section that an atom moving in a red-detuned standing wave experiences a cooling force. This is only true however as long as the intensity of the light is not too high (saturation parameter $sI \ll 1$). For high intensity the dependence of the force on the sign of the detuning is reversed: one finds that atoms are heated for negative detuning and cooled for positive detuning. Dalibard and Cohen-Tannoudji presented a beautiful physical picture for this behaviour [9] that is based on the dressed atom approach:

The total Hamiltonian describing the combined system laser field and two-level atom can be written as the sum of a free Hamiltonian H_0 and an interaction Hamiltonian H_I

$$\begin{aligned} H_0 &= \hbar\omega_a |e\rangle\langle e| + \hbar\omega_L a^\dagger a \\ H_I &= \hbar g\sqrt{n+1}\left(a^\dagger\sigma^- + \sigma^\dagger a\right) \\ H &= H_0 + H_I \end{aligned} \tag{9}$$

For weak coupling one can treat the effect of H_I by perturbation theory. The eigenstates of H_0 are unchanged and the interaction couples these states to each other. In the strong coupling regime, where H_I dominates H, atom and light have to be viewed as a single quantum mechanical entity. Thus one should switch from the eigenstates of H_0 (bare states) to the eigenstates of H, the so-called dressed states, given by

$$\begin{aligned} |+,n\rangle &= \sqrt{\frac{\Omega_n - \Delta_a}{2\Omega_n}}|e,n\rangle + \sqrt{\frac{\Omega_n + \Delta_a}{2\Omega_n}}|g,n+1\rangle \\ |-,n\rangle &= -\sqrt{\frac{\Omega_n + \Delta_a}{2\Omega_n}}|e,n\rangle + \sqrt{\frac{\Omega_n - \Delta_a}{2\Omega_n}}|g,n+1\rangle \end{aligned} \tag{10}$$

with eigenenergies

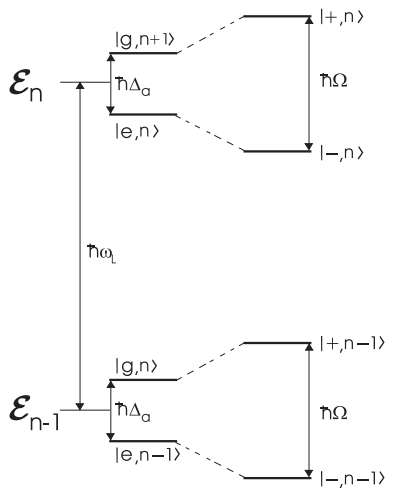

FIGURE 4. Bare states (left) and dressed states (right). The dressed states at photon number n are bunched into well-separated two-dimensional manifolds $\mathcal{E}_n$ separated by the energy of one photon $\hbar\omega_L$. The dependence of Ω_n on the photon number n in the manifold is neglected by assuming a laser beam in a coherent state with a Poissonian distribution for n with a width Δn much smaller than the average number of photons.

$$E_{\pm,n} = \hbar\omega_L n + \frac{\hbar\left(\omega_L + \omega_a\right)}{2} \pm \frac{\hbar}{2}\Omega_n, \tag{11}$$

where

$$\Omega_n = \sqrt{\Delta_a^2 + 4g^2\left(n+1\right)}. \tag{12}$$

Physically these dressed states are linear superpositions of atomic and laser field states. Fig. 4 shows how the bare states of the atom-laser mode system correspond to the dressed states. The energy split $\hbar\Omega$ between $|+,n\rangle$ and $|-,n\rangle$ depends on the atomic position z_a since, e. g. for a standing wave mode $g = g_0 \cos kz_a$.

Fig. 5 shows three adjacent dressed state manifolds for positive detuning Δ_a versus the laser standing wave. At a node of the light field g vanishes and the two dressed states $|+,n\rangle$ and $|-,n\rangle$, respectively become the unperturbed bare states $|g,n+1\rangle$ and $|e,n\rangle$ separated by $\hbar\Delta_a$, while at antinodes of the standing wave the splitting between $|+,n\rangle$ and $|-,n\rangle$ becomes largest. Note that the contamination of $|+,n\rangle$ by $|e,n\rangle$ is highest at antinodes, while $|n,-\rangle$ is maximally contaminated by $|e,n\rangle$ at nodes. Spontaneous emission by the atom causes radiative transitions between dressed levels of adjacent photon manifolds. Since both dressed states $|+,n\rangle$ and $|-,n\rangle$ of $\mathcal{E}_n$ are contaminated by $|e,n\rangle$ and both dressed states $|+,n-1\rangle$ and $|-,n-1\rangle$ of $\mathcal{E}_{n-1}$ are contaminated by $|g,n\rangle$, four transitions between $\mathcal{E}_n$ and $\mathcal{E}_{n-1}$ are allowed:

$$
\begin{aligned}
|+,n\rangle &\to |-,n-1\rangle \\
|-,n\rangle &\to |+,n-1\rangle \\
|+,n\rangle &\to |+,n-1\rangle \\
|-,n\rangle &\to |-,n-1\rangle
\end{aligned}
\tag{13}
$$

Consider now an atom moving in a blue-detuned laser field (fig. 5). Let us follow the exemplary trajectory of an atom that starts at a node of the standing wave in $|+,n+1\rangle$. It climbs uphill to the antinode of the field where its spontaneous decay rate is maximal, because the contamination of $|+,n+1\rangle$ by $|e,n+1\rangle$ is maximal. It may jump either into $|+,n\rangle$ or into $|-,n\rangle$. A transition to $|+,n\rangle$ does not change the mechanical energy of the atom, while a jump into $|-,n\rangle$ transfers the atom to a potential valley, from where it has to climb a hill again[1]. $|-,n\rangle$ is most unstable at a node of the standing wave, so the atom will have maximum probability to decay to the lower manifold $\mathcal{E}_{n-1}$, and so on. Clearly this leads to a decrease of the average atomic kinetic energy and thus to deceleration of the atom.

[1]This explains the denomination Sisyphus cooling referring to the ancient greek myth.

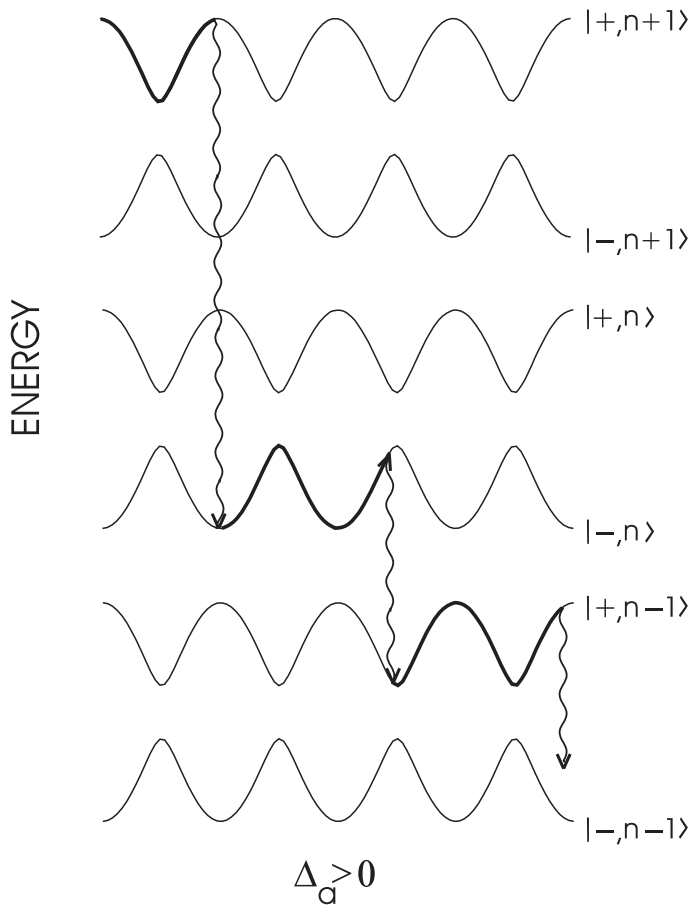

FIGURE 5. Sisyphus cooling in a blue-detuned standing laser wave. The full line represents an exemplary trajectory of the moving atom. The vertical wavy lines refer to spontaneous emission events. The atom sees on average more uphill parts than downhill parts and is therefore decelerated.

2.2.3. Sub-Doppler cooling

In 1988 researchers at the National Institute of Standards and Technology, Washington were surprised to find that they had cooled sodium atoms to temperatures much lower than the Doppler limit $\hbar\Gamma$, even approaching the recoil limit $k_B T_{Rec} = \hbar k^2/(2m)$ at very low laser powers [18]. It took theoreticians almost a year to find a possible explanation for these unexpected low temperatures [19, 20]. The broad outlines of the argument were the following:

The friction force experienced by an atom moving in a laser field is due to the existence of an internal time scale τ that describes how fast the atom can adjust its internal state to the variation of the field induced by the atomic motion. In a two-level atom there is only one such time-scale, the radiative lifetime of the excited state

$$\tau_{rad} = \frac{1}{\Gamma}. \tag{14}$$

For atoms with several Zeeman sublevels in their ground state (e. g. alkali atoms), there is another internal time scale, which is the optical pumping time

$$\tau_p = \frac{1}{\gamma_0 I}, \tag{15}$$

characterizing the mean time it takes for an atom to be transferred by a floures-cence cycle from one Zeeman sublevel to another, where $I = E^- E^+$ is the laser intensity. At low laser power, $\gamma_0 I \ll \Gamma$ and we have

$$\tau_{rad} \ll \tau_p. \tag{16}$$

This means that non-adiabatic effects can occur at velocities $kv \approx \gamma_0 I$ much smaller than those required for Doppler cooling $kv \approx \Gamma$, which explains the exis-tence of a friction force for very slow atoms. Furthermore a laser field not only leads to optical pumping between different Zeeman sublevels of the groundstate but also to lightshifts that can be different for each of the sublevels.

In the next two sections we will give a short overview on two different types of sub-Doppler cooling, associated with two different types of polarization gradients.

a. Polarization gradient cooling: Lin ⊥ Lin. In this section we consider atomic motion in the field of two counterpropagating plane laser wave modes with equal amplitudes and orthogonal linear polarization (see fig. 6)

$$\begin{aligned} \vec{E}^+ &= \mathcal{E}\left(e^{ikz}\vec{e}_x + e^{-ikz}\vec{e}_y\right) \\ &= \mathcal{E}\left[(\vec{e}_x + \vec{e}_y)\cos kz + i\,(\vec{e}_x - \vec{e}_y)\sin kz\right]. \end{aligned} \tag{17}$$

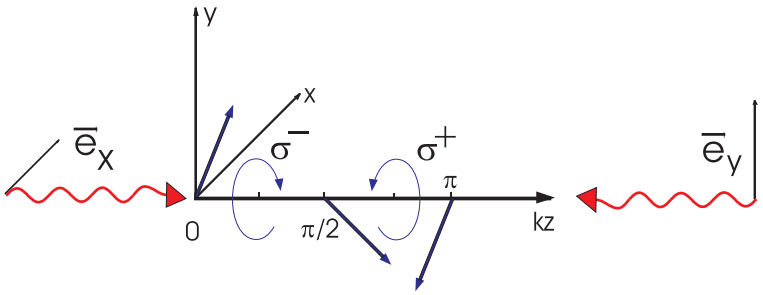

FIGURE 6. Polarization of laser field along z-axis for a lin ⊥ lin setup.

The polarization of the electric field changes, when one moves along the z-axis: In $kz = 0$ it is linear along $\vec{e}_x + \vec{e}_y$, in $kz = \pi/4$ it is circular (σ^-), in $kz = \pi/2$

linear along $\vec{e}_x - \vec{e}_y$, circular (σ^+) in $kz = 3\pi/4$ and linear again in $kz = \pi$ along $-(\vec{e}_x + \vec{e}_y)$.

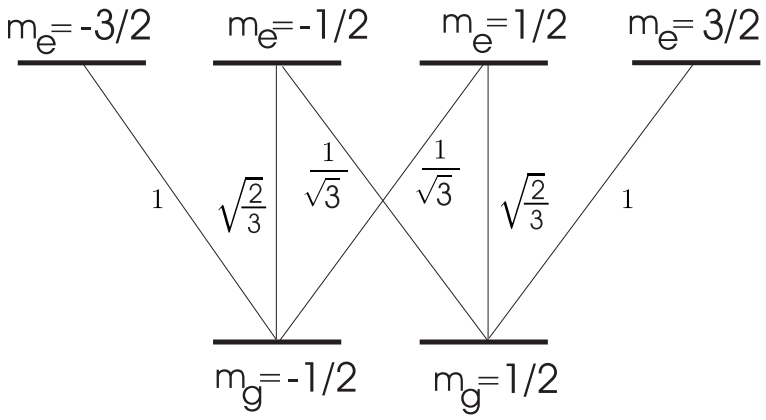

FIGURE 7. Level scheme and Clebsch-Gordan coefficients for a $J_g = 1/2 \rightarrow J_e = 3/2$ transition.

Let us consider the simple case of a $J_g = 1/2 \rightarrow J_e = 3/2$ atomic transition (fig. 7). For this transition there are two Zeeman sublevels $|g_{-1/2}\rangle$ and $|g_{1/2}\rangle$ in the groundstate and four Zeeman sublevels in the excited state. Since the Clebsch-Gordan coefficients of the various transitions between ground and excited state are not the same, and since the nature of the polarization changes with z, it can be easily shown [21], that the two light shifted energies of $|g_{-1/2}\rangle$ and $|g_{1/2}\rangle$ have the spatial dependence displayed in fig. 8: the $|g_{-1/2}\rangle$ sublevel has the largest shift for a σ^- polarization, the $|g_{1/2}\rangle$ sublevel has the largest lightshift for a σ^+ polarization and both sublevels are equally shifted for a linear polarization. Fig. 8 also shows how this gives rise to a Sisyphus type cooling effect due to the time lag τ_p caused by optical pumping.

For a slowly moving atom ($kv \ll \gamma_0 I$) the cooling force is linear in velocity $f = -\beta_\perp v$ with the friction coefficient

$$\begin{aligned} \beta_\perp &= \hbar k^2 \frac{U_0}{\gamma_0} \\ &= \hbar k^2 \frac{\Delta_a}{\Gamma} \end{aligned} \tag{18}$$

which is independent of the laser intensity $I = |\mathcal{E}|^2$. Choosing $\Gamma \ll \Delta_a$ the friction coefficient is much larger than the optimal friction coefficient for Doppler cooling $\beta_{Dopp} = \hbar k^2 I s$. Eq. 18 also shows that the weakness of the dipole force is compensated for by the length of the optical pumping times, since $U_0 \ll 1$ is divided by γ_0 which is also small, since the optical pumping time is very long. However the velocity capture range of this new friction force, given by $kv = \gamma_0 I$ is much smaller than the corresponding one for Doppler cooling.

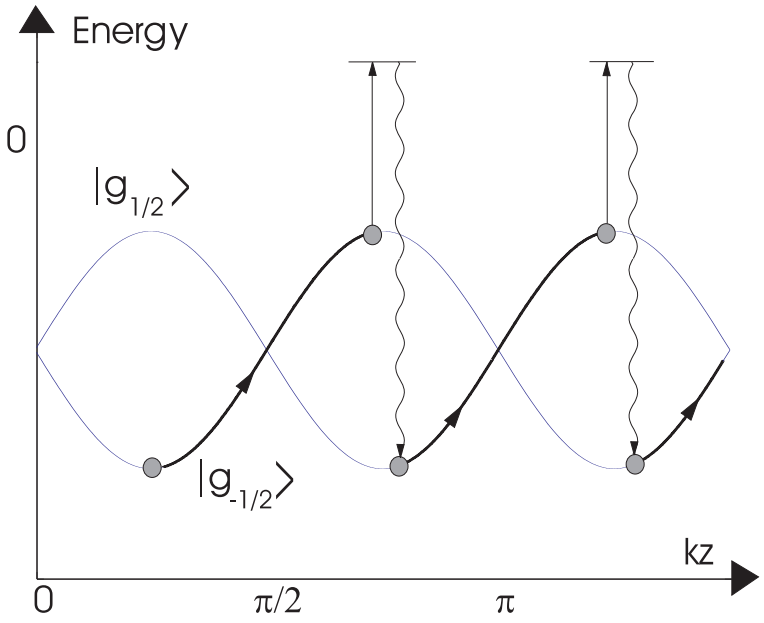

FIGURE 8. Low intensity Sisyphus cooling in the lin⊥lin configuration. The transition rate from $|g_{1/2}\rangle$ to $|g_{-1/2}\rangle$ via the excited state is maximal at the places where the energy of $|g_{1/2}\rangle$ is the highest, and vice versa for $|g_{-1/2}\rangle$. Therefore the atom leaves one of the oscillating potential curves at the top of one hill and is transferred to the valley of the other potential curve. In other words, because of the time lag τ_p the atom sees on average more uphill parts than downhill ones. Here the atomic velocity has been chosen such that the atom travels over one wavelength $\lambda/4$ in a relaxation time τ_p, which gives the maximal value for the cooling force.

b. Polarization gradient cooling: σ^+-σ^-. Choosing a setup where the two counterpropagating waves have polarization σ^- and σ^+ respectively,

$$\begin{aligned}\vec{E}^+ &= \mathcal{E}\left(e^{ikz}\vec{e}_+ + e^{-ikz}\vec{e}_-\right)\\ &= -i\sqrt{2}\mathcal{E}\left(\vec{e}_x \sin kz + \vec{e}_y \cos kz\right)\\ &\equiv -i\sqrt{2}\mathcal{E}\vec{e}_Y(z),\end{aligned} \tag{19}$$

where $\vec{e}_\pm = \mp 1/\sqrt{2}(\vec{e}_x \pm i\vec{e}_y)$, we see that the polarization of the laser field is always linear along $\vec{e}_Y$ and rotating in the $x-y$ plane as one moves along the z-axis.

As the field amplitude is position-independent in this setup, the light shifts of the groundstate sublevels remain constant when the atom moves along the z-axis and there is no possibility of a Sisyhus effect. In this section a different type of cooling scheme is described, depending on a highly sensitive motion-induced population difference in the groundstate sublevels even for very small velocities. The simplest atomic transition to observe this type of cooling is $J_g = 1 \to J_e = 2$ (see fig.10).

An atom moving along the z-axis with velocity v sees a linear polarization along $\vec{e}_Y$ rotating around the z-axis in the x-y-plane with a frequency $-kv$. Transforming

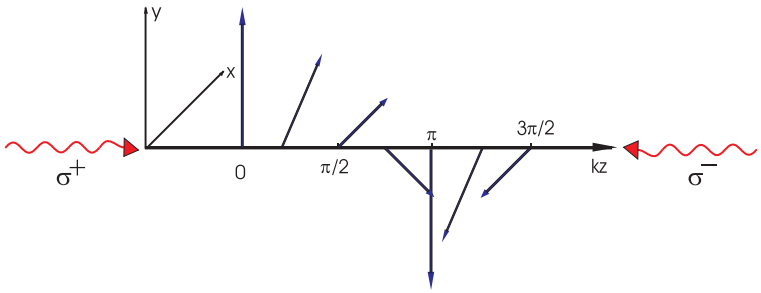

FIGURE 9. Polarization of laser field along z-axis for a σ^+-σ^- setup.

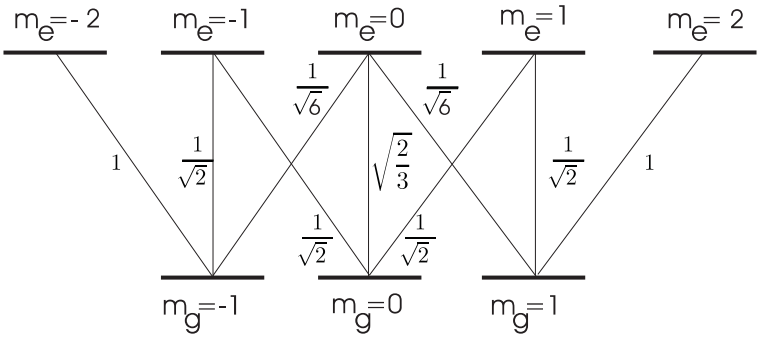

FIGURE 10. Level scheme and Clebsch-Gordan coefficients for a $J_g = 1 \rightarrow J_e = 2$ transition.

into a comoving rotating coordinate system the laser polarization keeps a fixed direction. In addition Larmor's theorem tells us that in this moving rotating frame, an inertial field parallel to the rotation axis will appear. This leads to a new term in the Hamiltonian equal to

$$H_{rot} = kvJ_z. \tag{20}$$

It can be shown [21] that this additional term leads to a population difference in the eigenstates of J_z proportional to kv. Choosing red detuning ($\Delta_a < 0$) it can be shown that $|g_-\rangle$ is more populated than $|g_+\rangle$ for an atom moving toward $z > 0$. Since there is a six times greater probability that an atom in $|g_-\rangle$ will absorb a σ^- photon propagating toward $z < 0$ than that it will absorb a σ^+ photon propagating toward $z > 0$, it follows that the radiation pressures exerted by the σ^+ and σ^- waves will be unbalanced. The atom will scatter more counterpropagating σ^- photons than copropagating σ^+ photons and its velocity will decrease. For a slowly moving atom the friction coefficient can be calculated to give

$$\begin{aligned} \beta_\sigma &= \hbar k^2 \frac{\gamma_0}{U_0} \\ &= \hbar k^2 \frac{\Gamma}{\Delta_a}. \end{aligned} \tag{21}$$

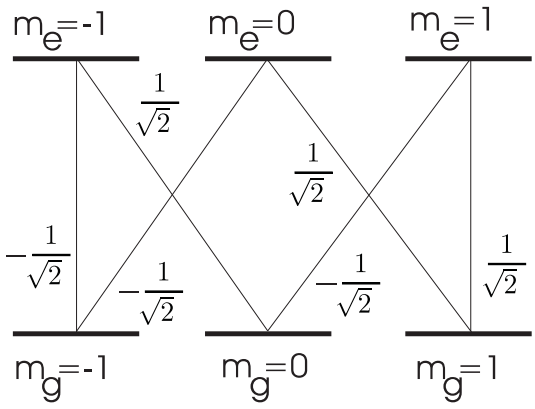

FIGURE 11. Level scheme and Clebsch-Gordan coefficients for a $J_g = 1 \rightarrow J_e = 1$ transition.

As in the $lin \perp lin$ setup it does not depend on the laser intensity I. Comparing β_σ with $\beta_\perp = \hbar k^2 U_0/\gamma_0$ we see that β_σ is much smaller as we assume $\Gamma \ll |\Delta|$. A detailed calculation taking into account heating processes shows however [21], that a steady-state temperature of the same order and below the Doppler limit can be reached in both cooling schemes, since the diffusion coefficient for the σ^+-σ^- setup is much smaller than the corresponding one for $lin \perp lin$.

2.2.4. VSCPT

All cooling mechanisms discussed so far rely on spontaneous emission to dissipate the kinetic energy of the atom. In all of these schemes spontaneous emission never stops, therefore the random recoil due to the emitted photons and the corresponding single photon recoil energy $E_{Rec} = \hbar^2 k^2/(2m)$ appears to limit the reachable steady-state temperature to the so-called recoil temperature

$$k_B T_{Rec} = \frac{\hbar^2 k^2}{2m}. \tag{22}$$

This shows that in order to reach sub-recoil temperatures spontaneous emission has to be "switched off" at some point. As we will show qualitatively in this section, the existence of the phenomenon of velocity selective coherent population trapping (VSCPT) for a $J_g = 1 \rightarrow J_e = 1$ atomic transition in a σ^+-σ^- laser setup allows for the cooling of atoms to temperatures well below the recoil temperature approaching $T = 0$.

The Hamiltonian for this system after adiabatic elimination of the excited atomic state can be written as

$$\begin{aligned} H = & U_0 I/2[|g_{-1}\rangle\langle g_{-1}| + |g_1\rangle\langle g_1| - \\ & e^{-2ikz_a}|g_{-1}\rangle\langle g_1| - e^{2ikz_a}|g_1\rangle\langle g_{-1}|]. \end{aligned}$$

This Hamiltonian has two eigenstates, namely the dark state[2] with eigenvalue $\lambda_{DS} = 0$

$$|\psi_{DS}\rangle = \frac{1}{\sqrt{2}}\left(e^{-ikz_a}|g_{-1}\rangle + e^{ikz_a}|g_1\rangle\right) \tag{23}$$

and the maximally coupled bright state with eigenvalue $\lambda_{BS} = U_0 I$

$$|\psi_{BS}\rangle = \frac{1}{\sqrt{2}}\left(e^{-ikz_a}|g_{-1}\rangle - e^{ikz_a}|g_1\rangle\right) \tag{24}$$

For an atom at rest the total population is pumped into $|\psi_{DS}\rangle$ as this state does not couple to the light field. It can be shown [22] that for a moving atom a motional coupling $\hbar kv$ appears between $|\psi_{DS}\rangle$ and $|\psi_{BS}\rangle$. This contamination of the dark state by the bright state leads to a non-vanishing fluorescence rate R_F of the perturbed state $\overline{|\psi_{DS}\rangle}$. This effect is proportional to $kv/(U_0 I)$ so that the variation of R_F with v occurs in a very small velocity range $\delta v \approx U_0 I/k$ around $v = 0$:

$$R_F(v) = \frac{(2kv)^2\Gamma}{g^2 I} \tag{25}$$

for $v \ll \delta v$ which does not depend on Δ_a. Calculating the force on a moving atom in such a setup shows that the dipole force and radiation pressure cancel each other exactly leading to $f_{tot} = 0$. However the fact that R_F varies rapidly within δv together with the observation that the momentum diffusion coefficient varies also rapidly with v around $v = 0$, since it is based on the random exchanges of momentum associated with fluorescence cycles, leads to a new cooling mechanism that can be considered as an optical pumping process in velocity space: An atom with $v > \delta v$ that undergoes a fluorescence cycle may end up with a velocity $v < \delta v$. Thus momentum diffusion transfers atoms with a velocity at which they absorb light to a region δv in velocity space around $v = 0$ where they remain trapped since all fluorescence stops.

A detailed full quantum mechanical treatment where the external atomic degrees of freedom (position, momentum) are quantized, shows [22] that the correct trapping states are linear superpositions of states that differ not only in $|g_{-1}\rangle$ and $|g_1\rangle$ but also in the momentum $|p + \hbar k\rangle$ for $|g_1\rangle$ and $|p - \hbar k\rangle$ for $|g_{-1}\rangle$, since a photon absorbed by $|g_{-1}\rangle$ has momentum $+\hbar k$ and a photon absorbed by $|g_1\rangle$ has momentum $-\hbar k$. For a long enough interaction time T_{int} between laser and atoms one can expect to find a two-peaked momentum distribution centered around $\pm\hbar k$ with a width of $\delta p \propto 1/\sqrt{T_{int}}$. Choosing a larger T_{int} decreases δp and increases the weight of both peaks since the atoms have more time to be pumped in momentum space towards

[2]Note that it is not the different sign of the Clebsch-Gordan coefficients for the transitions between $|g_{-1}\rangle$ and $|g_1\rangle$ to $|e_0\rangle$ that allows for the existence of a dark state uncoupled to the light field, but the non-existence of levels $|e_{\pm(J_e+1)}\rangle$ to which $|g_{\pm 1}\rangle$ would otherwise couple. In fact the role of $|\psi_{DS}\rangle$ and $|\psi_{BS}\rangle$ would simply be interchanged had the Clebsch-Gordans the same sign.

$p = 0$.
Hence this new type of cooling mechanism that is based on a combination of momentum diffusion and VSCPT is only limited by the interaction time T_{int} and is independent on the sign of the detuning Δ_a. It has however some serious limitations: As there is no cooling force that pushes the atoms to $p = 0$ cooling times are rather long in 3 D. VSCPT needs a closed optical transition and spontaneous atomic relaxation to reach the final dark states. Hence the reabsorption problem strongly limits the final atomic density and temperature. In chapter 6 we will present a generalized dark state cooling scheme which strongly diminishes these disadvantages of free-space VSCPT.
Sub-recoil cooling based on VSCPT has been observed experimentally in 1988 [22] where a one-dimensional temperature below the recoil limit of the chosen atoms has been reached.

	Doppler c.	Polarization gradient c.		VSCPT	Cavity c.
		$\text{lin} \perp \text{lin}$	$\sigma^+ - \sigma^-$		
Closed optical transition needed?	Yes	Yes		Yes	No
β	$\hbar k^2 \beta s$	$\hbar k^2 \frac{U_0}{\gamma_0}$	$\hbar k^2 \frac{\gamma_0}{U_0}$	0	$\hbar k^2 \beta s \left(\frac{g}{\kappa}\right)^2$
$v_{capt.}$	Γ/k	$\gamma_0 \beta/k$	$U_0 \beta/k$	—	κ/k
$k_B T$	$\hbar\Gamma$	$\hbar\omega_{rec} \leq k_B T < \hbar\Gamma$		0	$\hbar\kappa$

FIGURE 12. Table comparing friction coefficient β, velocity capture range $v_{capt.}$ and steady-state temperature T for the low-intensity cooling schemes discussed in chapter 2 and cavity cooling, discussed in chapter 3.

Fig. 12 concludes our brief qualitative overview on free space cooling techniques for neutral atoms in the low saturation limit by summarizing the most important parameters for each of the schemes and comparing them to the ones obtained for cavity cooling that is discussed in the next chapter.

CHAPTER 3

Single atoms in optical resonators

3.1. Introduction

It has been known for many decades that the radiative properties of an atom are changed inside a resonator [23], but it was only in the last decade that the modification of mechanical light effects by such a cavity came into the focus of interest of several research groups [4, 5, 6]. Partly this was due to the fact that in order to observe such effects experimentally, resonators with a very high finesse are needed.

In the 1990's cavities with a finesse > 100000 became experimentally feasible, and the present technical status is such that already one photon inside a cavity can exert a detectable force on an atom. On the other hand very cold atomic samples have to be available to allow for large interaction times with the resonator. This became possible after the development of efficient laser cooling and trapping techniques for neutral atoms, such as the Magneto-Optical Trap (MOT).

Typically in a cavity-QED experiment cold atoms are released from a MOT with a temperature of a few μK [4, 5, 6]. So far all experiments have been done using standing wave resonators. Although one might not expect any new mechanical effects in a ring resonator setup, it can be easily seen that this is not true: In a standing wave cavity the boundary conditions for the resonator field call for a node of the electric field $\vec{E}$ at the cavity mirrors (assuming perfect mirror conductivity). Thus the phase of $\vec{E}$ is fixed with respect to the mirrors, while the mode amplitude is a dynamical quantity that can be modified by the presence of an atom [3].

An atom moving along the standing wave of a resonator can be understood as a dielectric substance with position-dependent coupling to the cavity field. At a field node atom and cavity are uncoupled while the coupling gets maximal at antinodes of the standing wave. The intracavity photon number is maximal if the cavity is pumped resonantly. When the pump frequency ω_P does not match the cavity eigenfrequency ω_C, less light is trapped in the resonator. Fig. 13 illustrates how this leads to a intracavity photon number that depends on the position of the atom. Parameters have been chosen such that the empty cavity is on resonance with the external pump field. At the antinodes the cavity is shifted maximally out of resonance by the atom leading to a minimum of the photon number in the resonator.

In a ring cavity the boundary condition of a field node is replaced by the periodic boundary condition $\vec{E}(0) = \vec{E}(L)$, where L is the resonator length. This does not fix the phase of the intracavity field which is now subjected to the influence of an atom too. In order to get a physical understanding how this works let us assume that

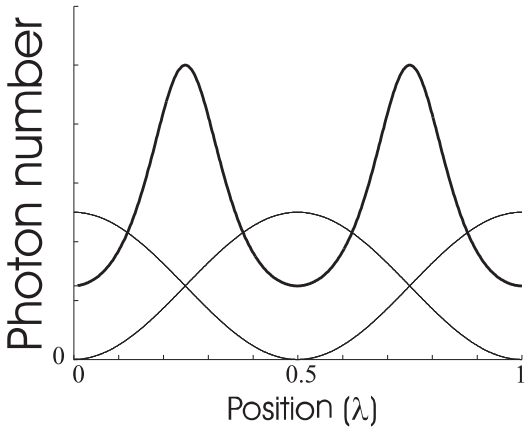

FIGURE 13. Photon number (thick line) and standing wave in a standing wave resonator versus z_a. At antinodes the cavity is shifted maximally out of resonance by the atom leading to a minimum in photon number.

there is an atom at position z_a on the axis of a ring resonator pumped from one side only. This means that only one of the two frequency-degenerate counterpropagating running waves has a non-zero photon number in the absence of an atom.

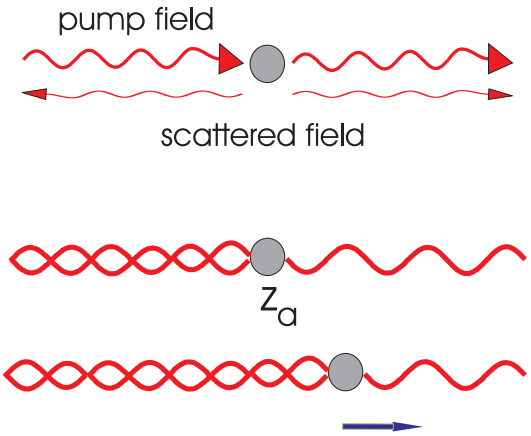

FIGURE 14. Photons scattered by an atom at z_a create a standing wave to the left of the atom. This standing wave is dragged along as the atom moves to the right.

An atom at position z_a will scatter photons out of the pumped mode. Some of these photons will be coherently redistributed to the unpumped mode, thus the atom creates a standing wave on top of the injected running wave, not necessarily with a potential minimum at its position (fig. 14).

The phase of the scattered standing wave depends on z_a and a moving atom drags the standing wave along with its motion. For a moving atom, cavity decay cannot instantaneously adjust the field amplitudes $\alpha_\pm$ to the values they would obtain in steady state for an atom at rest at z_a. There is a certain time-lag, given by $T_\kappa = 1/\kappa$,

where κ is the cavity decay rate. Fig. 15 shows that a moving atom will experience a non-zero gradient of the local intensity which can either lead to an acceleration or deceleration of the atom, depending on the chosen parameters (see chapter 3.5).

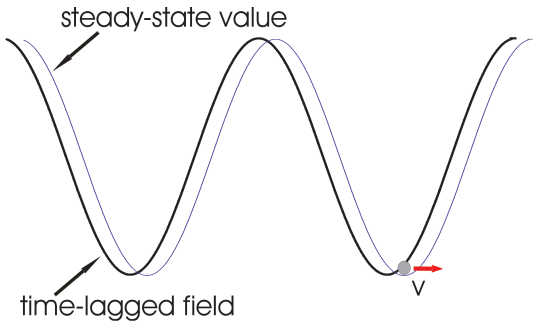

FIGURE 15. A moving atom experiences a non-zero gradient of the local intensity due to the cavity time-lag.

On the other hand if there are several atoms interacting with the cavity each of the atoms drags its scattered field along with its motion. As each atom can feel the other atoms by their scattered fields this will lead to collective motional effects. We will show below that this can be used as a quantum bus, i. e. to share information on a quantum level between these atoms, as has first been suggested by Hemmerich [24].

3.2. Model

In this chapter we describe the motion of a single two-level atom in the field of two counterpropagating running plane wave modes with field amplitudes $\alpha_{\pm}$. Each cavity mode is assumed to be driven at pump rates $\eta_{\pm}$ and frequency ω_P. The cavity decay rate is denoted by κ. $\gamma_0 = \Gamma g^2/(\Gamma^2 + \Delta_a^2)$ is the spontaneous emission rate per photon by the atom and $U_0 = \Delta_a g^2/(\Gamma^2 + \Delta_a^2)$ is the frequency shift induced by the atom for each mode. The intracavity field E can be split into the positive and negative frequency parts and written as

$$\begin{aligned} \vec{E}(Z,t) &= \vec{E}^{+}(Z,t)e^{-i\omega_P t} + \vec{E}^{-}(Z,t)e^{i\omega_P t} \\ \vec{E}^{+}(Z,t) &= \mathcal{E}\left(a_{+}(t)e^{ikZ} + a_{-}(t)e^{-ikZ}\right)\vec{e}_x \\ \vec{E}^{-} &= \left(\vec{E}^{+}\right)^{\dagger}, \end{aligned} \tag{26}$$

where $\mathcal{E} = \sqrt{\frac{\hbar\omega_P}{2\epsilon_0 V}}$ is the electric field per photon

For an atom moving into the positive z-direction α_+ (α_-) is the copropagating (counterpropagating) cavity mode.

The equations of motion for the cavity fields read

$$\dot{\alpha}_{\pm} = \left(-\kappa - \gamma_0 + i\left(\Delta_c - U_0\right)\right)\alpha_{\pm} - \left(\gamma_0 + iU_0\right)\alpha_{\mp}e^{\mp 2ikz_a} + \eta_{\pm} \tag{27}$$

where the excited atomic state has been adiabatically eliminated and $\Delta_C = \omega_P - \omega_C$. The force on the atom can be calculated by the gradient of the interaction hamiltonian (see section 3.5.3 for more details).

3.3. Mechanical light effects

Let us now come back to the mechanical light effects inside a ring resonator. The total force acting on an atom can be easily understood:

$$\begin{aligned} f_{tot} &= f_{rp} + f_{dip} \\ f_{rp} &= 2\hbar k\gamma_0 \left(\alpha_+^* \alpha_+ - \alpha_-^* \alpha_-\right) \\ f_{dip} &= 2\hbar k U_0 i \left(\alpha_+^* \alpha_- e^{-2ikz_a} - \alpha_-^* \alpha_+ e^{2ikz_a}\right) \end{aligned} \tag{28}$$

It consists of two parts. The dipole force f_{dip} comes from the interaction of the reactive atomic dipole moment induced by α_+ with α_- and vice versa. It is non-zero only if the atom is detuned from the pump field ($\Delta_a \neq 0$) and can be written as the gradient of the intracavity intensity at the position of the atom times U_0

$$f_{dip} = -\hbar U_0 \left\langle \frac{d}{dz} E^- E^+ \right\rangle \Bigg|_{z_a} . \tag{29}$$

The radiation pressure f_{rp} is caused by the dissipative component of the atomic dipole moment induced by α_+ interacting with α_- and vice versa. In the case of only two counterpropagating waves it is the difference of radiation pressures exerted separately by α_+ and α_-. In general a ring resonator can be pumped with different pump rates for α_+ and α_- modes, η_+ and η_-. Let us study the two instructive special cases of one-sided pump ($\eta_- > 0$, $\eta_+ = 0$) and symmetric pump ($\eta_+ = \eta_- \equiv \eta$).

3.3.1. One-sided pumping

Let us neglect cavity dynamics as a first step. Of course this is only correct for an atom at rest. For a single running wave mode interacting with an atom in free space one would expect $f_{rp} \neq 0$, $f_{dip} = 0$, as there is no intensity gradient in a plane wave. However eqs. 30 show that there is a non-zero reactive force inside a ring resonator stemming from coherent redistribution of photons between the pumped and unpumped modes.

$$\begin{aligned} f_{rp} &= -2\hbar k\gamma_0 I \left[1 + 2\frac{\kappa\gamma_0 - \Delta_c U_0}{\kappa^2 + \Delta_c^2}\right] \\ f_{dip} &= -4\hbar k U_0 I \frac{U_0\kappa + \gamma_0\Delta_c}{\kappa^2 + \Delta_c^2} \end{aligned} \tag{30}$$

where

$$I = \frac{\eta_-^2}{(2\gamma_0 + \kappa)^2 + (2U_0 - \Delta_C)^2} \tag{31}$$

is the photon number at the position of the atom. The free space situation corresponds to the limit where $\gamma_0, U_0, \Delta_C \ll \kappa$ together with I fixed to some constant value. We see that f_{dip} goes to zero as expected and radiation pressure assumes its free space value $f_{rp} = -2\hbar k\gamma_0 I$.

3.3.2. Symmetric pumping

In an empty symmetrically pumped cavity there is an equal number of photons in α_+ and α_-. Thus, neglecting the atomic backaction on the field, there would be no net radiation pressure. However every time a photon is coherently redistributed between α_+ and α_- by the atom, the photon numbers become unbalanced (fig. 16).

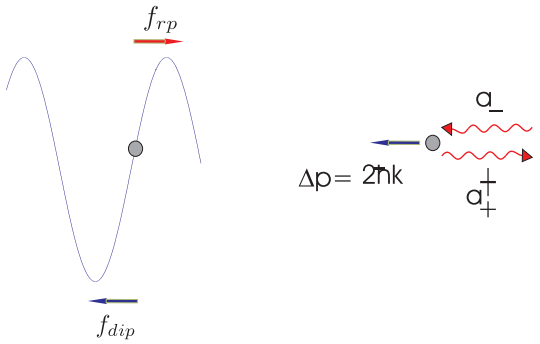

FIGURE 16. Coherent redistribution of photons causes different photon numbers for $\alpha_\pm$. This leads to a net radiation pressure force.

This gives rise to a non-zero radiation pressure even for symmetric pumping as can be seen in eqs. 32.

$$\begin{aligned} f_{rp} &= 4\hbar k\gamma_0 I \frac{U_0\kappa + \gamma_0\Delta_c}{\kappa^2 + \Delta_C^2} \sin 2kz_a \\ f_{dip} &= 2\hbar k U_0 I \left[1 + 2\frac{\kappa\gamma_0 - 2\Delta_c U_0}{\kappa^2 + \Delta_C^2}\right] \sin 2kz_a \end{aligned} \tag{32}$$

where $I = 2\eta^2/[(2\gamma_0 + \kappa)^2 + (2U_0 - \Delta_C)^2]$. In the free space limit this leads to the expected result $f_{rp} = 0$ and $f_{dip} = 2\hbar k U_0 I \sin 2kz_a$.

As can be expected the forces are modified for a slowly moving atom. Let us focus on the dipole force which will be much larger than radiation pressure in the limit $\gamma_0 \ll U_0$. It is straightforward to find an expression for the friction coefficient, i. e., the linear velocity dependence of the force for small velocities ($kv \ll \kappa$) due to the cavity dynamics, by expanding the field amplitudes in the form $\alpha_\pm \approx \alpha_\pm^0 + kv/\kappa\alpha_\pm^1$. Eq. 28 then gives to first order in v

$$f_{dip} = f^0_{dip} + f^1_{dip} v$$

for the dipole force. This force acting on the atom can now be averaged over one wavelength. In a symmetrically pumped cavity we get of course $\overline{f^0_{dip}}^{\lambda} = 0$ and

$$\overline{f_{dip}}^{\lambda} = \frac{16\hbar k^2 U_0^2 \kappa I}{\kappa^2 + (2U_0 - \Delta_C)^2} \frac{\Delta_C - U_0}{\kappa^2 + \Delta_C^2} \left[1 - 2\frac{\Delta_C U_0}{\kappa^2 + \Delta_C^2}\right] v. \tag{33}$$

Fortunately it is also possible to calculate the field amplitudes for arbitrary velocity v by solving eqs. 27 analytically. Setting $\Delta_c = 0$ to increase readability we get

$$\alpha_{\pm} = \frac{\kappa + i\left(U_0 \pm 2kv\right)}{\left(\kappa + i\left(U_0 \pm kv\right)\right)^2 + \Omega^2}\eta - \frac{iU_0 e^{\mp 2ik(z_0+vt)}}{\left(\kappa + i\left(U_0 \mp kv\right)\right)^2 + \Omega^2}\eta \tag{34}$$

Each mode has a contribution from the other one that is multiplied by a phase depending on the atomic position z_a. The first part in eq. 34 is the contribution from the pump light, shifted out of resonance by the moving atom, e. g. α_+ is frequency shifted by an amount of $U_0 - 2kv$. With eqs. 34 the dipole force for arbitrary velocity v can be written as the sum of the force exerted by the copropagating and the counterpropagating light alone.

$$\begin{aligned}
\overline{f_+}^{\lambda} &= \frac{4\hbar k \kappa U_0^2 \eta^2}{\left(\kappa^2 + 2U_0 kv\right)^2 + 4\kappa^2\Omega^2} \\
\overline{f_-}^{\lambda} &= -\frac{4\hbar k \kappa U_0^2 \eta^2}{\left(\kappa^2 - 2U_0 kv\right)^2 + 4\kappa^2\Omega^2} \\
\overline{f_{dip}}^{\lambda} &= \overline{f_+}^{\lambda} + \overline{f_-}^{\lambda}
\end{aligned} \tag{35}$$

or

$$\overline{f_{dip}}^{\lambda} = \frac{-32\hbar k \kappa^3 U_0^3 kv}{\left[\left(\kappa^2 + 2U_0 kv\right)^2 + 4\kappa^2\Omega^2\right]\left[\left(\kappa^2 - 2U_0 kv\right)^2 + 4\kappa^2\Omega^2\right]}\eta^2 \tag{36}$$

where $\Omega^2 = (kv)^2 + U_0^2$.

Fig. 17 shows the typical odd structure of the dipole force with respect to v. f_{dip} reaches its maximal value around $kv \approx \kappa/2$ which gives the velocity capture range of the cavity dipole force. As $\kappa \ll \Gamma$ in experiments, the cavity force is effective at velocities much slower than the free space Doppler force. Furthermore one would have to choose a red detuning between pump and atom ($U_0 < 0$) to achieve cooling, while in a cavity $U_0 > 0$ is the correct choice if $\Delta_C = 0$. A more thorough comparison between cavity force and Doppler force is given in the next section.

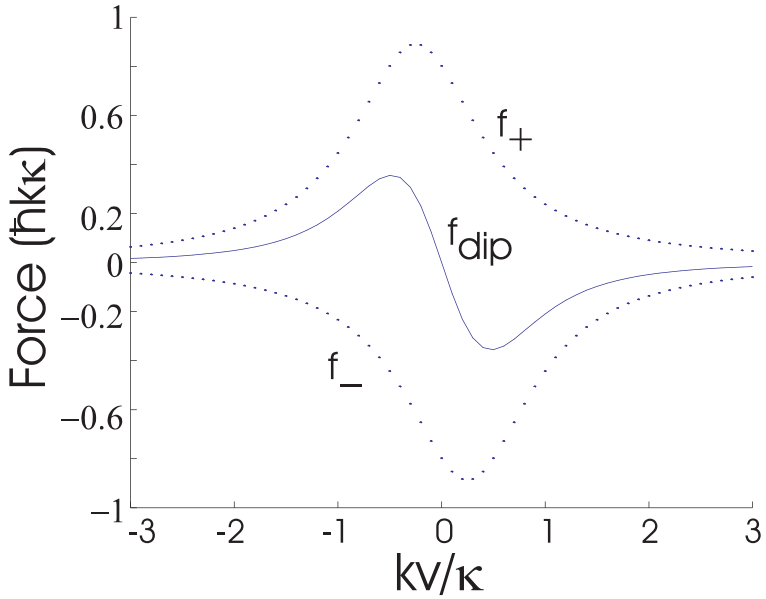

FIGURE 17. Mean dipole force f_{dip} acting on the atom versus its velocity for $U_0 = \kappa$, $\Delta_C = 0$ and $\eta = \kappa$. f_+ (f_-) is the force exerted by the copropagating (counterpropagating) beam alone.

3.3.3. Comparison between Cavity cooling and Doppler cooling

How effective is cavity cooling compared to conventional Doppler cooling? For a slowly moving atom ($kv \ll \kappa$) the force on the atom can be shown to be linear in v. For a correct choice of parameters this leads to a friction coefficient. In the optimal parameter regime, where $\Delta_C = -\kappa$, $2U_0 - \Delta_C = 0$ (pump detuned to half-width of cavity lorentzian, atom shifts cavity into resonance) and $\Gamma \ll \Delta_a$, eq. 33 can be simplified to give

$$\overline{f_{Cav}}^{\lambda} = -\hbar k^2 I s (2g/\kappa)^2 v, \tag{37}$$

where $sI = \eta^2 U_0^2/(g^2\kappa^2)$ is the saturation parameter. Comparing this with the well-known doppler friction force in free space

$$\overline{f_{Dopp}}^{\lambda} = -\hbar k^2 I s v, \tag{38}$$

it can be seen, that for $g > \kappa$ (strong coupling regime) the cavity force is larger by a factor of $(2g/\kappa)^2$. This friction coefficient can be used to estimate the cooling time τ_C, defined from the exponential decrease of the kinetic energy of the atom

$$E(t) = \left(E(0) - \frac{k_B T}{2}\right) e^{-t/\tau_C} + \frac{k_B T}{2}, \tag{39}$$

where $\tau_C = m/(2|f|)$. For $g > \kappa$ the cooling time inside a ring resonator

$$\tau_{C,Cav} = \frac{\omega_{Rec}^{-1}}{4s}\left(\frac{\kappa}{2g}\right)^2 \tag{40}$$

is smaller by a factor of $(\kappa/(2g))^2$ than in free space, where we have

$$\tau_{C,Dopp} = \frac{\omega_{Rec}^{-1}}{4s} \tag{41}$$

and $\omega_{Rec} = \hbar k^2/(2m)$ is the recoil frequency.

The reachable steady-state temperature in a ring resonator with 2 modes can be calculated to give $k_B T = \hbar\kappa/2$. For $\kappa < \Gamma$ this can be lower than the Doppler limit $k_B T = \hbar\Gamma$. We conclude that the modification of mechanical light effects in a ring resonator can be used to achieve faster cooling of atoms (if $g > \kappa$) to a lower temperature (if $\kappa < \Gamma$) than in free space. While it would seem that κ should be as small as possible compared to Γ and g, one should not forget that the velocity range where cavity cooling works is given by $kv \approx \kappa$. This means for smaller κ atoms precooled to a lower temperature have to be used.

3.4. Quantum gate

Another promising aspect of the interaction between a ring resonator and neutral atoms is the possible implementation of Quantum computation schemes. In 1999 Hemmerich suggested [24] to use cold atoms trapped in a ring resonator to build a quantum logic gate. A similar proposal had already been suggested by Cirac and Zoller [25] in 1995 for ions. The central idea is to use the internal degrees of freedom of each particle in a string of atoms as qubits in the sense of Quantum information. In an ion trap coulomb repulsion strongly couples the ions to each other thus permitting the generation of entanglement between different qubits needed to build e. g. a controlled-NOT gate. However the strong coupling between ions and electric field noise in the endcape electrodes leads to a decoherence time in the order of milliseconds. Additionally this system is not scalable in the number of particles. It seems to be experimentally impossible to go beyond a few 10 ions, which limits the practical applicability of this proposal. Optical lattices filled with neutral atoms on the other hand would have much more favorable properties. Decoherence time due to spontaneously emitted photons can be up to seconds. Furthermore high loading rates (up to 10 % of available lattice sites occupied) seem to be reachable within the next few years, which means easy scalability.

At first sight the only problem seems to be the complete lack of direct atom-atom interactions between atoms at different lattice sites. An optical lattice constituted by the standing wave of a symmetrically pumped ring resonator would easily overcome

this obstacle: Assume that there are N atoms trapped around nodes of a blue-detuned cavity field $\Delta_C = 0$, $U_0 > 0$ [1]. The position of the n-th atom can be written as $kz_n = \frac{2n-1}{2}\pi + \epsilon_n$, where $\epsilon_n \ll 1$ is the deviation of the n-th atom from the nearest cavity node. By focusing lasers on one of the atoms it can be kicked out of its equilibrium position. As the coupling between cavity and atom gets non-zero, the cavity field starts to notice the atom and gets dragged along with its motion. The intracavity intensity can be written as

$$\langle E^- E^+ \rangle = \frac{4\eta^2}{\kappa^2 + \Delta_c^2} \cos^2 (kz - \mu\epsilon_{CM}) \tag{42}$$

where the factor μ has been defined as

$$\mu = \frac{(2U_0 N)^2}{\kappa^2 + (2U_0 N)^2} \tag{43}$$

Now all of the atoms will feel a non-zero local intensity gradient and hence a force equal to

$$f_{dip,n} = -\hbar U_0 \left\langle \frac{d}{dz} E^- E^+ \right\rangle \Big|_{z=z_n}$$

(see fig. 18).

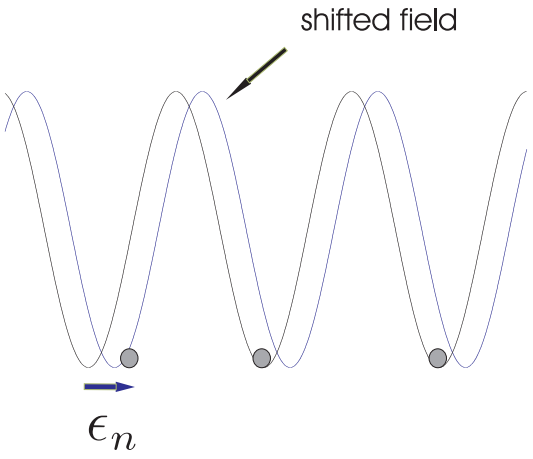

FIGURE 18. An atom is kicked out of its equilibrium position at a field node. The intracavity phase is shifted resulting in a non-zero intensity gradient at the positions of the other atoms.

Writing down the equation of motion for the deviation of the n-th atom from its equilibrium position

[1] An additional conventional lattice in the remaining two dimensions perpendicular to the resonator axis would have to be used in a 3 D setup. Alternatively one could choose a red detuned cavity which leads to higher spontaneous emission rates and decreased coherence times.

$$\ddot{\epsilon}_n + \omega_0^2 \epsilon_n = \omega_0^2 \mu \epsilon_{CM} \tag{44}$$
$$\omega_0^2 = \frac{8\hbar k^2 U_0 \eta^2}{m\kappa^2},$$

where ω_0 is just the usual oscillation frequency of an atom in a harmonic potential of strength $U_0\eta^2/\kappa^2$. One can calculate the possible vibrational modes by making the ansatz $\epsilon_n = \beta_n e^{i\omega_n t}$. Defining the center of mass of the individual displacements by $\epsilon_{CM} = \frac{1}{N}\sum_{n=1}^{N} \epsilon_n$ one can see that there are two different types of modes: A center of mass mode with $\omega_{CM} = \omega_0\sqrt{1-\mu}$ and relative motion modes with $\omega_n = \omega_0$. Let us illustrate this for N=2. The center of mass mode corresponds to two atoms oscillating in phase, hence the individual drags of the atoms on the cavity field add up (fig. 19).

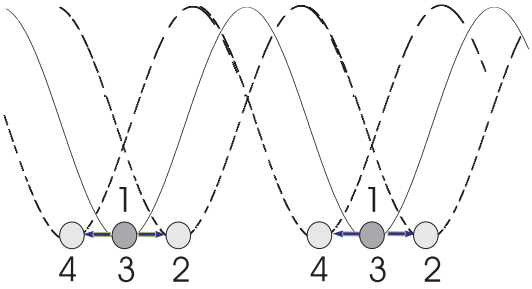

FIGURE 19. Two atoms oscillating in phase. Their individual drags on the field add up and the intracavity intensity is shifted.

The relative motional modes correspond to the atoms oscillating π out of phase, hence their individual drags on the field cancel each other. Each atom oscillates without noticing the presence of the other one (fig. 20).

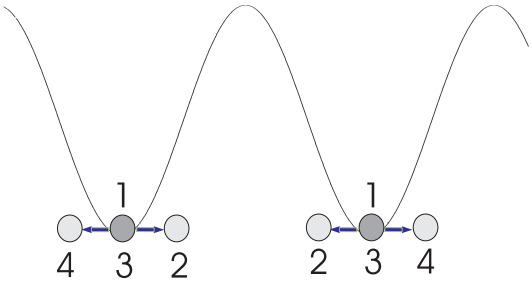

FIGURE 20. Two atoms oscillating π out of phase. Their individual drags on the field cancel and the intracavity phase is not shifted to first order in ϵ.

Obviously the center-of-mass mode would be used in any attempt to build a quantum gate.

In which regime should the resonator be operated as a Quantum Gate? One would like to have clearly separated individual and CM frequencies, so μ should not

be too small. Fig. 21 shows that $NU_0 \approx \kappa$ would already give $\omega_{CM}/\omega_0 = 0.6$ which should be experimentally acceptable. On the other hand cavity dynamics must not be neglected.

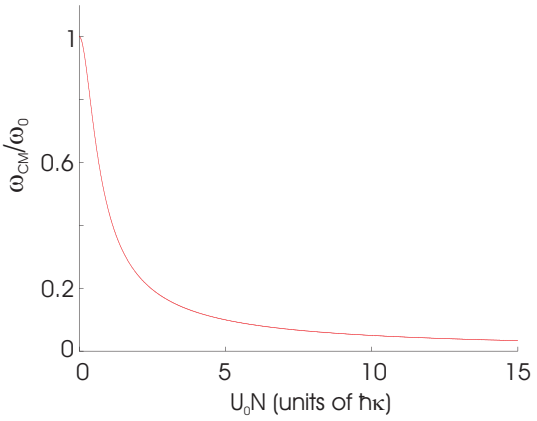

FIGURE 21. Frequency of the vibrational center of mass mode normalized to ω_0 over U_0N. $\Delta_c = 0$, $\kappa = 1$.

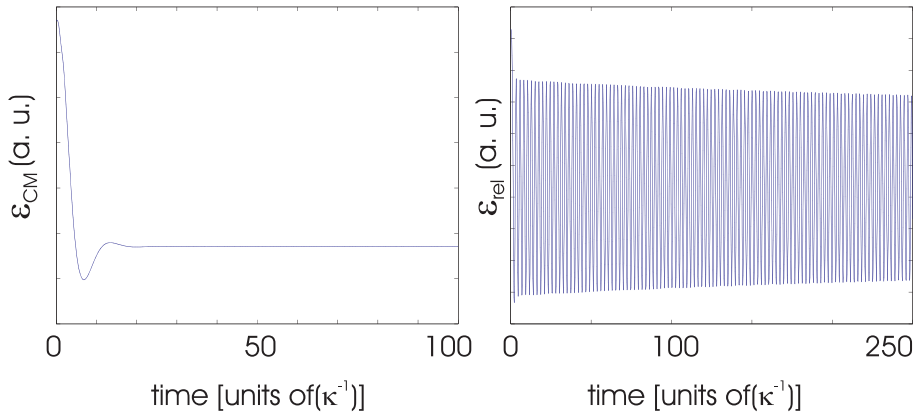

FIGURE 22. $NU_0 = 2\kappa$, $\kappa = 1$. Overdamped CM-oscillation (left) and almost undamped relative oscillation (right).

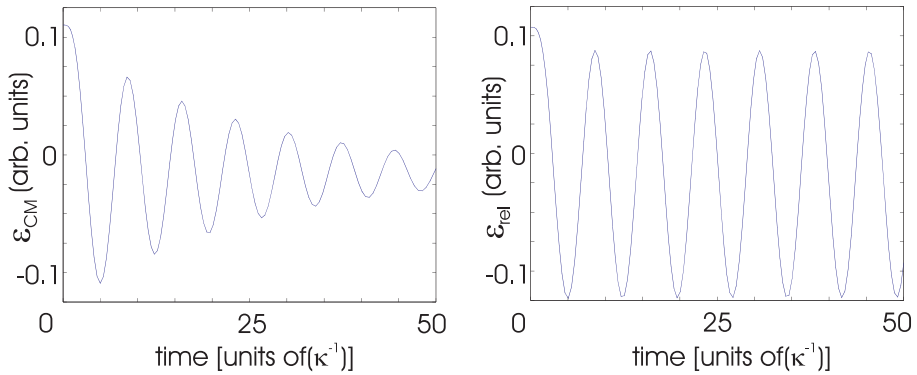

FIGURE 23. $NU_0 = 0.2\kappa$, $\kappa = 1$. Damped CM-oscillation (left) and relative oscillation (right).

Figs. 22 and 23 show widely differing damping rates for the different mode types due to cavity-induced friction. The numerical solution shows that the CM-mode is overdamped already for $NU_0 = 2\kappa$. $NU_0 < \kappa$ would have to be chosen in order to have enough time to operate the quantum gate. Hence the optimal parameters for cooling ($NU_0 \approx \kappa$) and for the operation of a quantum gate ($NU_0 < \kappa$) do not coincide. Future work should clarify how this can be changed using atoms with a more complicated level structure allowing e. g. dark states with respect to the light field.

3.5. Publication 1: Cold atoms in a high-Q ring cavity

Cold atoms in a high-Q ring cavity

Markus Gangl and Helmut Ritsch

Institut für Theoretische Physik, Universität Innsbruck,
Technikerstr. 25, A-6020 Innsbruck, Austria.

Abstract:
We investigate the coupled dynamics of N two-level atoms in the field of a weakly pumped multimode high-Q cavity. While the field mode amplitudes are coupled by the atoms depending on their positions, the motion of the atoms is influenced by the radiation pressure and dipole force induced by the total intracavity field. In the strong coupling regime, where the atom field coupling g dominates the atomic and cavity decay rates (Γ, κ) strong correlations between the atoms themselves and between the atoms and the light field build up. For suitable operating conditions an efficient motional cooling of the atoms occurs. At the example of two atoms coupled to two counterpropagating modes in a ring cavity, we show that this can lead to a strong binding force between atoms trapped at a large distance at different antinodes of the cavity field.
PACS number(s): 32.80.Pj, 42.50.Vk, 42.50.Lc

Published as Physical Review A **61**, 043405 (2000).

3.5.1. Introduction

Cavity-QED, i.e. the coupled quantum dynamics of a few atoms and field modes, has been a subject of intense research for several decades. The modified radiative properties of atoms inside optical cavities have already been studied back in 1946 by Pourcel [23] and a vast amount of theoretical and experimental effort was devoted to variations of the Jaynes-Cummings model. However, only recently with the availability of very cold atomic sources in connection with high-Q cavities [4, 5, 6] the dynamical aspects of the atomic motion (forces) inside a cavity field have been studied. In a series of papers by Parkins and co-workers [26, 27, 28] and ourselves [1, 2, 29, 30] many interesting properties of the motional dynamics of a single atom in a single high-Q cavity have been revealed and partly also have been experimentally confirmed [31, 32]. Extensions to two and more atoms have been discussed in some detail as well [29, 30]. In a recent paper Hemmerich [24] pointed out that a system of several atoms coupled to two counterpropagating modes in a ring cavity could provide for a new possibility to realize quantum logic gates similar to ion trap systems [25]. Here we will generalize our previous models to N atoms commonly interacting with M nearly degenerate cavity modes. In principle these could be various transverse modes in a quasi-planar or quasi-spherical cavity or various propagating modes in a ring cavity or several crossed cavities. This leads to a mode coupling which strongly depends on the momentary atomic positions implying effects such as phase locking and amplitude redistribution. Hence the total field reflects the atomic positions, which could be monitored by analysing the transmitted field. For cold moving atoms the intracavity field creates of course significant position dependent forces which in turn then modify the atomic motion. This can lead to energy exchange between atomic motion and the field as well as between the motion of different atoms. Besides such average forces, spontaneous emission, cavity decay and pumping will also create random forces yielding momentum diffusion and field intensity fluctuations. We will investigate and discuss several aspects of this rather involved dynamics in the following steps:

In section II we extend our previously developed simple classical model of a massive dipole in a high-Q cavity to N particles coupled to M modes and discuss a few basic aspects. Some of the key new physical properties of this system are then discussed in section III at the example of a two-level atom interacting with two quantized running waves inside a weakly driven ring cavity. We present the equations of motion for the two cavity modes in the good-cavity regime ($\Gamma \gg \kappa$) and calculate the average forces and momentum diffusion. We show the emergence of a new friction force which is based on the position-dependent phase of the intracavity field and compare it to the Sisyphus-type force arising in a standing-wave cavity. In section IV we study the collective dynamics of N atoms inside the two mode ring cavity and dicuss the strong motional correlations, which build up during the cooling process due to the cavity-mediated interaction.

3.5.2. Classical N-atom and M-mode model

Let us consider N linearly polarizable particles of mass m sitting at positions x_n coupled to M nearly degenerate weakly driven cavity modes with mode functions $u_m(\vec{x})$ and decay rates κ. In close analogy to Ref.[29] we then find the following equations for the mode amplitudes $\alpha_l(t)$ and induced atomic dipole moments $s_n(t)$, where $\beta(\vec{x},t)$ is the polarization density.

$$\dot{\alpha}_l(t) = (i\Delta_c - \kappa)\alpha_l(t) + i\frac{\omega_P}{2}\beta_l(t) + \eta_l \tag{45}$$

$$\beta_l(t) = \int dV \beta(\vec{x},t) u_l^*(\vec{x})$$

$$\beta(\vec{x},t) = \sqrt{\frac{2}{\hbar\omega_P\epsilon_0 V}} \sum_{n=1}^{N} s_n(t)\delta^3(\vec{x}-\vec{x}_n)$$

$$\dot{s}_n(t) = (i\Delta_a - \Gamma)s_n(t) + \frac{ie^2}{2\omega_P m}\sqrt{\frac{\hbar\omega_P}{2\epsilon_0 V}} \sum_{m=1}^{M} \alpha_m(t) u_m(\vec{x}_n), \tag{46}$$

where $\Delta_a = \omega_P - \omega_0$ is the detuning between pump and atom and 2Γ denotes the spontaneous emission width of the atomic excited state. We will assume the same driving frequency ω_P and decay rate κ for all modes. Assuming weak excitation and sufficiently large damping Γ, we can adiabatically eliminate the polarization and obtain

$$\dot{\alpha}_l(t) = -(\kappa - i\Delta_c)\,\alpha_l(t) - (\gamma_0 + iU_0) \sum_{n=1}^{N}\sum_{m=1}^{M} V_{ml}(\vec{x}_n)\alpha_m(t) + \eta_l \tag{47}$$

where the induced effective mode frequency shifts U_0 and dampings γ_0 are given by

$$U_0 = \frac{\Delta_a}{\Gamma^2 + \Delta_a^2} g^2 \tag{48}$$

$$\gamma_0 = \frac{\Gamma}{\Gamma^2 + \Delta_a^2} g^2 \tag{49}$$

$$V_{ml}(\vec{x}_n) = u_m(\vec{x}_n) u_l^*(\vec{x}_n) \tag{50}$$

where we have defined $g^2 = e^2/4\epsilon_0 m V$.

On the one hand we see that through the term $V_{ml}(\vec{x}_n)$ we get a position dependent mode coupling induced by the atoms, which leads to dynamical phase locking. On the other hand the induced optical dipole force on the n-th particle is then just proportional to the total intensity gradient and depends on the relative field phases. This yields the following equations of motion:

$$\dot{\vec{p}}_n(t) = -U_0 \left(\vec{\nabla} \left| \sum_{m=1}^{M} \alpha_m u_m(\vec{x}) \right|^2 \right) \Bigg|_{\vec{x}=\vec{x}_n} \tag{51}$$

$$\dot{\vec{x}}_n(t) = \vec{p}_n(t)/m. \tag{52}$$

Hence we see that different particles and modes will exhibit a strongly correlated motion. Obviously if all particles sit at the nodes or antinodes of the self consistent steady state solution of the field, all the forces vanish and we get a steady state for the motion of the atoms. Depending on the signs of the detunings this state can also be stable against small perturbations and we get a set of collective vibrational modes for the atoms. The excitation of a single particle will hence spread out over the whole system building up well defined particle and mode correlations. As the field modes are damped through their own losses κ and the position dependent photon scattering rate γ_0, the system evolution is non conservative and energy is extracted or fed into the particle motion. So besides optical trapping, there is also the possibility of cooling. The analysis of the time evolution of the field will thus provide ample information on the particles positions and motions.

3.5.3. Atoms in a ring cavity

Let us now proceed to a more refined description of the dynamics but reduce the complexity a bit. First let us study a single two-level atom moving in the field of two frequency-degenerated counterpropagating plane running wave modes $u_+(x), u_-(x)$ inside a ring cavity. Here we include incoherent processes like spontaneous emission (Γ) and cavity decay (κ) in our model via coupling to external reservoirs. For simplicity we consider only the atomic motion along the axis of the cavity and use a so called semiclassical approach for the center of mass dynamics, where only the expectation values of the atomic position and velocity enter our equations. This can be expected to be valid as long as the energy connected to the equilibrium temperature $k_B T$ is much larger than the recoil energy $E_R = \hbar^2 k^2/2m$, so that the atomic coherence length is much smaller than a wavelength. Each cavity mode is assumed to be driven with a monochromatic field of frequency ω_P at pump rates η_+, η_-. These simplifications now provide for the possibility to discuss some key aspects of the motional mode coupling in a largely analytically solvable model. A graphic scheme representing our model is shown in fig. 24.

The intracavity field E can be split into the positive and negative frequency parts and written as

$$\begin{aligned} \vec{E}(X,t) &= \vec{E}^{(+)}(X,t)e^{-i\omega_P t} + \vec{E}^{(-)}(X,t)e^{i\omega_P t} \\ \vec{E}^{(+)}(X,t) &= \mathcal{E}\left(a_+(t)e^{ikX} + a_-(t)e^{-ikX}\right)\vec{e}_z \\ \vec{E}^{(-)} &= \left(\vec{E}^{(+)}\right)^\dagger, \end{aligned} \tag{53}$$

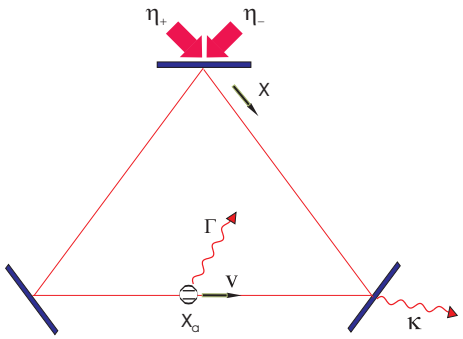

FIGURE 24. Two-level atom moving in a weakly driven ring cavity with losses from spontaneous emission Γ and cavity decay κ.

where $\mathcal{E} = \sqrt{\frac{\hbar\omega_P}{2\epsilon_0 V}}$ is the electric field per photon and $a_{+,-}$ denotes the photon annihilation operator of the $(+,-)$-mode. The Hamiltonoperator governing the unitary evolution of our system using dipole and rotating-wave approximation in a frame rotating with the pump frequency ω_P then reads ($\hbar = 1$):

$$\begin{aligned} H &= H_0 + H_{AC} + H_P \\ H_0 &= -\Delta_a \sigma^\dagger \sigma^- - \Delta_c \left(a_+^\dagger a_+ + a_-^\dagger a_- \right) \\ H_{AC} &= g \left(a_+^\dagger \sigma^- e^{-ikX} + \sigma^\dagger a_+ e^{ikX} \right) + g \left(a_-^\dagger \sigma^- e^{ikX} + \sigma^\dagger a_- e^{-ikX} \right) \\ H_P &= -i\eta_- \left(a_- - a_-^\dagger \right) - i\eta_+ \left(a_+ - a_+^\dagger \right), \end{aligned} \tag{54}$$

where the atomic and cavity detunings are defined as $\Delta_c = \omega_P - \omega_C$ and $g = -d_{eg}\mathcal{E}$ is the atom-field coupling, which is assumed to be equal for both modes (i.e. we assume the same polarization and geometry for both modes). In order to properly describe also the incoherent part of the system dynamics, we have to include reservoirs and deal with the master equation for the reduced atom-field density operator ρ. Using standard quantum optics assumptions and methods one gets:

$$\begin{aligned} \dot{\rho} &= -\frac{i}{\hbar}[H, \rho] + \left(\mathcal{L}_A + \mathcal{L}_{C_+} + \mathcal{L}_{C_-} \right) \rho \\ \mathcal{L}_A \rho &= -\Gamma \left(\sigma^\dagger \sigma^- \rho(t) - 2\sigma^- \rho(t) \sigma^\dagger + \rho(t) \sigma^\dagger \sigma^- \right) \\ \mathcal{L}_{C_\pm} \rho &= -\kappa \left(a_\pm^\dagger a_\pm \rho(t) - 2 a_\pm \rho(t) a_\pm^\dagger + \rho(t) a_\pm^\dagger a_\pm \right). \end{aligned} \tag{55}$$

As a first instructive step, let us write down the corresponding equations for the expectation values of the atomic and mode operators

$$\begin{aligned}
\langle \dot{a}_+ \rangle &= (i\Delta_c - \kappa)\langle a_+ \rangle - ige^{-ikx_a}\langle \sigma^- \rangle + \eta_+ \\
\langle \dot{a}_- \rangle &= (i\Delta_c - \kappa)\langle a_- \rangle - ige^{ikx_a}\langle \sigma^- \rangle + \eta_- \\
\langle \dot{\sigma}^- \rangle &= (i\Delta_a - \Gamma)\langle \sigma^- \rangle + 2ig\left(e^{ikx_a}\langle \sigma_z a_+ \rangle + e^{-ikx_a}\langle \sigma_z a_- \rangle\right)
\end{aligned} \tag{56}$$

which indeed look very similar to Eqs. 46 obtained in the previous section. However, we have a hierarchic coupling to products of higher operator number, which of course prevents a simple direct solution. As we will primarily investigate the strong-coupling regime with very weak pumping, we will truncate our Hilbert space $\mathcal{H} = \{|g,0,0\rangle, |g,1,0\rangle, |g,0,1\rangle, |e,0,0\rangle\}$ to states of one quantum of excitation at most. It can be easily shown, that in this regime products of system operators factorize [33],

$$\begin{aligned}
\langle a_\pm^\dagger a_\pm \rangle &= \langle a_\pm^\dagger \rangle \langle a_\pm \rangle, \\
\langle \sigma_z a_\pm \rangle &= -\frac{1}{2}\langle a_\pm \rangle,
\end{aligned} \tag{57}$$

which of course greatly simplifies the problem. Note that similar factorization can be performed, if one assumes the fields to be in a coherent state of sufficient amplitude. This property is, however, not exactly preserved during time evolution and hence only approximately valid. Nevertheless, for most of the properties discussed in the following, the results turn out to be very similar.

In this case the expectation value of the force operator $f \equiv \langle F \rangle$ in the semiclassical limit is then given by [14]

$$\begin{aligned}
f &= \langle -\frac{d}{dX} H_{AC} \rangle \\
&= -g\left(\langle a_+^\dagger \sigma^- \rangle \frac{d}{dx} e^{-ikx} + \langle \sigma^\dagger a_+ \rangle \frac{d}{dx} e^{ikx}\right)\Big|_{x=x_a} - \\
&\quad g\left(\langle a_-^\dagger \sigma^- \rangle \frac{d}{dx} e^{ikx} + \langle \sigma^\dagger a_- \rangle \frac{d}{dx} e^{-ikx}\right)\Big|_{x=x_a}
\end{aligned} \tag{58}$$

Again we assume weak atomic excitation and that the internal atomic time-scale is much faster than the external and the cavity time-scale, so that we can eliminate the excited atomic state to obtain

$$\langle \sigma^- \rangle_{ss} = \frac{ig}{i\Delta_a - \Gamma}\left(e^{ikx_a}\langle a_+ \rangle + e^{-ikx_a}\langle a_- \rangle\right) \tag{59}$$

Inserting this into the equations for the mode amplitudes we find

$$\langle \dot{a}_\pm \rangle = (-\kappa - \gamma_0 + i(\Delta_c - U_0))\langle a_\pm \rangle - (\gamma_0 + iU_0)\langle a_\mp \rangle e^{\mp 2ikx_a} + \eta_\pm, \tag{60}$$

where (61)

$$\gamma_0 = \frac{\Gamma}{\Gamma^2 + \Delta_a^2} g^2 \text{ and } U_0 = \frac{\Delta_a}{\Gamma^2 + \Delta_a^2} g^2.$$

Note that we now have a mode coupling of fixed absolute value, whose phase depends on the atomic position. In the steady state this will hence lead to a position dependent phase locking of the two fields. This is different from a standing-wave cavity, where the field geometry is independent of the atomic positions [1]. The force acting on the atom can be split into two different contributions as follows:

$$\begin{aligned} f &= f_{rp} + f_{dip} \\ f_{rp} &= 2\hbar k\gamma_0 \left(\langle a_+^\dagger a_+ \rangle - \langle a_-^\dagger a_- \rangle \right) \\ f_{dip} &= 2\hbar k U_0 i \left(\langle a_+^\dagger a_- \rangle e^{-2ikx_a} - \langle a_-^\dagger a_+ \rangle e^{2ikx_a} \right) \end{aligned} \tag{62}$$

The first part f_{rp} proportional to the photon scattering rate γ_0 has a rather simple interpretation as the sum of the two radiation pressure forces independently induced by the two counterpropagating modes. For a balanced situation it gives no average contribution as in a standing wave, but relative intensity fluctuations will induce extra diffusion. Note that in contrast to free space the amplitude of the modes is of course affected by the atom inside the cavity. The second part f_{dip} can be rewritten as $-U_0 \langle \frac{d}{dX} E^{(-)} E^{(+)} \rangle \mid_{x=x_a}$, and thus is proportional to the total intracavity intensity gradient. This contribution to the total force creates an effective optical potential and is identified as the dipole force. For the case of an atom at rest we can explicitly calculate the steady state field amplitudes and obtain:

$$\begin{aligned} \langle a_+ \rangle &= \frac{\left(-\kappa - \gamma_0 + i\left(\Delta_c - U_0\right)\right)\eta_+ + \left(\gamma_0 + iU_0\right)\eta_- e^{-2ikx_a}}{\left(\kappa + 2\gamma_0 + i\left(2U_0 - \Delta_c\right)\right)\left(i\Delta_c - \kappa\right)} \\ \langle a_- \rangle &= \frac{\left(-\kappa - \gamma_0 + i\left(\Delta_c - U_0\right)\right)\eta_- + \left(\gamma_0 + iU_0\right)\eta_+ e^{2ikx_a}}{\left(\kappa + 2\gamma_0 + i\left(2U_0 - \Delta_c\right)\right)\left(i\Delta_c - \kappa\right)} \end{aligned} \tag{63}$$

This can be inserted in Eqs. 62 so that we end up with

$$\begin{aligned} f_{rp} = & \frac{2\hbar k\gamma_0}{\left(\kappa^2 + \Delta_c^2\right)\left(\left(2\gamma_0 + \kappa\right)^2 + \left(2U_0 - \Delta_c\right)^2\right)} \\ & \Big[\left(\eta_+^2 - \eta_-^2\right)\left(\kappa^2 + 2\kappa\gamma_0 - 2\Delta_c U_0 + \Delta_c^2\right) - \\ & 4\eta_+\eta_-\left(U_0\kappa + \gamma_0\Delta_c\right)\sin 2kx_a \Big] \\ f_{dip} = & \frac{4\hbar k U_0}{\left(\kappa^2 + \Delta_c^2\right)\left(\left(2\gamma_0 + \kappa\right)^2 + \left(2U_0 - \Delta_c\right)^2\right)} \\ & \Big[\eta_+\eta_-\left(\kappa^2 + 2\kappa\gamma_0 - 2\Delta_c U_0 + \Delta_c^2\right)\sin 2kx_a + \\ & \left(\eta_+^2 - \eta_-^2\right)\left(U_0\kappa + \gamma_0\Delta_c\right) \Big] \end{aligned} \tag{64}$$

Let us now study the two instructive special cases of one-sided (3.5.4) and of symmetric pumping (3.5.5).

3.5.4. One-sided pumping

In the first case we set $\eta_- > 0, \eta_+ = 0$, so that there will be no light in the counterpropagating mode initially. During the interaction time photons are scattered by the atom into the empty mode. As this is in part a coherent process, it gives rise to a standing wave structure on top of the injected running wave field inside the cavity (second term on the r.h.s of eq. 65) as one finds:

$$\langle \dot{E}^{(+)} \rangle = (-\kappa + i\Delta_c) \langle E^{(+)} \rangle - 2 (\gamma_0 + iU_0) \langle E^{(+)} \rangle \mid_{x=x_a} \cos k (x - x_a) + \eta_- e^{-ikx} \tag{65}$$

Obviously for a fixed atom the phase of these ripples depends on the atomic position. Hence if these modulations do not have a simple maximum or minimum at the atomic position, the atom will see a field intensity gradient and a force. This explains the surprising result of a non-zero contribution of the dipole force acting on the atom even for single sided pump. Note that the steady state force for single sided pump is position-independent, as one can expect from the translational symmetry of the setup. Surprisingly it turns out that depending on the chosen detunings, the atom can sit on either side of a field maximum, yielding a force along or opposite to the radiation pressure force, which of course always points along the injected field. Interestingly a sufficiently slow moving atom will drag the standing wave along with its motion. Hence it feels a constant acceleration (its like surfing on a self created co-moving wave). Elaborating this picture a bit further, one finds that for a faster moving atom there will be a time-lag in the self-adjustment of the cavity field to the atomic position and the relative atom field position gets velocity dependent. For a certain limiting velocity the atom will sit in a co-moving potential minimum and no longer feel the dipole force. Hence within certain limitations one gets a final atomic velocity independent of the initial velocity.

Note that the very same mechanism also provides for a strong long distance atom-atom interaction, as the co-moving wave can be felt by any other atom somewhere in the cavity. We will elaborate on this in more detail in section 3.5.6.

3.5.5. Symmetric pumping

The second typical case which we discuss here is symmetric pumping $\eta_- = \eta_+ \equiv \eta$, where the external fields create a standing wave with fixed phase inside the cavity. As can be seen from eq. 66 the presence of the atom will lead to a spatial shift of this standing wave phase in steady state.

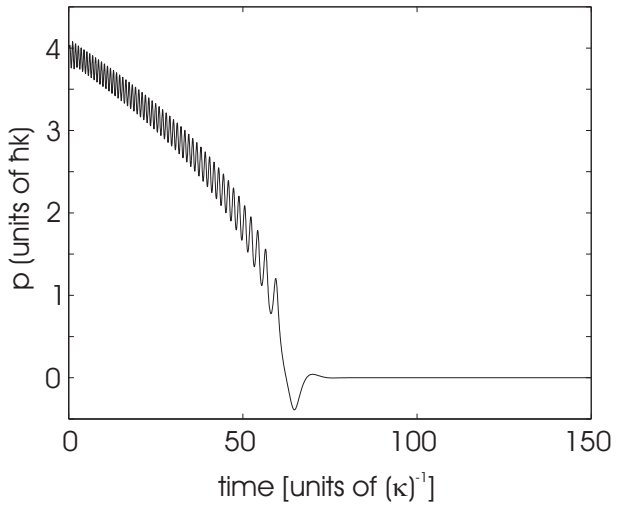

FIGURE 25. The atom is cooled while moving along the cavity standing wave until its kinetic energy gets so low that it is trapped in a potential well where it is finally damped to $p = 0$. $\Gamma = 3\kappa$, $g = 5\kappa$, $\Delta_a = 10\kappa$, $\Delta_c = 0$, $\eta_+ = \eta_- = \kappa = 1$.

$$\langle E^{(+)} \rangle = \frac{2\eta}{\kappa - i\Delta_c} \cos kx - \frac{2\left(\gamma_0 + iU_0\right)}{\kappa - i\Delta_c} \frac{2\eta \cos kx_a}{\kappa + 2\gamma_0 - i\left(\Delta_c - 2U_0\right)} \cos k\left(x - x_a\right) \tag{66}$$

Similarly to the nonvanishing dipole force for single sided pumping the radiation pressure force does not vanish for symmetric pumping due to the position dependent redistribution of light. This can be viewed as follows: If the atoms sits at a certain position where the dipole force pushes it to the right, photons will be scattered from the right to the left running wave, which will acquire a higher steady state intensity. Hence at this point the radiation pressure forces will not cancel any more yielding a net force towards left opposing the dipole force. This behaviour is strongly different from the free space standing wave case and induces extra friction and diffusion. Note that all average forces on the atom only cancel if the atom is at a node or antinode of the injected wave. Comparing the cooling force on a moving atom with the one in a standing wave cavity we see that the atom is much more rapidly slowed down to zero momentum in the ring cavity as compared to a standing wave cavity (see fig. 25) as the motional coupling influences the position and the intensity of the intracavity field.

a. Friction force on a slowly moving atom. As can be expected the forces are modified for a slowly moving atom. Fortunately, it is straightforward to find an expression for the friction coefficient, i. e., the linear velocity dependence of the force for small velocities ($kv \ll \kappa$) due to the cavity dynamics. We expand the

field operators in the form $\langle a_\pm \rangle \approx \langle a_\pm^0 \rangle + kv/\kappa \langle a_\pm^1 \rangle$ and insert this into eqs. 60 to compare equal orders of v. To first order in v we get:

$$f_{dip} = f_{dip}^0 + \alpha_{dip} v$$
$$f_{rp} = f_{rp}^0 + \alpha_{rp} v.$$

This force acting on the atom can now be averaged over one wavelength. In a symmetrically pumped cavity we get of course $\overline{f_{dip}^0}^\lambda = \overline{f_{rp}^0}^\lambda = 0$ and

$$\overline{\alpha_{dip}}^\lambda = \frac{8\hbar k^2 \eta^2 U_0 \beta}{\left(\kappa^2 + \Delta_c^2\right)^2 \left(\left(\kappa + 2\gamma_0\right)^2 + \left(2U_0 - \Delta_c\right)^2\right)^2} \left(\kappa^2 + 2\kappa\gamma_0 - 2\Delta_c U_0 + \Delta_c^2\right) \quad (67)$$

$$\overline{\alpha_{rp}}^\lambda = \frac{-8\hbar k^2 \eta^2 \gamma_0 \beta}{\left(\kappa^2 + \Delta_c^2\right)^2 \left(\left(\kappa + 2\gamma_0\right)^2 + \left(2U_0 - \Delta_c\right)^2\right)^2} 2\left(U_0 \kappa + \gamma_0 \Delta_c\right) \quad (68)$$

where

$$\beta = 2\gamma_0 \left(\gamma_0^2 + U_0^2 - \left(\kappa + \gamma_0\right)^2 + \left(\Delta_c - U_0\right)^2\right) + 4U_0 \left(\kappa + \gamma_0\right)\left(\Delta_c - U_0\right).$$

The total friction coefficient is then $\overline{\alpha_{tot}}^\lambda = \overline{\alpha_{dip}}^\lambda + \overline{\alpha_{rp}}^\lambda$.

Figs. 26 and 27 show numerical examples for the dipole and the radiation pressure friction force in a symmetrically pumped cavity. Comparing these figures with our previous results in a standing wave cavity [2] the most striking difference is the far-stretched appearance of the dipole friction force with respect to Δ_a. We think that this difference is due to the fact that the physical origin of the dipole force lies in the spatial shift of the intracavity field, while in a standing wave cavity the physical origin is the position dependence of the amplitude of the cavity field. Furthermore we see again that the areas of cooling and heating are interchanged in the dipole and the radiation pressure friction force, as we have already mentioned before for an atom at rest in a symmetrically pumped cavity. In Fig. 28 we show the sum of both friction forces. It can be seen that the areas of cooling and heating are the same as for the dipole friction force because the radiation pressure friction force approaches zero faster than the dipole force for large detunings. Interestingly even for very large atomic detunings $\Delta_a \approx 100\Gamma$, where spontaneous emission is strongly reduced, one can get a significant cavity induced friction force on the atom. This implies a much larger capture range for the injected particles and could prove important for applications in cooling molecules.

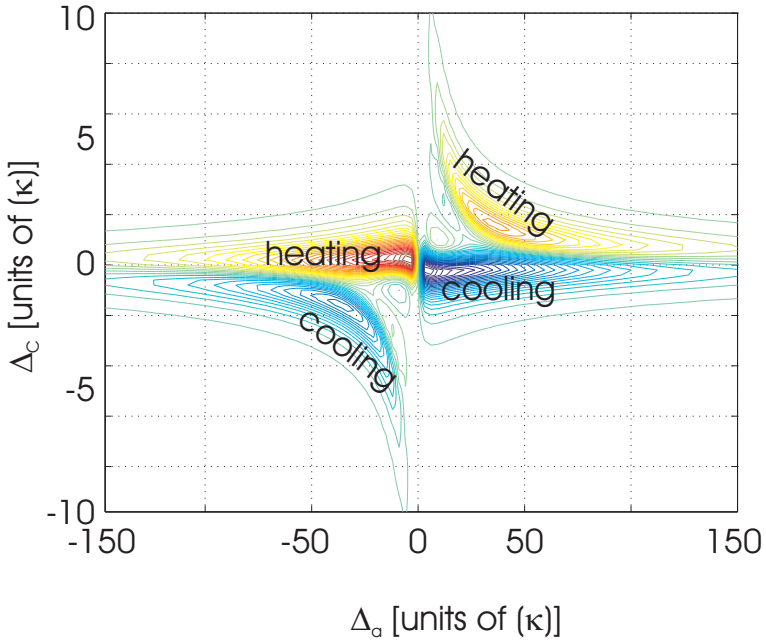

FIGURE 26. Contour plot of the dipole friction force. $\eta_- = \eta_+ = \kappa = 1$, $g = 5\kappa$, $\Gamma = 3\kappa$.

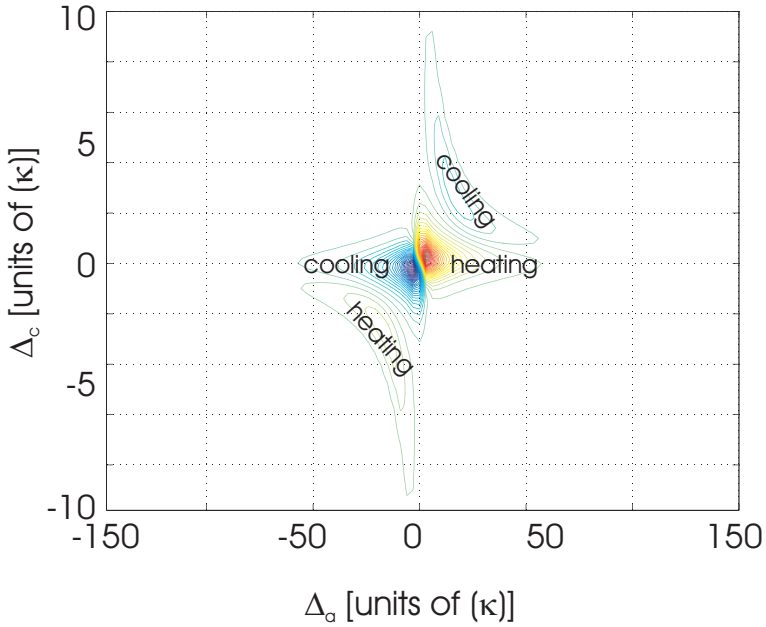

FIGURE 27. Contour plot of the radiation pressure friction force. $\eta_- = \eta_+ = \kappa = 1$, $g = 5\kappa$, $\Gamma = 3\kappa$.

b. Analytic solutions for a moving atom. An interesting limit of this model is the case of a large atomic detuning Δ_a, so that spontaneous emission plays almost no role in the dynamics. Setting $\gamma_0 = 0$ and assuming that the velocity of the atom

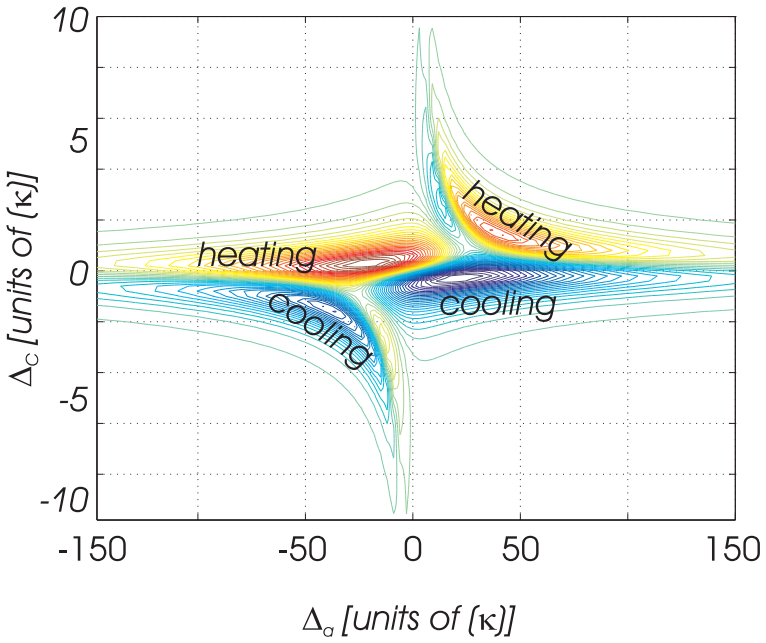

FIGURE 28. Contour plot of the total friction force. $\eta_- = \eta_+ = \kappa = 1$, $g = 5\kappa$, $\Gamma = 3\kappa$.

does not change much as it moves over a wavelength, we can find analytic expressions for the time evolution of the fields $\langle a_\pm \rangle$ for arbitrary initial conditions.

$$\begin{aligned}
\langle a_+ \rangle = e^{-(\kappa + iU_0 + ikv)t} \Bigg[& \left(C_+(t) + \langle a_+(0) \rangle\right) \left(\cos \Omega t + i \frac{kv}{\Omega} \sin \Omega t \right) - \\
& \left(C_-(t) + \langle a_-(0) \rangle\right) i \frac{U_0}{\Omega} e^{-2ikx_0} \sin \Omega t \Bigg] \\
\langle a_- \rangle = e^{-(\kappa + iU_0 - ikv)t} \Bigg[& \left(C_-(t) + \langle a_-(0) \rangle\right) \left(\cos \Omega t - i \frac{kv}{\Omega} \sin \Omega t \right) - \\
& \left(C_+(t) + \langle a_+(0) \rangle\right) i \frac{U_0}{\Omega} e^{2ikx_0} \sin \Omega t \Bigg]
\end{aligned} \tag{69}$$

with

$$
\begin{aligned}
C_+(t) = & \frac{iU_0 e^{-2ikx_0}\eta_-}{(\kappa + iU_0 - ikv)^2 + \Omega^2}\left\{\frac{e^{(\kappa+iU_0-ikv)t}}{\Omega}\cdot\ldots\right. \\
& \left.\ldots\left[(\kappa + iU_0 - ikv)\sin\Omega t - \Omega\cos\Omega t\right] + 1\right\} + \\
& \frac{\eta_+}{(\kappa + iU_0 + ikv)^2 + \Omega^2}\left\{e^{(\kappa+iU_0+ikv)t}\left[(\kappa + iU_0 + ikv)\cdot\ldots\right.\right. \\
& \left.\left.\ldots\left(\cos\Omega t - \frac{ikv}{\Omega}\sin\Omega t\right) + \Omega\left(\sin\Omega t + \frac{ikv}{\Omega}\cos\Omega t\right)\right] - (\kappa + iU_0 + 2ikv)\right\} \\
C_-(t) = & \frac{iU_0 e^{2ikx_0}\eta_+}{(\kappa + iU_0 + ikv)^2 + \Omega^2}\left\{\frac{e^{(\kappa+iU_0+ikv)t}}{\Omega}\cdot\ldots\right. \\
& \left.\ldots\left[(\kappa + iU_0 + ikv)\sin\Omega t - \Omega\cos\Omega t\right] + 1\right\} + \\
& \frac{\eta_-}{(\kappa + iU_0 - ikv)^2 + \Omega^2}\left\{e^{(\kappa+iU_0-ikv)t}\cdot\ldots\right. \\
& \left.\ldots\left[(\kappa + iU_0 - ikv)\left(\cos\Omega t + \frac{ikv}{\Omega}\sin\Omega t\right) + \right.\right. \\
& \left.\left.\Omega\left(\sin\Omega t - \frac{ikv}{\Omega}\cos\Omega t\right)\right] - (\kappa + iU_0 - 2ikv)\right\} \qquad (70)
\end{aligned}
$$

and $\Omega = \sqrt{(kv)^2 + U_0^2}$. We see that the atom dynamically couples the right to the left running wave, yielding a velocity dependent periodic redistribution of the light between the two directions in form of damped Rabi-oscillations of the mode amplitudes with a coupling $U_0 e^{-2ikx_a}$ and an effective detuning of kv. Of course due to momentum conservation this yields a periodically alternating force on the atom. If these forces are non-negligible we get rather complicated combined atom field oscillations.

c. Steady-State Momentum Distribution and Temperature. Lets now turn back to the kinetic equations for the atom. Besides the average forces discussed above we find force fluctuations, which lead to momentum diffusion. Similar to the case of laser cooling in a free standing wave field we can calculate the total diffusion coefficient $D_{tot} = D_{rp} + D_{dip}$ for an atom at rest [2]. Averaged over one wavelength $\overline{D_{tot}}^{\lambda}$ with $\eta_+ = \eta_- \equiv \eta$ we find

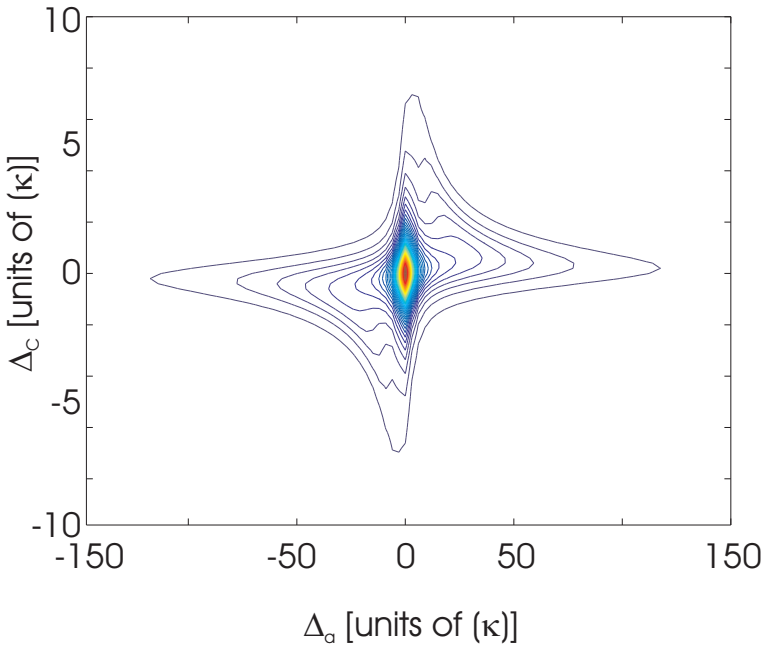

FIGURE 29. Contour plot of the total diffusion averaged over one wavelength. $\eta = \kappa = 1$, $g = 5\kappa$, $\Gamma = 3\kappa$.

$$\overline{D_{tot}}^{\lambda} = \frac{8\hbar^2 k^2 \left(\kappa + \gamma_0\right)\left(U_0^2 + \gamma_0^2\right)}{\left(\kappa^2 + \Delta_c^2\right)\left(\left(2\gamma_0 + \kappa\right)^2 + \left(2U_0 - \Delta_c\right)^2\right)}\eta^2. \tag{71}$$

Using eq. 66 the total averaged diffusion coefficient can be written as

$$\overline{D_{tot}}^{\lambda} = \left(2\hbar k\right)^2 \left(\kappa + \gamma_0\right) \frac{U_0^2 + \gamma_0^2}{\kappa^2 + \Delta_c^2} \overline{\left(\langle E^{(-)} E^{(+)} \rangle \mid_{x=x_a}\right)}^{\lambda}, \tag{72}$$

showing contributions proportional to the square of the potential U_0 and the photon scattering rate γ_0.

In the regime where the incoherent scattering is much smaller than the coherent one ($\gamma_0 \ll \kappa, U_0$) the dominant contribution to $\overline{D_{tot}}^{\lambda}$ comes from the redistribution of photons between the two cavity modes at a rate $U_0^2/\kappa \overline{\left(\langle E^{(-)} E^{(+)} \rangle \mid_{x=x_a}\right)}^{\lambda}$.

Note that this quantity is rather important in context with possible applications in quantum information processing, as it gives the heating rate out of the atomic groundstate and limits the coherence time of the vibrational atomic motion.

With the friction coefficients calculated earlier, it is easy to estimate the steady state temperature using

$$k_B T = \frac{\overline{D_{tot}}^{\lambda}}{-\overline{\alpha_{tot}}^{\lambda}} \tag{73}$$

In the regions where we have cooling for slow velocities, the denominator of expression 73 is positive (e. g. $U_0 > 0$, $\Delta_c = 0$), and we get the following rather simple expression for the final temperature:

$$k_B T = \hbar \left(\kappa + \gamma_0\right) \frac{\left(U_0^2 + \gamma_0^2\right)\left(\left(\kappa + 2\gamma_0\right)^2 + 4U_0^2\right)}{2U_0\kappa\left(\kappa\gamma_0 + 2\gamma_0^2 + 2U_0^2\right)} \tag{74}$$

Considering $k_B T$ as a function of U_0 we see that $k_B T \approx \hbar U_0 \left(1 + \gamma_0/\kappa\right)$ for $\kappa, \gamma_0 \ll U_0$. The final temperature is thus limited by the single photon light shift. Hence we cannot expect effective trapping in the single photon case. Nevertheless for a good cavity the temperature can be much below the Doppler limit.

3.5.6. N atoms in a ringcavity

Lets us now further extend our model and discuss the N-atom dynamics in such a twomode ring cavity. Fortunately for a given set of atoms at positions $\{x_n\}$ the field equations for the mode amplitudes are modified only in a very simple manner, namely we have to replace $e^{\mp 2ikx_a}$ by the collective sum $\sum_{n=1}^{N} e^{\mp 2ikx_n}$ and γ_0, U_0 by $N\gamma_0, NU_0$

$$\langle \dot{a}_\pm \rangle = \left(-\kappa - N\gamma_0 + i\left(\Delta_c - NU_0\right)\right)\langle a_\pm \rangle - \left(\gamma_0 + iU_0\right)\langle a_\mp \rangle \sum_{n=1}^{N} e^{\mp 2ikx_n} + \eta_\pm \tag{75}$$

Analogously to eq. 65 we can write the equation of motion for the positive part of the electric field operator as

$$\langle \dot{E}^{(+)} \rangle = \left(-\kappa + i\Delta_c\right)\langle E^{(+)} \rangle - 2N\left(\gamma_0 + iU_0\right) \sum_{n=1}^{N} \langle E^{(+)} \rangle \mid_{x=x_n} \cos k\left(x - x_n\right) + 2\eta \cos kx \tag{76}$$

a. Two atoms. It is rather instructive to write this down explicitly for two atoms using center of mass $x_{CM} = \frac{x_1 + x_2}{2}$ and relative $x_{rel} = x_2 - x_1$ coordinates

$$\langle \dot{a}_\pm \rangle = \left(-\kappa - 2\gamma_0 + i\left(\Delta_c - 2U_0\right)\right)\langle a_\pm \rangle - 2\left(\gamma_0 + iU_0\right)\langle a_\mp \rangle e^{\mp 2ikx_{CM}} \cos(kx_{rel}) + \eta_\pm \tag{77}$$

We see that the coupling between the atoms and the cavity field has now a position-dependent magnitude as well as a position-dependent phase. For both atoms at rest it is easy to calculate the steady state values of the cavity modes

$$\langle a_+\rangle = \frac{\left[-\kappa - 2\gamma_0 + i\left(\Delta_c - 2U_0\right)\right]\eta_+ + 2\left(\gamma_0 + iU_0\right)\eta_- e^{-2ikx_{CM}}\cos(kx_{rel})}{\Big\{\left[\kappa + 4\gamma_0\cos^2(kx_{rel}/2) + i\left(4U_0\cos^2(kx_{rel}/2) - \Delta_c\right)\right]\cdot\ldots}$$
$$\ldots\left[-\left(\kappa + 4\gamma_0\sin^2(kx_{rel}/2)\right) + i\left(\Delta_c - 4U_0\sin^2(kx_{rel}/2)\right)\right]\Big\}$$
$$\langle a_-\rangle = \frac{\left[-\kappa - 2\gamma_0 + i\left(\Delta_c - 2U_0\right)\right]\eta_- + 2\left(\gamma_0 + iU_0\right)\eta_+ e^{2ikx_{CM}}\cos(kx_{rel})}{\Big\{\left[\kappa + 4\gamma_0\cos^2(kx_{rel}/2) + i\left(4U_0\cos^2(kx_{rel}/2) - \Delta_c\right)\right]\cdot\ldots}$$
$$\ldots\left[-\left(\kappa + 4\gamma_0\sin^2(kx_{rel}/2)\right) + i\left(\Delta_c - 4U_0\sin^2(kx_{rel}/2)\right)\right]\Big\} \tag{78}$$

Similarly to the previous section we get for the stationary forces on atoms 1(2)

$$f_{rp_1} = f_{rp_2} = 2\hbar k\gamma_0\left(\langle a_+^\dagger a_+\rangle - \langle a_-^\dagger a_-\rangle\right)$$
$$f_{dip_{1(2)}} = 2\hbar kU_0 i\left(\langle a_+^\dagger a_-\rangle e^{-2ikx_{1(2)}} - \langle a_-^\dagger a_+\rangle e^{2ikx_{1(2)}}\right) \tag{79}$$

Inserting the stationary values of $\langle a_\pm\rangle$ the forces on each atom can be written as

$$f_{rp_{1(2)}} = \frac{2\hbar k\gamma_0}{\Big\{\left[(\kappa + 4\gamma_0\cos^2(kx_{rel}/2))^2 + ((4U_0\cos^2(kx_{rel}/2) - \Delta_c))^2\right]\cdot\ldots}$$
$$\ldots\left[\left(\kappa + 4\gamma_0\sin^2(kx_{rel}/2)\right)^2 + \left(\Delta_c - 4U_0\sin^2(kx_{rel}/2)\right)^2\right]\Big\}$$
$$\Big\{\Big[\left(\kappa + 2\gamma_0\right)^2 + \left(\Delta_c - 2U_0\right)^2 - 4\left(\gamma_0^2 + U_0^2\right)\cos^2(kx_{rel})\Big]\left(\eta_+^2 - \eta_-^2\right) -$$
$$8\eta_+\eta_-\left(U_0\kappa + \gamma_0\Delta_c\right)\cos(kx_{rel})\sin(2kx_{CM})\Big\}$$
$$f_{dip_{1(2)}} = \frac{2\hbar kU_0}{\Big\{\left[(\kappa + 4\gamma_0\cos^2(kx_{rel}/2))^2 + ((4U_0\cos^2(kx_{rel}/2) - \Delta_c))^2\right]\cdot\ldots}$$
$$\ldots\left[\left(\kappa + 4\gamma_0\sin^2(kx_{rel}/2)\right)^2 + \left(\Delta_c - 4U_0\sin^2(kx_{rel}/2)\right)^2\right]\Big\}$$
$$\Big\{\left(\eta_+^2 + \eta_-^2\right)2\sin 2kx_{rel}\left[U_0\left(\Delta_c - 2U_0\right) - \gamma_0\left(\kappa + 2\gamma_0\right)\right] -$$
$$\left(\eta_+^2 - \eta_-^2\right)4\cos^2 kx_{rel}\left(\gamma_0\Delta_c + U_0\kappa\right) +$$
$$\eta_+\eta_-\left[16\left(\gamma_0^2 + U_0^2\right)\cos 2kx_{CM}\sin kx_{rel} -\right.$$
$$\left.2\sin 2kx_{1(2)}\left(\kappa^2 + 4\kappa\gamma_0 + \Delta_c^2 - 4U_0\Delta_c\right)\right]\Big\} \tag{80}$$

One clearly can see the strong influence of the atoms on each other even if they are at large distance. It is only the relative position in the standing wave which is important. In particular the extension of one atom out of its equilibrium position is immediately felt by the second atom. Similar effects occur as well for the friction

forces yielding to collective cooling or heating, as outlined in some examples in the next section.

b. Linear chain of N atoms. Let us return to the general case of N atoms interacting with the two cavity modes. Of special interest to the field of quantum information is the linear chain of atoms interacting with each other via the cavity standing wave. This can be realized e. g. by using blue detuned light ($\Delta_a > 0, \Delta_c = 0$) because then atoms are low-field seekers and will get trapped around the nodes of the intracavity field. A transversal confinement could be achieved by adding laser beams to create a conventional free-space lattice in the remaining two dimensions perpendicular to the cavity axis.

With the atoms located around the nodes of the standing wave we can expand their positions by $kx_n = \frac{2n-1}{2}\pi + \epsilon_n$, where the ϵ_n denote small displacements around the potential minima which implies $e^{\mp 2ikx_n} \approx -(1 \mp 2i\epsilon_n)$ Defining the center of mass of the small displacements by $\epsilon_{CM} = \frac{1}{N}\sum_{n=1}^{N} \epsilon_n$ one can calculate the back-action of the atoms on the cavity field, neglecting the cavity dynamics as a first step. This means that the cavity field is assumed to adjust itself immediately to the atomic positions. By making this crude assumption we neglect of course any damping of the motion of the atoms by friction forces.

Our calculation shows that the only effect of the atoms is to shift the cavity standing wave pattern at an amount of $\mu\epsilon_{CM}$

$$\langle E^{(-)} E^{(+)} \rangle = \frac{4\eta^2}{\kappa^2 + \Delta_c^2} \cos^2 (kx - \mu\epsilon_{CM}) \tag{81}$$

where the factor μ has been defined as

$$\mu = \frac{2U_0 N (2U_0 N - \Delta_c)}{\kappa^2 + (2U_0 N - \Delta_c)^2} \tag{82}$$

Note that μ approaches unity very fast for increasing $U_0 N$. Furthermore the better the cavity (smaller κ) the more the intensity gets shifted.

To establish the equations of motion for the trapped atoms we calculate the dipole force acting on the n-th atom by taking the local derivatives of the potential at the site of each atom.

$$\begin{aligned} f_{dip,n} &= -U_0 \langle \frac{d}{dx} E^{(-)} E^{(+)} \rangle \mid_{x=x_n} \\ &= \frac{4\hbar k U_0 \eta^2}{\kappa^2 + \Delta_c^2} \sin 2 (kx_n - \mu\epsilon_{CM}) \end{aligned} \tag{83}$$

Expanding eq. 83 around the field nodes gives the equation of motion for the displacement of atom n under the influence of the dipole force in the form

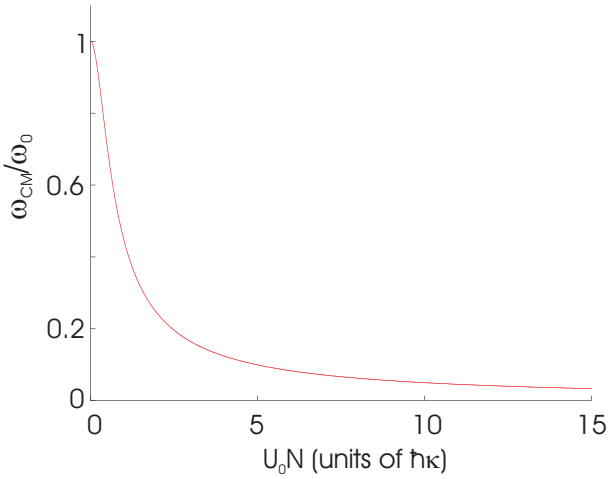

FIGURE 30. Frequency of the vibrational center of mass mode normalized to ω_0 over U_0N. $\Delta_c = 0$, $\kappa = 1$.

$$\ddot{\epsilon}_n + \omega_0^2 \epsilon_n = \omega_0^2 \mu \epsilon_{CM} \tag{84}$$

$$\omega_0^2 = \frac{8\hbar k^2 U_0 \eta^2}{m\left(\kappa^2 + \Delta_c^2\right)} \tag{85}$$

ω_0 is just the usual oscillation frequency of an atom in a harmonic potential of strength $U_0\eta^2/\left(\kappa^2 + \Delta_c^2\right)$. Using a normal mode ansatz in the form $\epsilon_n = \beta_n e^{i\omega_n t}$ we can investigate the mode spectrum of the collective oscillations. There are two different kinds of modes: Type (1) fulfills $\sum_{n=1}^{N} \beta_n = 0$ which means that there is no center of mass motion. The frequencies of all of these modes are degenerate and just given by $\omega_n^2 = \omega_0^2$, i. e. each particle oscillates in a well defined phase with the others so that the individual effects of the dragging of the field by each of the atoms cancels in sum. If we perturb one of the atoms all of the others will immediately feel this through a shift of their potential wells with the change of the center of mass. Of course, the more atoms we have, the smaller this shift induced by a single atom gets. This can be explicitly seen by looking at the second mode type (2), which satisfies $\sum_{n=1}^{N} \beta_n = N\beta_n$ (center of mass mode) with frequency $\omega_{CM}^2 = \omega_0^2\left(1 - \mu\right)$. Note that as μ approaches unity, the cavity field follows the motion of the center of mass without delay. The atoms always stay in the vicinity of the field nodes and consequently ω_{CM} approaches zero because the restoring force goes to zero. (see fig. 30).

With this the general motion of the n-th atom can be written as a linear superposition of the two types of modes:

$$\epsilon_n(t) = \left(\epsilon_n(0) - \epsilon_{CM}(0)\right)\cos\omega_0 t + \epsilon_{CM}(0)\cos\omega_{CM} t \tag{86}$$

Of course incoherent effects in this motion will lead to damping/amplification of these vibrational excitations. We have done some numerical studies to include

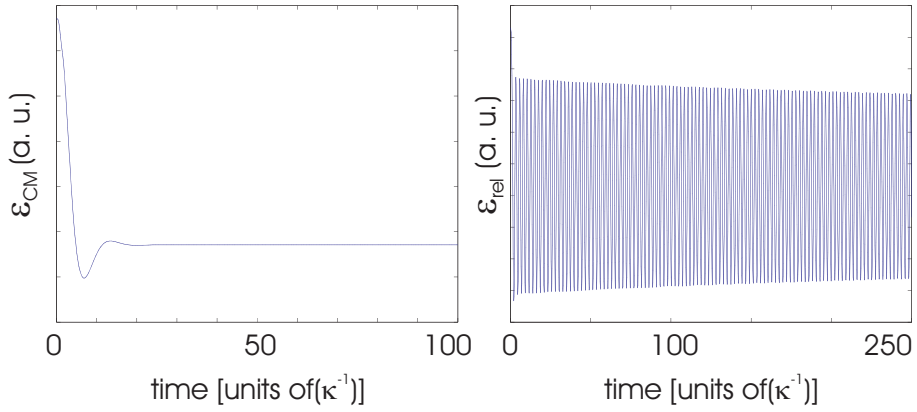

FIGURE 31. $NU_0 = 2\kappa$, $\kappa = 1$. Overdamped CM-oscillation (left) and almost undamped relative oscillation (right).

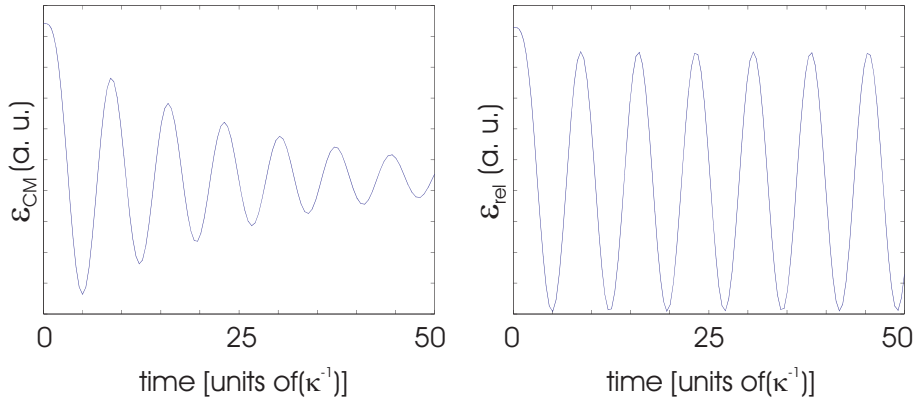

FIGURE 32. $NU_0 = 0.2\kappa$, $\kappa = 1$. Damped CM-oscillation (left) and relative oscillation (right).

the effect of the friction forces on either type of oscillation. In general one finds that the modes with no center of mass oscillation ($\omega_n^2 = \omega_0^2$) are only very weakly damped, while the center of mass motion ($\omega_{CM}^2 = \omega_0^2\,(1-\mu)$) is in the overdamped regime even for moderate values of $U_0 N$ (see fig. 31). Only for small values of the effective potential the CM-mode shows real oscillations as shown in Fig. 32. (In these simulations we have restricted ourselves to 2 atoms although the results stay basically the same for a larger number of atoms.) Fast damping of the center of mass mode means of course that the two atoms get perfectly anticorrelated in their motion around the field node. This of course implies exchange of energy and phase information at a large distance.

For a discussion on how the coupled dynamics between the atoms could be used to implement a quantum information processing scheme see the work of Hemmerich [24].

3.5.7. Conclusion

The generalization of the dynamical cavity cooling model to more modes and more atoms provides for a great deal of new physics with several possible applications to multiparticle cooling, the study of nonlocal interactions and the controlled generation and manipulation of classical and quantum correlations. This could provide for an interesting basis for many experiments in quantum information processing and quantum measurement theory. As compared to ion traps one could expect much higher particle numbers and higher coupling strengths at the expense of a shorter effective interaction time and less control of interaction strength. Of course a generalization to a Bose-condensate as atomic medium[34, 71] seems straightforward, although technically not so simple. In this context the dipole force acceleration mechanism discussed in section 2 could provide for a controlled fast output coupling mechanism. Another important application seems to be the cooling and trapping of molecules with a sufficient effective optical dipole moment in the spirit of stochastic cooling via the induced cavity dynamics. As the cooling occurs without the need of spontaneous emission one can avoid the problems connected to the vibrational spreading of the wavefunction in this case.

Acknowledgments

We thank A. Hemmerich, C. Lamprecht and T. Calarco for stimulating discussions. This work has been supported by the Austrian Fonds zur Förderung der wissenschaftlichen Forschung under grant numbers P13435 and F1512 as part of the Spezialforschungsbereich Quantenoptik.

3.6. Publication 2: Single-atom detection in high-Q multimode cavities

Single atom detection in high-Q multimode cavities

P. Domokos, Markus Gangl and Helmut Ritsch

Institut für Theoretische Physik, Universität Innsbruck,
Technikerstr. 25, A-6020 Innsbruck, Austria.

Abstract:
We propose a new method for detecting and monitoring the motion of a single atom in high Q optical resonators based on the position sensitive dispersive coupling of different field modes. Using sufficient atom-field detuning the irreversible evolution of the internal state and external motion of the atom can be kept small still allowing for a fast and reliable detection. As an implementation we discuss the case of two counterpropagating modes in a microscopic ring resonator with spatially localized output coupler. The analytical estimates yielding 100% signal contrast for suitable parameters are then confirmed by numerical solution of the time dependent equations for the coupled atom-cavity dynamics.
PACS number(s): 32.80.Pj, 42.50.Vk

Published as Optics Communications **185**, 115 (2000).

3.6.1. Introduction

Versatile manipulation of the center-of-mass dynamics of neutral atoms is today possible with a large variety of techniques. Trapping, guiding, and coherent splitting of atomic wave packets have been demonstrated in numerous experiments. The miniaturization of these components and their combination into matter wave circuits, yielding powerful devices on compact "atom chips" [35, 36], is in progress. Efficient and practical methods for state-selective and non-destructive detection of a single neutral atom are actually in high demand.

The basic concept of single-atom detection consists in coupling the atom strongly enough to another physical "sensor" system. An apparent choice for the sensor is the electromagnetic field where the atom acts as an absorber or phase shifter. The possibility of nondestructive measurement rests on this latter, dispersive effect [37]. By sufficiently detuning the radiation frequency from the atomic resonance, the atom cannot absorb photons from the field, and remains in an only weakly perturbed internal state. Spontaneous emission, and the accompanying "noisy" mechanical effects (heating) are reduced in nonresonant interaction. However, the phase of the detection field is shifted providing the basis of the detection schemes [38].

As the dipole moment of a single atom is rather small the atom field interaction has to be enhanced by "recycling" the radiation field in a resonator with high Q quality factor. Several cavity QED experiments have recently been performed [39, 40, 31, 41] where the following scheme was implemented. A weak stationary field is sustained in a single-mode of a microscopic cavity driven resonantly by an external monochromatic source. The outgoing field transmitted through the cavity is monitored by a photodetector. An atom, crossing the cavity, shifts the cavity mode frequency out of resonance, which yields a dip in the transmitted signal. Changes as large as two orders of magnitude of the resonant transmission have been observed for a single atom passage [39].

In this paper we study a generalization of these single-atom detection schemes to multimode cavities. As a particular example we use circulating fields in a ring cavity (or alternatively the evanescent fields of a high Q-microsphere) and propose a detection mechanism based on dispersive atom-field interaction. The underlying physical mechanism here is the atom-induced phase-locking between different cavity modes. The scheme is shown to be suitable for monitoring the atomic motion inside the cavity and the signal can be simply read off an intensity sensitive detector. There is no need for the homodyne technique as it were the case for monitoring the instantaneous phase shift induced by the atom in a single-mode cavity [42]. The necessary conditions for detecting a single atom are elucidated and compared to that of previously demonstrated schemes using a single-mode cavity. The central condition turns out to be invariant under an appropriate rescaling of the detuning and the photon number. Thus the proposed scheme allows for an operation regime involving large photon numbers where high temporal resolution can be achieved. After deriving some analytical estimates for fringe contrast and detection time scales we investigate the system behaviour in different regimes by numerical simulations.

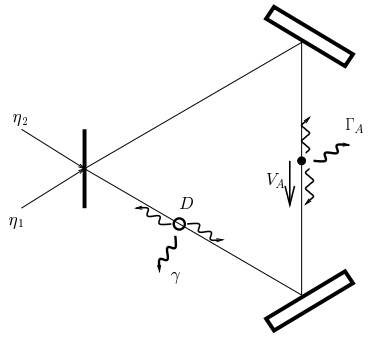

FIGURE 33. The multimode cavity detection scheme. The field in the ring cavity comprises two running wave modes (pumping η_1 and η_2, respectively). In the cavity, there is a moving atom A and an absorber (D, "detector") in a fixed position. Both the atom A and the detector D couples the counterpropagating modes by backscattering. In addition, they introduce extra losses via spontaneous emission into lateral modes.

3.6.2. Semiclassical model

Let us consider a ring cavity in which the radiation field is composed of two, frequency and polarization degenerate, counterpropagating running wave modes. We can restrict the model to one spatial dimension without masking any important physical effect relevant to the detection problem. The positive frequency part of the electric field can be decomposed into

$$E^{(+)}(r,t) = i \sum_{\nu=1,2} \sqrt{\frac{\hbar\omega_c}{2\epsilon_0 V}} \vec{e}\alpha_\nu(t) f_\nu(r) e^{-i\omega t} \ , \tag{87}$$

where the mode functions read

$$f_1(r) = e^{ikr} \ , \quad f_2(r) = e^{-ikr} \ . \tag{88}$$

The slowly varying amplitudes $\alpha_1(t)$ and $\alpha_2(t)$ have been defined in a rotating frame fixed to the frequency ω of the driving fields. This external source can be, in general, detuned from the mode frequency, by $\Delta_C = \omega - \omega_c$.

The internal dynamics of a two-level atom located in the ring cavity is governed by the Hamiltonian

$$\hat{H}_A = -\hbar\Delta_A \hat{\sigma}_+ \hat{\sigma}_- - i\hbar g \sum_{\nu=1,2} (\alpha_\nu f_\nu(R_A)\hat{\sigma}_+ - \alpha_\nu^* f_\nu^*(R_A)\hat{\sigma}_-) \ , \tag{89}$$

where the detuning is $\Delta_A = \omega - \omega_A$, $g = \sqrt{\omega_c/2\epsilon_0\hbar V}\ |\vec{ed}|$ is the coupling constant to the field modes and R_A is the position of the atom. The operators $\hat{\sigma}_\pm$ are the usual raising and lowering atomic operators. We restrict our study to nonresonant interaction, i. e., when the detuning Δ_A is much larger than the coupling constant g. The atom is subject to incoherent relaxation processes described by the damping rate Γ_A. We assume that the evolution of the internal atomic state can be adiabatically eliminated in the nonresonant regime. Then the atom is, at any instant, in a quasi

stationary state determined by the actual position R_A, with induced dipole

$$\langle\hat{\sigma}_-\rangle = -\frac{iU_0+\Gamma_0}{g(1+s)}\sum_{\nu=1,2}\alpha_\nu f_\nu(R_A)\ , \tag{90}$$

where

$$U_0 = \frac{g^2\Delta_A}{\Delta_A^2+\Gamma_A^2}\ , \quad \Gamma_0 = \frac{g^2\Gamma_A}{\Delta_A^2+\Gamma_A^2}\ . \tag{91}$$

The saturation s is given by $s = n_A/n_{sat}$, i. e. , the ratio of the photon number $n_A = |\sum\alpha_\nu f_\nu(R_A)|^2$ at the atomic position and the saturation photon number $n_{sat} = (\Delta_A^2+\Gamma_A^2)/2g^2$. For nondestructive detection of the atom, the saturation s must be kept low in order to avoid spontaneous emission.

The two modes contribute to the atomic polarization, and in turn, the atomic dipole can radiate into both of them. Hence, the atom (or any other particle with suitable dipole moment) couples two different field modes via photon scattering. This model can easily be generalized to more contributing modes, e. g. , modes with different transverse profile.

The total system under study is schematically depicted in Figure 1. The specific feature is that it contains an output coupler at a fixed localized position. It is a resonant (unsaturated) medium absorbing photons from the cavity field, and can therefore be viewed as a detector. Indeed, we will use the fluorescence of this "absorber" simply modeled by another two-level atom as our measurement signal. The effective coupling constant, analogous to Γ_0 in Eq. (91), is denoted by γ here.

The dynamics of the field amplitudes under the effects of the moving atom, the absorber, and the pumping is described by the coupled equations [3]

$$\begin{aligned}
\dot{\alpha}_1 = \eta_1 + & \left[i\left(\Delta_C - \frac{U_0}{1+s}\right) - \left(\kappa+\gamma+\frac{\Gamma_0}{1+s}\right)\right]\alpha_1 \\
& - \left[\frac{iU_0+\Gamma_0}{1+s}e^{-2ikR_A} + \gamma e^{-2ikR_{abs}}\right]\alpha_2\ , \\
\dot{\alpha}_2 = \eta_2 + & \left[i\left(\Delta_C - \frac{U_0}{1+s}\right) - \left(\kappa+\gamma+\frac{\Gamma_0}{1+s}\right)\right]\alpha_2 \\
& - \left[\frac{iU_0+\Gamma_0}{1+s}e^{2ikR_A} + \gamma e^{2ikR_{abs}}\right]\alpha_1\ ,
\end{aligned} \tag{92}$$

where R_{abs} is the position of the absorber. The external pumping is represented by the terms $\eta_{1,2}$. It is normalized such that the stationary photon number is η^2/κ^2 in a resonantly driven empty cavity. Let us remark that in general there can be additional mechanisms coupling the counterpropagating modes of a ring cavity (impurities, mirror imperfections, etc.). For the sake of simplicity, we assume these effects negligible compared to the coupling by the atom.

Equations (92) contain the atomic position which is itself a variable. The atomic motion will be treated semiclassically, which is a good approximation as far as the coherence length of the atomic de Broglie wavepacket is much shorter than the

wavelength of the radiation field. In this case, the center–of–mass dynamics follows

$$\begin{aligned}\dot{R}_A &= V_A \ , \\ \dot{V}_A &= -2V_{rec}\frac{iU_0}{1+s}\left(\alpha_1\alpha_2^* e^{2ikR_A} - c.c.\right) + 2V_{rec}\frac{\Gamma_0}{1+s}\left(|\alpha_1|^2 - |\alpha_2|^2\right) \ , \end{aligned} \tag{93}$$

where $V_{rec} = \hbar k/m$ is the recoil velocity. In the latter equation, the first term represents the dipole, the second term is the radiation force exerted on the atom. These equations do not contain the effect of random recoils accompanying a spontaneous emission. To be consistent with this simplification, only the low saturation regime, $s \ll 1$, can be studied with this semiclassical model.

Equations (92) and (93) form a closed set of equations. A general analytical solution has not been found so far. We will solve this semiclassical model numerically. Beforehand, we calculate the steady–state solution, which gives us an insight in the dynamics for slow enough atoms.

3.6.3. Competitive phase–locking

Let us suppose that the atom moves on a given trajectory and the field can adapt itself to the actual atomic position. The condition for the validity of this approach can roughly be formulated as $\kappa > kV_A$, i. e. , on the time scale of the field relaxation the atomic displacement is small compared to the wavelength.

The steady–state solution of Eqs. (92) can easily be determined in the low saturation regime. Note that the saturation parameter s depends on the field amplitude variables, yielding a nonlinear set of equations in (92). However, we concentrate only on the nonresonant interaction regime between the atom and the fields. In this regime the saturation is automatically small, $s \ll 1$, and it is a reasonable approximation to neglect the saturation effect. The resulting set of coupled equations is linear, having the solution

$$\begin{pmatrix}\alpha_1\\ \alpha_2\end{pmatrix} = \frac{1}{D}\mathbf{A}\begin{pmatrix}\eta_1\\ \eta_2\end{pmatrix} \tag{94}$$

where

$$\mathbf{A} = \begin{pmatrix} -i(\Delta_C - U_0) + \kappa + \gamma + \Gamma_0 & -(iU_0 + \Gamma_0)e^{-2ikR_A} - \gamma e^{-2ikR_{abs}} \\ -(iU_0 + \Gamma_0)e^{2ikR_A} - \gamma e^{2ikR_{abs}} & -i(\Delta_C - U_0) + \kappa + \gamma + \Gamma_0 \end{pmatrix}, \tag{95}$$

and $D = \det \mathbf{A}$. We will need the modulus of the determinant, which is

$$|D|^2 = \left(\kappa^2 + 2\kappa\gamma + U_0^2\right)^2 + 4U_0^2\gamma^2\cos^2 2k(R_A - R_{abs}) \ . \tag{96}$$

In the detection scheme the radiation field is far detuned from the atomic resonance, $\Delta_A \gg \Gamma_A$, in order to avoid significant atomic excitation. As a consequence $U_0 \gg \Gamma_0$, and it is enough to take into account the dispersive coupling of the modes in the nondiagonal terms of matrix $\mathbf{A}$. In the diagonal terms, Γ_0 is generally negligible compared to κ. The detuning Δ_C can be chosen so that one atom pulls the mode frequency into resonance with the pump, i. e. $\Delta_C = U_0$.

Let us suppose that only mode 1 is pumped ($\eta_1 = \eta$, $\eta_2 = 0$). Then the electric field is composed of three terms:

$$E^{(+)}(r) \propto \frac{\eta}{D}\left[(\kappa+\gamma)e^{ikr} - iU_0 e^{ik(2R_A - r)} - \gamma e^{ik(2R_{abs}-r)}\right] . \tag{97}$$

The first term originates directly from the source. The second and the third terms represent the backscattered waves radiated coherently by the atom and by the absorber, respectively. The double-centered backscattering gives rise to an interference in the backward propagating field. As both mode 1 and mode 2 can then be excited, a standing wave pattern is superimposed on the pumped, running wave field. The position of the fringes is determined by the competitive phase locking exerted by the atom and by the absorber. The absorber alone would fix the phase so as it sits in a node (seeks for minimum field). However, the atom can drag the standing wave pattern and induce a modulation in the local field at the absorber position.

The absorber scatters photons at a rate 2γ. Thus the measurable signal, the fluorescence, is proportional to the local intensity at the absorber. The intensity $E^{(-)}E^{(+)}(R_{abs})$ can be expressed in terms of photon number as

$$n_{abs} = \frac{|\eta|^2}{\kappa^2}\frac{\kappa^2(\kappa^2+U_0^2)}{|D|^2}\left[1 + \frac{2\kappa U_0}{\kappa^2+U_0^2}\sin 2k(R_A - R_{abs})\right] , \tag{98}$$

where $|\eta|^2/\kappa^2$ gives the order of magnitude of the photon number in the cavity, the next factor is close to one in most of the cases of interest, and finally, the last term describes the oscillations as a function of the atom–detector distance. The oscillatory behaviour of the local intensity n_{abs} permits to measure the position (modulo λ) and the velocity of the atom. As the atom moves along the cavity axis, the detector experiences a perfect contrast corresponding to the maximum visibility 1, if $\kappa = U_0$. This is evidently a sufficient condition for an *ideal* detection scheme. The visibility does not depend on the absorption rate γ. Since the atom shifts the cavity mode frequency by U_0, the above condition implies a frequency shift comparable to the mode linewidth, i. e. , the possibility of detection also by using the frequency pulling effect.

Let us analyze how to maximize the single–atom dispersive effect described by U_0. In the nonresonant regime $\Delta_A \gg \Gamma_A$, one can approximate $U_0 \approx g^2/\Delta_A$. To increase U_0, the field must be tuned as close to the resonance as possible without exciting the atom. Suppose that the excited state population is tolerated below a given saturation $s \ll 1$. The requirement of low saturation is necessary to avoid atomic excitation accompanied by noisy mechanical effects on the atomic motion. It is then necessary to have $n_{sat}^{-1} \approx 2g^2/\Delta_A^2 < s/n_A$ (n_A is the photon number at the atom). The largest U_0, being about $U_0^{max} \approx g\sqrt{s/n_A}$, corresponds to small photon numbers. However, if the field intensity is very low, the detection needs a long time to accumulate enough photons to reconstruct the signal induced by the atom. In the following section we present an operation regime appropriate for single-atom detection, where many photons are involved. The detuning Δ_A is very large and U_0 is considerably reduced ($U_0 \ll \kappa$ resulting in a visibility much less than 1), nevertheless, the resolution of the intensity oscillations predicted in Eq. (98) can be

fulfilled provided $g \geq \kappa/\sqrt{s}$. In this way we can detect a small phase shift of a large amplitude signal.

3.6.4. Limit of small phase shift effect

In what follows we calculate the fluorescence signal detected by the absorber in the limit of very large detunings yielding $U_0 \ll \kappa$. The expression (98) for the local field intensity at the position of the absorber can be expanded to power series of the small parameter U_0/κ. On keeping just the leading order, one gets

$$n_{abs} = \frac{|\eta|^2}{\kappa^2}(1 + 2\gamma/\kappa)^{-2}\left[1 + \frac{2U_0}{\kappa}\sin 2k(R_A - R_{abs})\right] . \tag{99}$$

In fact, the resolution of the intensity oscillations requires that the amplitude is larger than the quantum noise inherent to the radiation field. Hence, the considerably reduced visibility ($2U_0/\kappa \ll 1$) can be compensated by increasing the photon number by strong pumping $|\eta|^2$. On the other hand, the intensity is limited in order to keep the saturation s low. The intensity at the atom,

$$n_A = \frac{|\eta|^2}{\kappa^2}\left(1 + \frac{2(\kappa+\gamma)\gamma}{(\kappa+\gamma)^2+\gamma^2}\right)^{-1}\left[1 - \frac{2(\kappa+\gamma)\gamma}{(\kappa+\gamma)^2+\gamma^2}\cos 2k(R_A - R_{abs})\right] , \tag{100}$$

is at most $n = |\eta|^2/\kappa^2$. Thus the pumping is limited by $|\eta|^2/\kappa^2 \ll n_{sat}$.

Let us denote the time resolution of the detection by τ. We assume the ideal case when the detector collects all the photons scattered by the absorber (some collection efficiency could be taken into account, nevertheless it can be quite large using for example a single-molecule probe glued on a fiber tip [43]), that is $\bar{n} = n2\gamma\tau(1 + 2\gamma/\kappa)^{-2}$ photons on average. The associated quantum fluctuations, on assuming a coherent field, is approximately $\sqrt{\bar{n}}$. The amplitude of the modulation due to the atom is $4U_0/\kappa$ times the average. This signal should be larger than the intrinsic quantum noise, which leads to the criterion

$$\kappa < 2U_0\sqrt{n\kappa\tau}\,\frac{2\sqrt{2\gamma/\kappa}}{1 + 2\gamma/\kappa} . \tag{101}$$

The last fraction can be maximized to 1 by choosing $\gamma = \kappa/2$. In the limit of large detuning, $\Delta_A \gg \Gamma_A$, the maximum allowed photon number is $n \approx s\Delta_A^2/2g^2$, and $U_0 \approx g^2/\Delta_A$. From these scaling laws it follows that $\sqrt{n}U_0 \approx g\sqrt{2s}$ is independent of Δ_A. Eq. (101) can then be transformed into the general condition for observing a single atom

$$\kappa < g\sqrt{2s\kappa\tau} . \tag{102}$$

The time resolution τ of the measurement is a crucial parameter. In one hand, it is possible to accumulate the signal for long periods $\tau \gg \kappa^{-1}$. Without the atom, the absorber sits in a minimum field. Hence the presence of the atom yields an increase of the fluorescence regardless of the atomic position and motion. The detection time τ can then be as long as the interaction time which is limited by Γ_A^{-1} to avoid spontaneous atomic decay. On the other hand, owing to the large photon number in the cavity, the atomic motion modulo $\lambda/2$ along the cavity axis

could be completely mapped to the fluorescence signal. To this end, τ must be short enough to resolve that the moving atom pushes a node or an antinode of the induced standing wave pattern to the absorber. In the adiabatic limit, $\tau \approx \kappa^{-1}$ provides a sufficient temporal resolution. Then the condition (102) leads to $\kappa < g\sqrt{s}$ which, as was already shown at the end of the previous section, is equivalent to $U_0 \geq \kappa$ at very low photon numbers, $n_A \approx 1$. However, it is not always possible to choose a detuning as close to the coupling as $\Delta_A \approx 3g$ corresponding to $s \approx 0.1$. For example, this is the case when $g < \Gamma_A$, since the nonresonant excitation requires $\Gamma_A \ll \Delta_A$.

In the experiments [40, 31] using the frequency pulling effect, the observation of the atomic signal has been accomplished by increasing the time window τ. The very weak transmitted intensity collected in periods of hundreds of κ^{-1} was necessary to overcome the intrinsic noise. In fact, the operating point can be pushed towards high photon numbers in the standing-wave cavity experiments as well. Instead of applying resonant driving, the source should be detuned to have $\Delta_c \approx \kappa/\sqrt{3}$. On the slope of the Lorentzian resonance curve, even if $U_0 \ll \kappa$, a small modulation U_0 could be amplified by increasing the photon number. Apart from some numerical factor of the order of 1, the same condition (102) can be derived for detecting a single atom. Nevertheless, for both the frequency pulling and the phase-locking effect, the option of detecting the atom at a weak visibility is no longer possible when the technical noise becomes dominant.

3.6.5. Numerical solution

The complete dynamics can be solved by integrating numerically the equations (92) and (93). The numerical calculation includes also the effect of saturation. As an example we chose the $5^2S_{1/2} \leftrightarrow 5^2P_{3/2}$ transition of Rb at 780 nm. The dipole relaxation rate is $\Gamma_A = 3$ MHz, the recoil velocity is $V_{rec} = 6$ mm/s. As an initial condition for the velocity $v_A = 0.6$ m/s is taken (for comparison, the Doppler velocity characteristic of this transition is $v_D = 0.4$ m/s). We consider a cavity with $\kappa = 10^7\,\mathrm{s}^{-1}$ and $g = 4 \cdot 10^7\,\mathrm{s}^{-1}$. Note that the coupling constant is comparable with the dipole damping rate $\Gamma_A = 1.85 \cdot 10^7\,\mathrm{s}^{-1}$. However, the condition (102) is fulfilled, hence the atom could be observed in principle.

Figures 2 and 3 show the time evolution of some relevant quantities of the atom-cavity system for two different settings of the detuning and the pumping parameters. In order to get a better understanding of the dynamics, the evolution is presented on a time scale longer than required for the detection itself. In the first example (Fig. 2), the field is tuned close to the atomic resonance, $\Delta_A = 1.6 \cdot 10^8\,\mathrm{s}^{-1}$, which corresponds to $U_0 \approx \kappa$. The saturation photon number n_{sat} is about 8, thus the intracavity photon number must be kept below 1 in order to avoid atomic excitation ($\eta = 15$). In the second example (Fig. 3), the detuning Δ_A is set to $1.2 \cdot 10^9\,\mathrm{s}^{-1}$, which is very large compared to the coupling constant g. The saturation photon number is then high ($n_{sat} = 450$), which allows for pumping as many as 40 photons in the cavity ($\eta = 60$).

The local intensity at the absorber is depicted in Figs. 2a and 3a. The measurable fluorescence signal is proportional to this quantity. In the first case the signal to noise

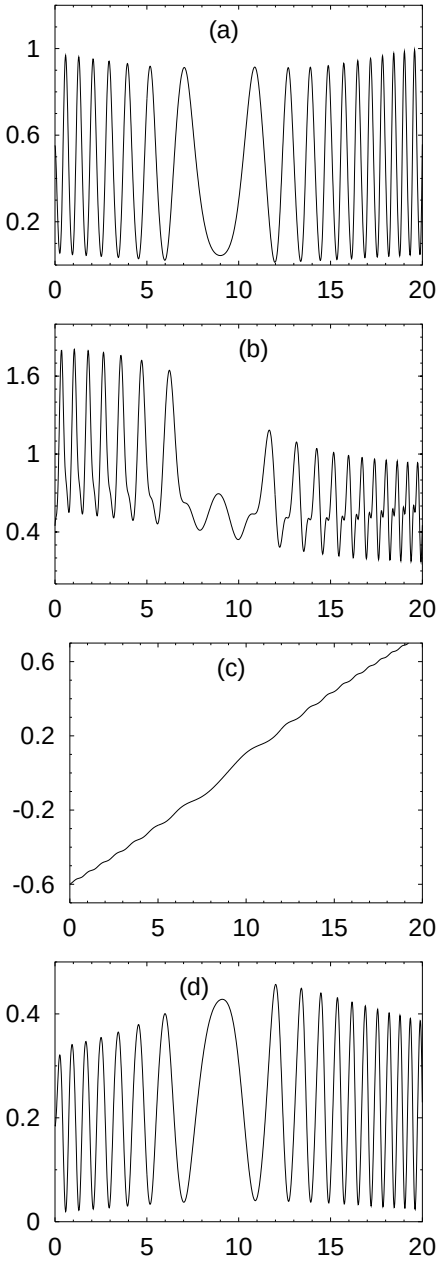

FIGURE 34. Time evolution of the atom-cavity system. Time is given in units of μs. (a) The photon number at the position of the absorber; (b) the photon number at the position of the atom; (c) the atomic velocity in m/s; (d) backscattered photon number at the output mirror. Important parameters are $\kappa = 10$, $\gamma = 18.5$, $g = 40$, $\Delta_A = 160$ (all in units of $10^6 \mathrm{s}^{-1}$), and $\eta = 15$. This setting corresponds to $\kappa = U_0$.

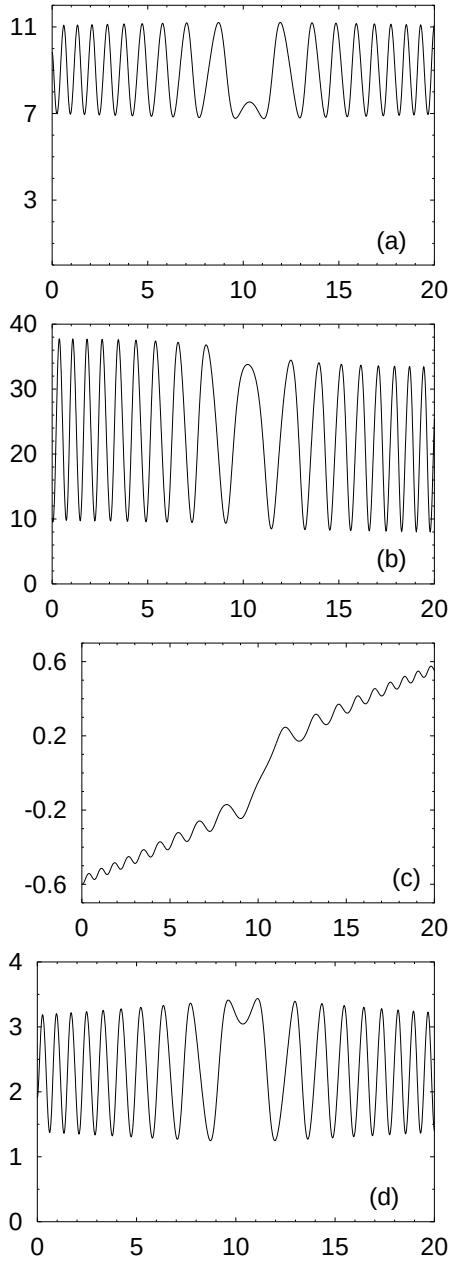

FIGURE 35. Same as Figure 2, but with $\Delta_A = 1.210^9 \mathrm{s}^{-1}$, $\eta = 60$, corresponding to the limit $\kappa \gg U_0$.

ratio is almost 1. Nevertheless, when the atom pushes an antinode to the absorber, the local intensity becomes 1 in units of photon numbers. The single photon must be detected in a time $\kappa^{-1} = 0.1\mu$s, which is a quite rigorous requirement. In the second case (Fig. 3a), the photon number at the position of the absorber oscillates around 9 with an amplitude 4. For comparison, the quantum noise limit would be only 3. The intensity at the position of the atom (Figs. 2b and 3b) exhibits strong

oscillations, however, it remains always below 1.6 and 40, corresponding to $s \approx 0.2$ and $s \approx 0.08$, respectively for the first and second case.

From Figs. 2c and 3c, representing the time evolution of the atomic velocity V_A, it becomes evident that the cavity field has an important mechanical effect on the atom. The average deceleration is due to the dipole force. It originates from the coherent redistribution of the photons between the two counterpropagating modes. Because of the single-sided pumping, the redistribution process is not balanced, hence the net force in a given direction. Let us stress that the center-of-mass dynamics of the atom is a coherent evolution. The detection introduces just a minimum irreversibility in the atomic motion, according to the low saturation parameter s. In a given setup with well defined geometrical conditions, the momentum transfered to the atom can be compensated after the detection process is accomplished.

The increase of the oscillation period in the measured signal (Figs. 2a and b) reflects the deceleration of the atom. Thus the detection also provides information *in vivo* about the atomic velocity. The visibility of the signal does not change considerably as the atomic velocity decreases. This proves that the field can follow adiabatically the center–of–mass dynamics in the entire velocity range involved. The period is 1 μm, thus the $\tau = \kappa^{-1}$ resolution is enough to monitor the atomic motion. When the atoms are injected into the cavity in a given, controlled direction, the dipole force slows down rapid atoms to the Doppler velocity range. This leads automatically to the highest possible visibility of oscillations corresponding to the adiabatic motion limit.

Finally, in Figs. 2d and 3d the photon number in the mode 2 is presented. This field results from the superposition of the fields backscattered by the atom and by the absorber, which gives rise to interference for varying distance between the two sources. The interference fringes have a very high contrast for parameter settings such as $\gamma \approx U_0$, e. g. our second example. The backscattered intensity is easily measurable from the output power. The plots 2d and 3d can be considered as alternative signals for the single–atom detection.

3.6.6. Conclusions

We presented a multimode cavity scheme for detecting a single neutral atom with imposing only a minimal irreversible evolution on its internal state and motion. The proposed scheme relies on far off resonance dispersive interaction, and is very sensitive as it locks the phase of two counterpropagating field modes in a ring cavity, without changing the total photon number. The condition for observing the atom is shown to be invariant under a properly chosen scaling of the detuning and the photon number in the cavity. When operating in the large detuning and large photon number regime, high temporal resolution can be achieved that allows for the monitoring of the atomic motion in the cavity.

Sufficient detection sensitivity can be achieved if the atom–field coupling constant g is at least a few times the mode linewidth κ. This condition requires small mode volumes and good mirrors, i. e. a microscopic ring cavity. One possible option would be the use of the degenerate counterpropagating whispering gallery modes of

a microsphere. Close to the surface of the microsphere, the evanescent field–atom coupling can be much larger than κ and the atomic linewidth Γ_A [44, 45]. Here the single–atom phase locking effect is also strong enough to dominate the coupling of the running wave modes due to the Rayleigh backscattering on impurities [46]. The absorber can be implemented by using eroded fiber tips [47] locally coupled to the sphere. The application of microspheres is also promising because they could possibly be integrated in complex atom chips [36]. These chips permit to guide cold atoms in a well controlled way and to make them collide with the evanescent field of the microsphere, which could be an experimental realization of the scheme presented in this paper.

Acknowledgments

We are grateful for useful discussions with Peter Horak, Ron Folman, Hideo Mabuchi, and Jörg Schmiedmayer. This work was supported by the Österreichischer Fonds zur Förderung der wissenschaftlichen Forschung under Projects No. 13435 and F1512 as a part of the Spezialfoschungbereich Quantenoptik. P. D. acknowledges the financial support by the National Scientific Fund of Hungary under contracts No. T023777 and F032341.

CHAPTER 4

Cavity cooling of many atoms

4.1. Scaling laws for many atoms

In the previous chapter we have shown that for a single particle strongly coupled to a high-Q optical cavity motional energy can be extracted from the particle using the dissipative dynamics of the cavity mode. We showed that cooling times much shorter than in free space and temperatures well below the Doppler limit are possible without relying on atomic spontaneous emission. In this chapter we study the possibility of applying cavity cooling to an ensemble of N atoms coupled to M modes inside a coherently driven high-Q optical resonator.

The scaling properties of this cooling scheme for many atoms depend on the temperature of the atoms. Different results are obtained for ensembles of well-trapped particles and for free particles with large kinetic energies.

Starting with a flat initial distribution of atoms in space with large kinetic energies it was shown numerically by Horak et al. [48] that the single-atom cooling time given in section 3.3 is still valid in the many-atom situation. This might be surprising at first sight but can be understood easily: Each atom leads to fluctuations in the cavity field and is influenced by the fluctuations induced by itself as well as those induced by the other atoms. Assuming a temperature $k_B T > \hbar U_0 I$ so that the atoms are not trapped, all fluctuations induced by the $N-1$ other atoms on one atom average out due to the anharmonicity of the light potential and only the atom's own fluctuations will be correlated with its motion resulting in an appreciable mechanical effect. In other words, although every atom feels all the other atoms through their influence on the cavity field it will be cooled individually with a time scale comparable to the single particle cooling time. Experimentally, however it is not possible to use the parameters of section 3.3 ($\Delta_C = -\kappa$, $MNU_0 - \Delta_C = 0$) for this optimal situation for an arbitrary number of atoms. If the same (small) value of U_0 was used in the one and N particle situation and all other parameters except N were kept constant too, the steady-state temperature would remain constant as long as $NU_0 < \kappa$. For larger N the cavity is shifted into positive detuning where the friction force changes sign and the atoms are not cooled anymore but accelerated. This shows that for the many atom case the parameters have to be rescaled such that NU_0 and the optical potential depth $\propto U_0(\eta/\kappa)^2$ are constant meaning $U_0 \propto 1/N$ and $\eta \propto \sqrt{N}$. Consequently the cooling time for N particles $\tau_{C,Cav}$(N particles) scales linearly with the number of particles

$$\tau_{C,Cav}(\text{N particles}) = N\tau_{C,Cav}(\text{1 particle}). \tag{103}$$

As soon as the atoms get cold enough ($k_BT \ll U_0 I$) so that they experience a harmonic potential correlations between the atoms build up leading to collective atomic motional modes as has been shown in section 3.5.

Numerical simulations (see sections 4.4, 4.5) and the work of Horak et al. [48]) show exactly this behaviour: As long as the atoms are hot enough not to be trapped, cooling progresses individually. After the atoms are trapped the center-of-mass component of their collective motion gets damped away rapidly and some of the atoms end up in a steady state where they do not couple to the light field any more (relative motion modes).

4.2. Experimental realization of many-atom cooling

At the moment (December 2001) an experimental group led by A. Hemmerich in Hamburg is preparing an experiment to detect collective motional modes of cold neutral atoms trapped in a high-Q optical cavity (see section 3.4 and [24]). They want to cool and trap Rb^{85} atoms loaded from a MOT in a high finesse ring resonator [49]. Rb^{85} has a recoil frequency $\omega_{Rec} = 2\pi \cdot 3.8$ kHz and an atomic dipole moment around $d = 17.37 \cdot 10^{-30}$ Cm for its 780.2 nm transition. The electric field inside the cavity has a decay rate of $\kappa = 100$ kHz and the electric field per photon $\mathcal{E} = \sqrt{\frac{\hbar\omega_P}{\epsilon_0 V}} \approx 3.44$ V/m. Together with the dipole moment this gives a Rabi frequency per photon of $g = d\mathcal{E}/\hbar \approx 2\pi \cdot 90.5$ kHz. Thus one can expect forces in the resonator that are stronger by a factor of $(2g/\kappa)^2 \approx 130$ compared to free space. For $N = 10^7$ atoms the cavity is phase-shifted by a total amount of $NU_0 = -150$ kHz which shows that $NU_0 \approx -\kappa$.

Choosing $\Delta_C = -\kappa$ and $2N|U_0| = \kappa$ one is in the optimal cooling regime and the formulas obtained in section 3.3 show that a steady-state temperature of $T_{cav} = \frac{\hbar\kappa}{2k_B} \approx 380nK$ can be reached in the resonator which is much below the Doppler limit of Rb^{85}, $T_{Dopp} = 141\mu$K and around the recoil limit $T_{Rec} = 380nK$, where our semiclassical results are not valid anymore (see next section). The cooling time for $N = 10^7$ particles is of the order of $\tau_C \approx 3.3 \cdot 10^{12} \cdot 1/(\frac{\eta}{\kappa})^2$ s. Increasing the laser intensity (as long as $sI \ll 1$) reduces the time needed and a cooling time below a second seems to be realistic.

4.3. Tight binding regime

For ultracold atoms $k_BT \ll \hbar\omega_{Rec}$ a full quantum mechanical description where the atoms are treated as a quantum gas is needed. In section 4.5 we present some of the results obtained in such a treatment. It is interesting to note that this full

quantum mechanical model gives the same qualitative results as our more semiclassical approximation of section 3.5 with the only difference that the optical potential U_0 is multiplied by a correction factor δ_{qm} equal to

$$\delta_{qm} = \sqrt{1 - \frac{\omega_{Rec}}{\omega_0}} \tag{104}$$

due to the finite width of the atomic wavefunction.

4.4. Publication 3: Collective dynamical cooling of neutral particles in a high-Q optical cavity

Collective dynamical cooling of neutral particles in a high-Q optical cavity

Markus Gangl and Helmut Ritsch

Institut für Theoretische Physik, Universität Innsbruck,
Technikerstr. 25, A-6020 Innsbruck, Austria.

Abstract:
We show that an ensemble of two-level atoms commonly coupled to a single, driven, damped high-Q cavity mode could be cooled and trapped via the correlated dynamics of cavity field and the atomic motion. For sufficiently large detuning between the atoms and the field, spontaneous emission plays no role in the dynamics and the cooling scheme can be applied to all particles with a sufficient optical dipole moment. The time scale of this collective cooling process increases with the particle number and can be optimized by suitably tailoring the pump field amplitude and frequency. The key properties of the underlying mechanism are discussed using a linearized model, where one can derive a closed set of equations for certain ensemble averages and the field. The results are then compared with N-particle dynamical simulations of the full equations.
PACS numbers:32.80.Pj,32.80.Lg,42.50.Vk

Published as Physical Review A **61**, 011402(R) (2000).

4.4.1. Introduction

Laser cooling of neutral atoms has proven very successful to obtain very cold ensembles of neutral atoms. Nevertheless there are limitations in the final phase space density and the atomic species to which it can be applied. Almost all of the optical cooling methods developed so far are linked to atomic spontaneous emission to provide for irreversible energy extraction out of the system. This creates the need of a closed optical level scheme and poses the problem of light reabsorption. Recently, we have shown that for a single particle strongly coupled to a high-Q optical cavity the dissipative dynamics of the cavity mode can be used to extract motional energy from the particle. The procedure does not rely on spontaneous emission and allows final kinetic energies well below the Doppler limit[1, 2]. In an alternative approach Raizen and coworkers[50, 51] discussed stochastic cooling of an ensemble of trapped atoms using a sequence of momentum measurements and light induced kicks. In this work we investigate the possibility to apply cavity induced dynamic cooling to an ensemble of neutral particles, which are commonly coupled to a single cavity mode via their optical dipole moment. As a first guess one could expect, that the method should not work for a large number of independent particles as they move uncorrelated. Hence their influence on the cavity mode would just cancel on average. However, we will demonstrate in this work that this argument is only partly valid and that these ideas can also be generalized to a multiparticle system on the basis of the fluctuations of ensemble averages.

According to their momentary position distribution the particles induce a certain total phase shift (i.e. refractive index) inside the mode volume, which shifts the cavity resonances. As all the particles are coupled to the same modes, the total induced frequency shift of a particular mode compared to its empty cavity value is a collective property of the particle ensemble, which contains information on the position distribution. This frequency shift determines the effective detuning between this cavity field mode and an externally applied pump laser field with fixed frequency. Hence we get the following coupled atom-field dynamics: On the one hand the average distance of the particles from the field antinodes (i.e. the points of maximal atom field coupling) influences the intracavity intensity. On the other hand the intracavity light field induces an optical potential for the atoms, which influences the particle motions and modifies their position distribution. The central idea is now to use this interplay in a controlled way to extract motional energy from the atomic cloud, without inducing spontaneous emissions or particle loss. Note that this scheme possesses a close analogy to stochastic cooling as a collective property of the ensemble (i.e. the total potential energy of the atoms) is used for a feedback mechanism onto the ensemble. In contrast to the conventional approach the feedback in our case is, however, automatically contained in the system evolution via the cavity field dynamics and does not require external control.

4.4.2. Model

Let us consider a large number N of two-level atoms with resonance frequency ω_0 and mass m interacting with a single cavity mode field $E(x,t) = \mathcal{E}(\alpha(t)exp(-i\omega_p t)+ cc)u(x)$ with eigenfrequency ω_c and amplitude $\alpha(t)$. Here $\mathcal{E}$ gives the electric field per photon. The cavity is externally driven by a laser field of amplitude η and frequency ω_P and damped with a field decay rate κ. We assume that the detuning $\Delta_a = \omega_P - \omega_0$ between the atomic transition and the field is large enough, so that we can adiabatically eliminate the upper state yielding only a small spontaneous decay rate $\gamma(x)$ and an effective optical potential $U(x)$. Following the standard procedure of adiabatic elimination of the excited atomic state, we obtain the following expressions for these quantities at the position x_i of the $i-th$ particle:

$$\begin{aligned} U(x_i) &= \frac{\Delta_a}{\Delta_a^2 + \Gamma^2} g_0^2 u^2(x_i) \equiv U_0 u^2(x_i) \\ \gamma(x_i) &= \frac{\Gamma}{\Delta_a^2 + \Gamma^2} g_0^2 u^2(x_i) \equiv \gamma_0 u^2(x_i), \end{aligned} \tag{105}$$

where $g(x) = g_0 u(x) \equiv -d\mathcal{E}u(x)$ gives the position dependent atom-cavity mode coupling. Here $u(x)$ is the normalized cavity mode function and Γ the spontaneous half width of the atomic transition and d the atomic dipole moment.

In the following we assume $\gamma(x_i) \ll \kappa$, which can be obtained for large enough detuning Δ_a and we will use a semiclassical approach treating the atomic positions and velocities as c-numbers. This is of course only valid as long as the temperatures are not too low. In principle an extension to a very cold atomic ensemble (condensate), where one needs a quantum description of the atomic motion is straightforward[34, 60] but beyond our scope here. The equations of motion for the normalized field mode amplitude α and the atomic polarizations in the weak excitation limit then read[29]:

$$\begin{aligned} \dot{\alpha}(t) &= (i\Delta_c - \kappa)\alpha(t) - i\sum_{i=1}^{N} g(x_i)\langle\sigma_i^-(t)\rangle + \eta \\ \langle\dot{\sigma_i}^-(t)\rangle &= (i\Delta_a - \Gamma)\langle\sigma^-(t)\rangle - ig(x_i)\alpha(t), \end{aligned} \tag{106}$$

where $\Delta_c = \omega_P - \omega_c$ denotes the detuning between the pump field and the empty cavity mode and σ_i^- denotes the atomic lowering operator of the $i-th$ two-level atom. Note that this is true for any particle with a suitable optical polarizability. After adiabatic elimination of the polarization dynamics, we obtain the following set of equations:

$$\begin{aligned}\dot{\alpha} &= \left(-\kappa - \bar{\gamma} + i\Delta_c - i\bar{U}\right)\alpha + \eta \\ \dot{p_i} &= -\left|\alpha\right|^2 \frac{d}{dx} U(x)|_{x=x_i} \\ \dot{x_i} &= \frac{p_i}{m},\end{aligned} \tag{107}$$

where $\bar{\gamma} = \sum_{i=1}^{N} \gamma(x_i)$ and $\bar{U} = \sum_{i=1}^{N} U(x_i)$ are the total mode losses and frequency shift commonly induced by all atoms. p_i denotes the momentum of particle i. Note that recoil due to spontaneous emission is not contained in these equations. As it is well known it averages out but leads to momentum diffusion [2], which is assumed to be small here. Similarly Doppler cooling (heating) plays only a negligible role under these conditions and is not included.

Let us emphasize here that the force exerted on an atom at position x_i is proportional to the square of the intracavity mode function $u(x_i)$ and the intracavity intensity (photon number) $I = |\alpha|^2$, which depends on the positions of all of the other atoms. This of course correlates all the particles and can be seen as a sort of long distance interaction. We will use here a simple plane standing wave configuration $g(x) = g_0 sin(kx)$, so that for $\Delta_a > 0$ (*blue detuning*) atoms are pushed towards field nodes, which tends to decrease atom field interaction. For red detuning $\Delta_a < 0$ they are pushed towards field antinodes, where they maximally interact with the field. If the total intracavity photon number changes during the atomic motion over one wavelength, the averaged net dipole force is nonzero and the particle energy is not conserved.

For a single strongly coupled particle all this entangled dynamics is theoretically fairly well understood and has been proposed as a possibility to cool and trap a particle[1, 2]. The efficiency of this mechanism has also been experimentally confirmed to a large extend recently[58]. Let us now discuss the behavior for many particles with a correspondingly weaker individual coupling. As all the particles interact with the same mode, correlations between them will build up and they cannot be considered as independent. Hence we cannot expect to simply find individual cooling of each particle. Naturally a straightforward solution of the nonlinear N-particle equations (107) is rather complicated. Fortunately the spatial dynamics of the particles enters the field mode equation only via the collective quantities $\{\bar{\gamma}, \bar{U}\}$, which gives some hope for finding a not too complicated behavior for suitable operating conditions.

In order to get some physical understanding of the ongoing processes, we will now further simplify the model and discuss as a starting point the special case of a rather cold ensemble of N particles in a far blue detuned standing wave. This allows us to expand the optical potential around the nodes to obtain:

$$\bar{U} \approx U_0 \sum_{i=1}^{N} x_i^2 \tag{108}$$
$$\dot{p_i} = -2\left|\alpha\right|^2 U_0 x_i$$

Introducing the collective quantities $V_x = \sum_{i=1}^{N} x_i^2, V_p = \sum_{i=1}^{N} p_i^2$ and $V_{xp} = \sum_{i=1}^{N} x_i p_i$, we then find the following closed set of differential equations (again disregarding spontaneous emission):

$$\begin{aligned}
\dot{\alpha}(t) &= (i\Delta_c - iU_0 V_x - \kappa)\alpha(t) + \eta \\
\dot{V}_x &= 2V_{xp}/m \\
\dot{V}_{xp} &= V_p/m - 2\left|\alpha\right|^2 U_0 V_x \\
\dot{V}_p &= -4\left|\alpha\right|^2 U_0 V_{xp}.
\end{aligned}$$

Note that for vanishing ensemble average values of x_i, p_i these quantities just correspond to the variances of the atomic position and momentum distribution and are related to the mean energy of the whole ensemble. Similar equations can also be derived for a red detuned standing wave by expanding the potential around the field antinodes, but as the atoms sit at field maxima in this case, spontaneous emission poses more severe limitations.

Although still not analytically solvable these equations look rather simple and can help to understand the collective atomic dynamics. Let us first note that besides the obvious steady state solution $V_x = V_p = V_{xp} = 0, \alpha = \eta/(\kappa + i\Delta_c)$, where all particles sit exactly at the field nodes, there exists a second nontrivial steady state for any given V_x, which reads:

$$V_{xp} = 0,\ V_p = 2\left|\alpha\right|^2 U_0 V_x,\ \alpha = \frac{\eta}{(\kappa + i\Delta_c - iU_0 V_x)}. \tag{109}$$

Hence for certain conditions the influence of the motion of the particles on the field mode dynamics simply cancels and nothing happens. (These values are closely related to thermal equilibrium. Note that the steady state equations are not uniquely solvable for V_x as a function of V_p !) In other cases one gets an oscillatory behavior of the collective atomic variables. Depending on the chosen parameters energy is extracted out or fed into the common atomic motion.

One of the most interesting features of these equations is their scalability. Increasing the particle number by a factor r, dividing the interaction potential U_0 by r and increasing the pump strength η by $\sqrt{r}$ leads to identical solutions for properly scaled initial values. Hence we can scale up the model to a large number of particles being cooled at the same rate. Interestingly this scaling corresponds to an enlargement of the field mode volume with an adjustment of pump strength to maintain the same local intensities. Let us further emphasize here that the number of particles only enters via the initial conditions.

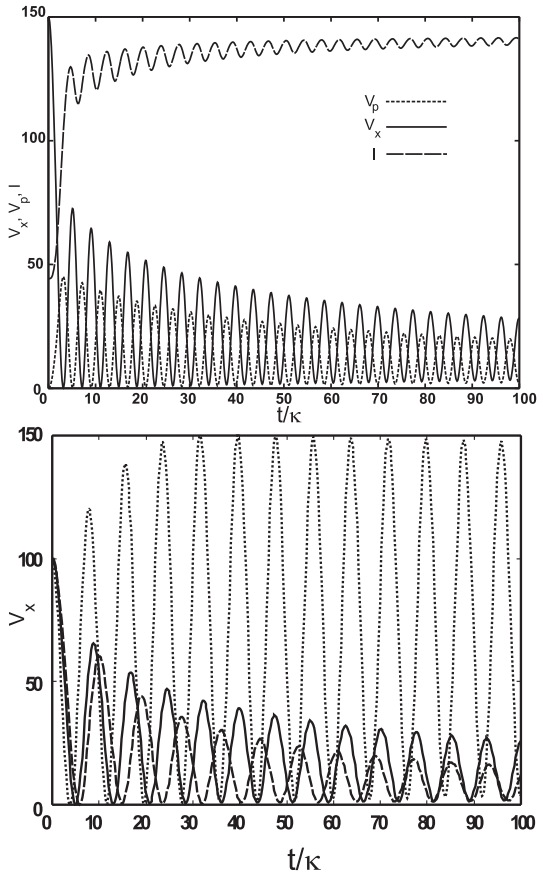

FIGURE 36. (a) Variances V_x (solid line) ,V_p (short-dashed line) and intracavity intensity I (dashed line) as a function of time for an interaction potential of $U_0 = 0.03\kappa$ and resonant cavity pumping $\Delta_c = 0$. (b) Variance V_x for different values of the cavity detuning $\Delta_c = 0$ (solid line), $\Delta_c = \kappa$ (dotted line) and $\Delta_c = -\kappa/2$ (dashed line).

As can be expected from the one-particle results cooling will occur in the case $U_0 > 0$ and $\Delta_c = 0$. This is shown in the following figures. In Fig. 1a we show the collective variables V_x, V_p and the intensity I as a function of time for rather weak coupling $U_0 = 0.01\kappa$ and weak resonant pumping $\Delta_c = 0$ with amplitude $\eta = 2\kappa$. We use a finite V_x and $V_p = 0$ as initial condition corresponding to a slow cold atomic beam entering the cavity through a narrow slit as e.g. in an atomic fountain experiment[5, 32]. Clearly V_x decreases by about one order of magnitude within 300 inverse cavity lifetimes and the system tends towards a nonzero steady state. In Fig. 1b we demonstrate the detuning dependence of this behavior by plotting $V_x(t)$ for three different values of the cavity detuning. While for positive $\Delta_c = \kappa$ (dotted line) we find heating of the atomic ensemble, negative detuning $\Delta_c = -\kappa/2$ (dashed line) even leads to improved cooling as compared to the resonant case $\Delta_c = 0$ (solid line).

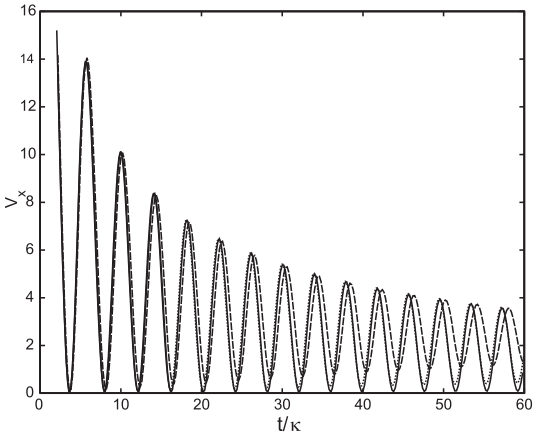

FIGURE 37. Comparison of the variance V_x as a function of time obtained from the linearized theory above (solid line) with a direct numerical solution of the full equations for N=1000 atoms (dotted line) and 250 atoms (dashed line) for the same potential $U_0 = 0.05\kappa$, detuning $\Delta_c = 0$ and the same initial variances $V_x = 30, V_p = V_{xp} = 0$.

Hence a careful choice of the operating conditions can significantly improve the system efficiency. Note that after some time the system comes close to the nontrivial steady state and cooling slows down considerably when the system approaches a steady state. This unwanted behavior can be removed by a change of the pump field strength or detuning after a certain cooling time. Similarly one could use a more sophisticated feedback scheme for the pump amplitude and frequency as a function of time and intracavity intensity[52].

Let us now return to the full potential and numerically solve Eqs. (107) for various particle numbers and parameters. As this requires a rather large numerical effort we will limit our particle numbers to 1000 and present the results only for some typical values and compare it to our previous simple model. Let us first start with a rather cold ensemble in a blue detuned light field, which is resonant with the cavity mode. Fig. 37 shows the time evolution for the full equations as compared to the linearized version, which agrees the better the more localized the particles are initially (in fact we choose N=1000 particles (dotted line) and N=250 particles (dashed line) with the same initial value of the collective spread V_x).

As a second example we consider an ensemble of atoms in a red lattice. The results of the corresponding simulation for $N = 1000$ particles is shown in Fig.38. Initially the energy of many particles is larger than the potential depth, i.e. those particles are initially not trapped. For a sufficiently long time of the order of $10^5\kappa^{-1}$, we see a substantial drop of the mean energy (curve (a)), while the average field intensity (curve (c)) increases. Note that the position spread $\sqrt{V_x}$ (curve b) increases faster at the beginning, where many particles are not confined to a potential well and reaches almost a steady state for long times, when most of the particles are trapped. This trapping also shows up in the initial and final energy distribution drawn in Fig. 39. Note that it is the correlated fluctuations of field and atomic position distributions,

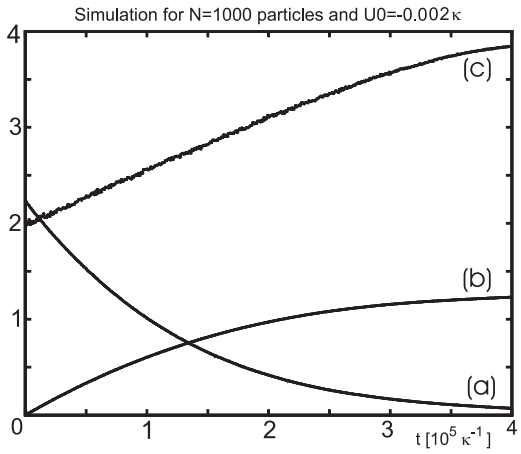

FIGURE 38. Time evolution of mean energy(a) mean spatial width $\sqrt{V_x}$ (b) and field mode photon number I (c) (arb. units) as a function of time for N=1000 particles in an attractive potential $U_0 = -0.002\kappa$ and for negative detuning $\Delta_c = -2\kappa$.

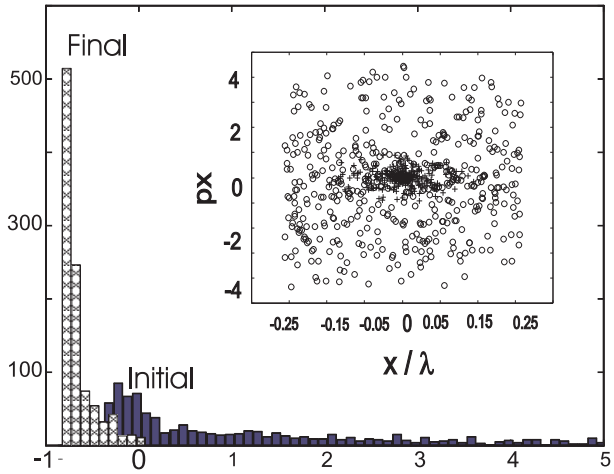

FIGURE 39. Initial (filled bars) and final (empty bars) energy distribution (in units of $\hbar\kappa$) for N=1000 particles in an attractive potential $U_0 = -0.002\kappa$, and for negative detuning $\Delta_c = -2\kappa$. The insert shows the initial (circles) and final (crosses) phase space distributions projected on one half wavelength.

which is responsible for the energy extraction from the system. These fluctuations are only barely visible in Fig. (38c) as they are rather small and fast on the plotted time-scale.

In order to make the phase space compression more visible we have inserted a graph of the initial (circles) and final (crosses) phase space distribution in Fig. 39. Clearly the distribution shrinks in momentum as well as in position space (Actually the position is plotted relative to the nearest field minimum.)

In general we have shown that collective dynamic cooling provides an alternative method to enlarge the phase space density of a cold atomic sample without particle loss and avoiding the spontaneous emission reabsorption problem. In principle one does not require a closed transition but a sufficient optical dipole moment and a high-Q optical cavity. One of the main problems of this process seems to be the rather long time-scales needed for the cooling process. This certainly can be substantially improved by more refined cooling strategies and feed back type manipulation of the cavity pump. Naturally a 3D generalization in the red detuned case is straightforward, as one automatically finds transverse confinement. The blue detuned case is more delicate in 3D and would require either a setup using higher order doughnut modes[53, 54] or some other extra (magnetic) confinement. Nevertheless the method seems to work sufficiently well in principle to provide an alternative cooling scheme for particles, where conventional methods are not applicable.

Acknowledgments

We thank M.G. Raizen and P. Horak for helpful discussions. This work was supported by the Austrian Fonds zur Förderung der wissenschaftlichen Forschung under grants P13435 and F1512.

4.5. Publication 4: Cooling neutral particles in multimode cavities without spontaneous emission

Cooling neutral particles in multimode cavities without spontaneous emission

Markus Gangl, Peter Horak and Helmut Ritsch

Institut für Theoretische Physik, Universität Innsbruck,
Technikerstr. 25, A-6020 Innsbruck, Austria.

Abstract:
We discuss a scheme to cool, trap and manipulate an ensemble of polarizable particles moving in the field of a multimode optical cavity via the correlated dynamics of the field and the particle motion. Using a large detuning between the atoms and the field, spontaneous emission plays a negligible role in this dynamics and the cooling scheme only requires a sufficiently large optical dipole moment. Increasing the particle number slows down the cooling process but it can be accelerated using an increasing number of field modes with higher pump amplitudes. For the special case of a two mode ring cavity and assuming small deviations of the particle positions from the potential minima, the frequencies and damping rates of the vibrational excitation modes can be explicitly calculated. We find a rapid damping of the center of mass motion and relatively slow damping rates for the relative particle oscillations. These predictions agree quite well with a quantum treatment of the atomic motion as used for the excitations of a noninteracting Bose gas (at T=0) inside the cavity field. Due to the position dependent mode coupling the cooling process in a multimode configuration in general happens much faster than for a standing wave geometry. These analytical results are confirmed by N-particle simulations of the semiclassical equations and show even enhanced damping due to the anharmonicity of the full potential.
PACS numbers:32.80.Pj,32.80.Lg,42.50.Vk

Published as Journal of Modern Optics **47**, 2741 (2000).

4.5.1. Introduction

Laser cooling of neutral atoms has seen dramatic improvements towards lower and lower temperatures and higher phase space densities [55, 56, 57]. Nevertheless there are limitations in the final phase space density and the atomic species to which it can be applied, as most schemes rely on spontaneous emission to provide for irreversible energy extraction out of the system. As an essential ingredient this creates the need of a closed optical level scheme and poses the problem of light reabsorption. This severely limits the applicability to molecules (rotational and vibrational couplings) and atoms with no suitable closed transition. Lately Raizen and coworkers [50, 51] proposed stochastic cooling of an ensemble of trapped atoms using a sequence of ensemble momentum measurements via Bragg scattering followed by controlled light induced kicks. This method provides for an alternative in principle but there are some practical limitations (mainly time) on this scheme. As a related option we recently suggested the use of a strongly coupled high-Q optical cavity field to extract motional energy from a cloud of trapped polarizable particles. The procedure relies on cavity damping and allows final average kinetic energies well below the Doppler limit [1, 2]. The scheme has been shown to work well for single atoms [58, 59]. As one might expect it can be generalized to trap and manipulate a Bose condensate [60] inside a cavity in the small saturation regime. In principle the system works as follows: Due to their momentary positions the atoms experience a certain position dependent lightshift, the gradient of which is of course the dipole force experienced by the atoms. The sum of all of the lightshifts for the atoms is just equivalent to the frequency shift of the cavity resonance induced by the atoms. Hence this frequency shift is a collective property of the atomic ensemble and can be used for backaction on the atoms via the pump field. In its simplest form one uses a constant pump of fixed frequency. The atom cavity system is then dynamically shifted in and out of resonance with the pump depending on the momentary atomic positions. This dynamically changes the intracavity intensity and forces on the ensemble. Choosing the right parameters motional energy can be extracted from the atoms. This process can be even enhanced by using a suitable feedback scheme of the intracavity intensity on the pump or an auxiliary light field to apply some extra forces [59, 26, 28, 61]. Some key properties of this mechanism for a single high-Q cavity mode have been investigated before [2]. In this work we generalize this system to several nearly degenerate cavity modes commonly involved in the dynamical cooling process of many atoms. Again we work in the low saturation limit and assume large atom-field detunings, so that spontaneous emission plays no role and the model is valid for any sufficiently polarizable particle. As a major difference to the single mode approach the atoms now influence the intensity and the relative phases of the intracavity modes. Light can be scattered between the various modes without any input-output coupling. For a single particle in a ring cavity a strong enhancement of the cooling has been predicted [3], as small shifts of the particle positions couple more efficiently to relative phase shifts of the two counterpropagating fields than to intensity changes. Generalizing this to many particles the effect should be clearly visible in the center of mass motion in the ensemble. Going beyond a simple harmonic approximation for

the potential wells should even enhance this effect as the relative particle oscillations are not separable any more.

This work is organized as follows: In section II we define a classical model and present the coupled equations for N particles coupled to M cavity modes. In section III we specialize to the case of N two-level atoms in a symmetrically driven ring cavity and in a semiclassical approach we derive some approximative results for the eigenfrequencies and damping rates obtained for small oscillations of the particles around their steady state positions and compare these to the case of a Bose-Einstein condensate (BEC). The system dynamics and parameter dependence of the full N particle dynamics using numerical simulations are then presented in section IV.

4.5.2. Classical model

Let us consider a large number N of linearly polarizable particles with electric charge e, resonance frequency ω_a, mass m and positions $\vec{x}_n$ interacting with a cavity field of several (nearly) degenerate eigenmodes

$$E(\vec{x},t) = \sum_{m=1}^{M} \mathcal{E}\left(\alpha_m(t) u_m(\vec{x}) exp(-i\omega_C t) + cc\right) \tag{110}$$

with mode eigenfrequency ω_C and mode amplitudes $\alpha_m(t)$. Here $\mathcal{E}$ gives the electric field per photon and $u_m(\vec{x})$ are the normalized cavity mode functions. The M cavity modes are externally driven by laser fields of amplitude η_l and frequency ω_P and the modes are damped with a field decay rate κ_l. Solving for the combined dynamics of the mode amplitudes $\alpha_l(t)$ and the induced atomic dipole moments $s_n(t)$, we obtain the following expressions, where $\beta(\vec{x}_n,t)$ is the polarization density and $\vec{x}_n$ denotes the position of the n-th particle:

$$\dot{\alpha_l}(t) = (i\Delta_c - \kappa_l)\alpha_l(t) + i\frac{\omega_P}{2}\beta_l(t) + \eta_l \tag{111}$$

$$\dot{s}_n(t) = (i\Delta_a - \Gamma)s_n(t) + \frac{ie^2}{2\omega_P m}\sqrt{\frac{\hbar\omega_P}{2\epsilon_0 V}}\sum_{m=1}^{M}\alpha_m(t)u_m(\vec{x}_n), \tag{112}$$

with

$$\beta_l(t) = \int dV \beta(\vec{x},t) u_l^*(\vec{x}),$$

$$\beta(\vec{x},t) = \sqrt{\frac{2}{\hbar\omega_P\epsilon_0 V}}\sum_{n=1}^{N} s_n(t)\delta^3(\vec{x}-\vec{x}_n).$$

Here $\Delta_c = \omega_P - \omega_C$, $\Delta_a = \omega_P - \omega_a$ is the detuning between pump and atom and 2Γ denotes the spontaneous emission width of the atomic excited state. We will assume the same driving frequency ω_P and decay rate κ for all modes. Presumably this is not the best possible case but the main features of our model can be well

demonstrated in this limit. Assuming weak excitation and sufficiently large detuning Δ_a, we can adiabatically eliminate the polarizations $s_n(t)$ and obtain

$$\dot{\alpha}_l(t) = -(\kappa - i\Delta_c)\,\alpha_l(t) - (\gamma_0 + iU_0)\sum_{n=1}^{N}\sum_{m=1}^{M} V_{ml}(\vec{x}_n)\alpha_m(t) + \eta_l \tag{113}$$

where the induced effective mode frequency shifts U_0 and dampings γ_0 are given by

$$U_0 = \frac{\Delta_a}{\Gamma^2 + \Delta_a^2} g^2, \tag{114}$$

$$\gamma_0 = \frac{\Gamma}{\Gamma^2 + \Delta_a^2} g^2, \tag{115}$$

$$V_{ml}(\vec{x}_n) = u_m(\vec{x}_n) u_l^*(\vec{x}_n), \tag{116}$$

with $g^2 = e^2/4\epsilon_0 mV$. Note that γ_0 scales as $1/\Delta_a^2$ for large detunings whereas U_0 scales as $1/\Delta_a$. If the detuning Δ_a is very large we can therefore neglect the small spontaneous emission rate γ_0 compared to the induced optical potential U_0.

On the one hand we see that through the term $V_{ml}(\vec{x}_n)$ we get a position dependent mode coupling induced by the atoms, which leads to dynamical phase locking. On the other hand the induced optical dipole force on the n-th particle is then just proportional to the total intensity gradient. Hence in contrast to the single mode case, the force strongly depends on the relative field phases in addition to the intensities. This difference will turn out to be very important for the scaling properties of the involved cooling dynamics.

The corresponding equations of motion for the momenta $\vec{p}_n$ and positions $\vec{x}_n$ of the atoms are then as follows:

$$\dot{\vec{p}}_n(t) = -U_0 \left(\vec{\nabla} \left| \sum_{m=1}^{M} \alpha_m u_m(\vec{x}) \right|^2 \right) \Bigg|_{\vec{x}=\vec{x}_n} \tag{117}$$

$$\dot{\vec{x}}_n(t) = \vec{p}_n(t)/m. \tag{118}$$

In the limit of small saturation this classical model, Eqs. (113), (117) and (118), corresponds to the so called semiclassical approach treating the atomic positions and velocities as c-numbers but describing the internal atomic dynamics and the cavity field quantum mechanically. This is of course only valid as long as the temperatures are not too low. In principle an extension to a very cold atomic ensemble (condensate), where one needs a quantum description of the atomic motion is straightforward [60, 34] and we will include some of the corresponding results for comparison later.

4.5.3. N particles in a two mode ring cavity

Let us now discuss the N-atom dynamics in a ring cavity. For a single particle or a few particles this entangled dynamics is theoretically fairly well understood and

has been presented in some detail [3, 24]. We will discuss here the behavior for a large number of particles with a correspondingly weaker individual coupling. As all the particles interact with the same modes, correlations between them will build up and they cannot be considered as independent. Hence a simple naive scaling cannot work and in general we have to solve the full N-particle equations.

We thus specialize our model to the case of only two counterpropagating travelling wave cavity modes with amplitudes $\alpha_\pm$ and mode functions $u_\pm(x) = \exp(\pm ikx)$ being excited. This implies a sufficiently large transverse and longitudinal mode spacing and Equation (113) then reads

$$\dot{\alpha}_\pm = \left(-\kappa - N\gamma_0 + i\left(\Delta_c - NU_0\right)\right)\alpha_\pm - \left(\gamma_0 + iU_0\right)\alpha_\mp \sum_{n=1}^{N} e^{\mp 2ikx_n} + \eta, \tag{119}$$

where we assumed a unique pumping rate η for both modes. From this we get the equation for the positive frequency part of the total electric field (110)

$$\dot{E}^{(+)}(x) = \left(-\kappa + i\Delta_c\right)E^{(+)}(x) - 2N\left(\gamma_0 + iU_0\right)\sum_{n=1}^{N} E^{(+)}(x_n)\cos k\left(x - x_n\right) + 2\eta\cos kx. \tag{120}$$

In order to get some physical understanding of the ongoing processes, we will now further simplify the model and discuss as a starting point the special case of a rather cold ensemble of N particles sitting near the antinodes of a far blue detuned field and we will assume that the detuning Δ_a is large enough to neglect γ_0.

With the atoms located around the nodes of the standing wave we can expand their positions by $kx_n = \frac{2n-1}{2}\pi + \epsilon_n$, where the ϵ_n denote small displacements around the potential minima which implies $e^{\mp 2ikx_n} \approx -\left(1 \mp 2i\epsilon_n\right)$. Defining the center of mass of the small displacements by $\epsilon_{CM} = \frac{1}{N}\sum_{n=1}^{N}\epsilon_n$ one can calculate the back-action of the atoms on the cavity field, neglecting the cavity dynamics at a first step. This means that the cavity field is assumed to adjust itself immediately to the atomic positions. With this assumption we neglect, of course, any damping of the atomic motion by friction forces, which contradicts our initial intention. However, for weak enough damping, this should be valid for short timescales and will allow us to classify the vibrational excitations.

In this limit the total intensity of the cavity light field only depends on the collective quantity ϵ_{CM},

$$I(x) = E^{(-)}(x)E^{(+)}(x) = \frac{4\eta^2}{\kappa^2 + \Delta_c^2}\cos^2\left(kx - \mu\epsilon_{CM}\right), \tag{121}$$

where the factor μ has been defined as

$$\mu = \frac{2U_0N\left(2U_0N - \Delta_c\right)}{\kappa^2 + \left(2U_0N - \Delta_c\right)^2}. \tag{122}$$

Hence the effect of the atoms is to shift the cavity standing wave pattern by an amount of $\mu\epsilon_{CM}$. Note that μ approaches unity very fast for increasing U_0N. In this limiting case the center of mass always coincides with a field node and atomic phaselocking dominates over the external pumping.

To establish the equation of motion for the center of mass we calculate the dipole force acting on the n-th atom by taking the local derivatives of the potential at the site of each atom,

$$f_{dip,n} = -U_0 \frac{dI}{dx}(x_n) = \frac{4\hbar k U_0 \eta^2}{\kappa^2 + \Delta_c^2} \sin 2\left(kx_n - \mu\epsilon_{CM}\right). \tag{123}$$

Expanding Eq. (123) around the field nodes and adding up these single-atom contributions gives a rather simple equation of motion for the center-of-mass coordinate ϵ_{CM} in the form

$$\ddot{\epsilon}_{CM} + \omega_0^2(1-\mu)\epsilon_{CM} = 0 \tag{124}$$

where

$$\omega_0^2 = \frac{8\hbar k^2 U_0 \eta^2}{m\left(\kappa^2 + \Delta_c^2\right)}, \tag{125}$$

would be the oscillation frequency of a single atom in a potential well for a fixed externally given field. Hence, the center of mass oscillates in the light field of a ring cavity with a reduced frequency $\omega_{CM}^2 = \omega_0^2(1-\mu)$. This is due to the spatial shift which the optical potential experiences because of the moving center of mass. Note that as μ approaches unity, the cavity field follows the motion of the center of mass without delay. The atoms always stay in the vicinity of the field nodes and consequently ω_{CM} approaches zero because the restoring force goes to zero, see fig. 40.

In the harmonic approximation discussed here, all other collective atomic modes, i.e., those comprising the relative motion of the atoms, decouple from the light field and simply oscillate at the bare frequency ω_0. The coupling of these modes to the light by the anharmonicity of the potential will be discussed in the next section using a numerical integration of the full model.

Relaxing the assumption of a very large cavity decay rate κ, the cavity field does not adiabatically follow the atomic positions, but changes with a finite delay time. This effect gives rise to damping or amplification of the atomic vibrational excitations. We have done some numerical studies to include the effect of the friction forces on the center of mass motion. We find that this oscillation is strongly damped regime even for moderate values of U_0N, see fig. 41. Only for very small values of the effective potential the center-of-mass mode shows real oscillations as shown in Fig. 42. Again this is in strong contrast to the single standing wave mode case, where small oscillations are only very weakly damped. For the numerical simulations we have restricted ourselves to 2 atoms as the results are very similar for a larger number of atoms. Fast damping of the center-of-mass mode of course means that the two atoms get perfectly anticorrelated in their motion around the field node. Hence the

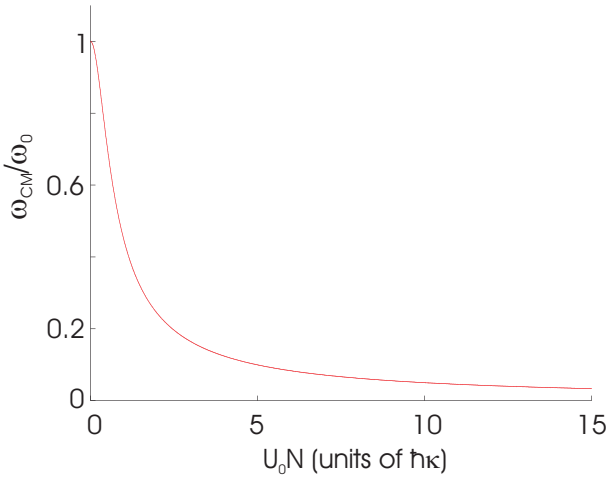

FIGURE 40. Frequency of the vibrational center of mass mode normalized to ω_0 over U_0N. $\Delta_c = 0$, $\kappa = 1$.

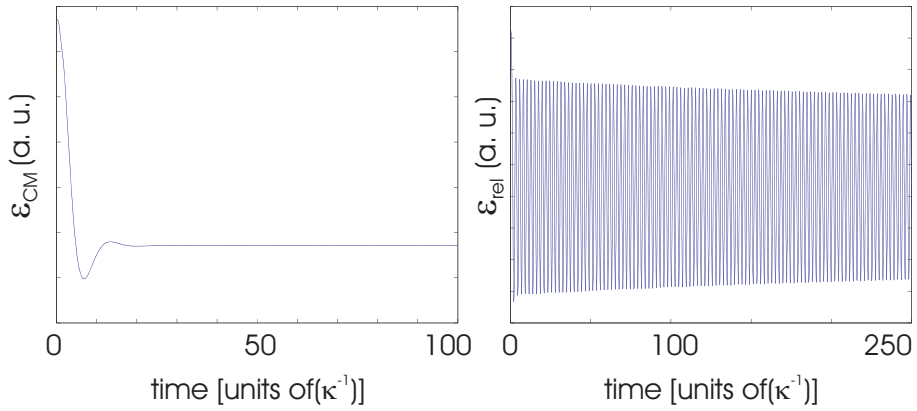

FIGURE 41. $NU_0 = 2\kappa$, $\kappa = 1$. Overdamped CM-oscillation (left) and almost undamped relative oscillation (right).

atoms exchange energy and momentum, as well as oscillation phase information at a large distance. For a discussion on how this effect could be used to implement a quantum information processing scheme see the work of Hemmerich [24].

Let us now derive an analytic expression for the damping rate of the center-of-mass motion in the limit where this damping is much slower than the oscillation frequency. We use the result for the friction force on a single atom in the field of a ring cavity [3] and incorporate this into Eq. (124) for the center-of-mass motion. This yields

$$\ddot{\epsilon}_{CM} + 2\gamma_{fric}\dot{\epsilon}_{CM} + \omega_{CM}^2\epsilon_{CM} = 0, \tag{126}$$

where

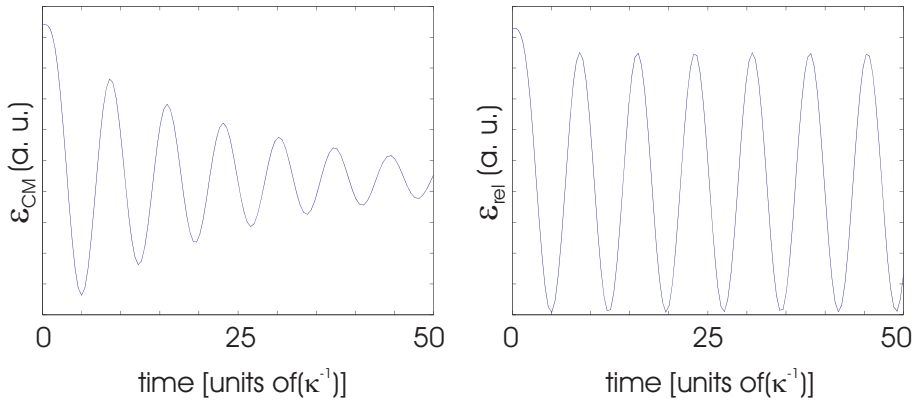

FIGURE 42. $NU_0 = 0.2\kappa$, $\kappa = 1$. Damped CM-oscillation (left) and relative oscillation (right).

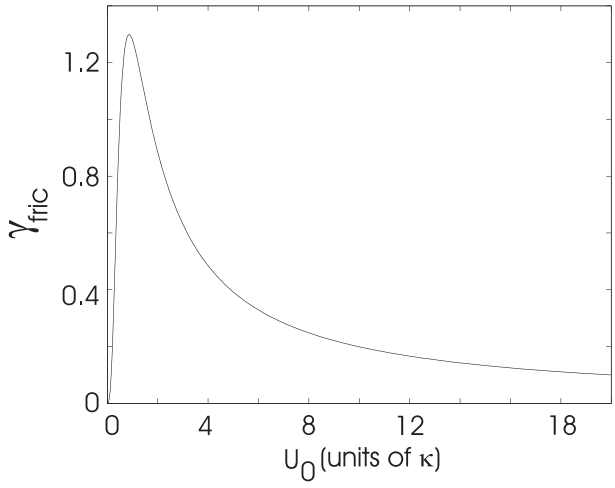

FIGURE 43. Damping constant γ_{fric} of the vibrational center of mass mode over U_0. $\Delta_c = 0$, $\eta = 1$, $\kappa = 1$.

$$\gamma_{fric} = \omega_0^2 \frac{2NU_0\kappa\,(2NU_0 - \Delta_c)}{\left(\kappa^2 + (2NU_0 - \Delta_c)^2\right)^2}. \tag{127}$$

The friction coefficient was derived assuming a prescribed atomic velocity $v(t)$ in the limit where the atomic motion is slow compared to the cavity decay rate $kv \ll \kappa$. Equation (126), which holds only for $\gamma_{fric} \ll \omega_{CM}$, simply describes a damped harmonic oscillation around the field node. In fig. 43 we plot this damping constant as a function of U_0. One can see clearly a maximum of γ_{fric} around $U_0 \approx \kappa$. As the optical potential increases the damping constant goes to zero as the time lag between the atomic motion and cavity response causing this damping effect vanishes.

One of the most interesting aspects of the N-atom system dynamics is their scalability. For a standing wave cavity field [3] we have seen that increasing the particle number by a factor r, dividing the interaction potential U_0 by r and increasing the

pump strength η by $\sqrt{r}$ leads to identical equations for the mean kinetic and potential energy of the atoms coupled to the field dynamics. This allows to scale up the system to higher particle numbers by increasing the cavity volume and the pump field. Although we cannot explicitly show such a behavior here, we see that the number of atoms enters the oscillation frequency only via the parameter μ, which contains only the combination U_0N. Hence the dynamics can be expected to be very similar if we keep U_0N as well as the intracavity intensity constant. Thus by changing the pump intensity we now can expect to have an extra handle on the cooling time scale. This could be very helpful for very large particle numbers, where the cooling process could get rather slow. We will discuss this in some more detail in the next section.

Let us now get back to analytically solvable cases and compare these results with the dynamics of ultracold atoms, more specifically, a temperature T=0 Bose-Einstein condensate subject to a ring cavity field [60]. For this one has of course to leave the semiclassical picture and treat the external motion of the atom quantum mechanically. The corresponding Schrödinger equation has then to be solved together with the cavity field equations, i.e. we have:

$$\frac{d}{dt}\alpha_{\pm}(t) = \left[i\Delta_c - iNU_0 - \kappa\right]\alpha_{\pm}(t) - iNU_0\langle e^{\mp 2ik\hat{x}}\rangle\alpha_{\mp} + \eta, \tag{128}$$

$$i\frac{d}{dt}\psi(x,t) = \left\{\frac{\hat{p}^2}{2m} + Ng_{coll}|\psi(x,t)|^2 + U_0\left|\alpha_+(t)e^{ikx} + \alpha_-(t)e^{-ikx}\right|^2\right\}\psi(x,t) \tag{129}$$

The only change in the equation of motion (128) for the field modes is that the sum over all particles in Eq. (119) is replaced by the corresponding expectation value taken with the momentary matter wave function. The equations for the particle dynamics (117) and (118) are replaced by the non-linear Schrödinger equation (129) which includes the effects of atom-atom interactions in the condensate via the binary collision rate g_{coll}.

For a comparison with our results here we will neglect atom-atom interactions and therefore set $g_{coll} = 0$. Moreover, for simplicity we will assume a resonant cavity, $\Delta_c = 0$. In the Lamb-Dicke limit (harmonic approximation for the optical potential) the stationary ground state of Eqs. (128) and (129) can be calculated analytically and yields the harmonic oscillator frequency

$$\omega_0^2 = \frac{16U_0\omega_R\eta^2}{\kappa^2}\left(1 - \frac{N^2U_0\omega_R}{4\eta^2}\right), \tag{130}$$

where $\omega_R = \hbar k^2/(2m)$. We see that the finite width of the wave function leads to a small modification compared to the value (125) for N point-like particles. It is then straightforward to calculate the spectrum of collective excitations, that is, the eigenfrequencies of small deviations of the wave function and the cavity fields from their respective ground states in a linearized model. In the limit of $\kappa \gg \omega_0$ we find the following analytic expressions for the oscillation frequency ν_1 and the damping

rate γ_1 of the lowest excited mode:

$$\nu_1 = \omega_0 \sqrt{1 - \frac{4N^2U_0^2(1-\frac{\omega_R}{\omega_0})}{\kappa^2 + 4N^2U_0^2(1-\frac{\omega_R}{\omega_0})^2}}, \tag{131}$$

$$\gamma_1 = \omega_0^2 \kappa \frac{4N^2U_0^2(1-\frac{\omega_R}{\omega_0})}{[\kappa^2 + 4N^2U_0^2(1-\frac{\omega_R}{\omega_0})^2]^2}. \tag{132}$$

Although derived via a quite different approach we see that the results of this fully quantum model agree with the classical results for the center-of-mass frequency ω_{CM} and the corresponding damping rate γ_{fric} up to corrections of the order of $(1 - \omega_R/\omega_0)$ which are related to the spatial width of the wave function. We thus can expect our cooling scheme to work also at very low temperatures and maybe even provide for an alternative to evaporative cooling on the route to BEC.

4.5.4. Numerical simulations

Let us now return to the exact expressions for the lightshift potentials and numerically solve Eqs. (113), (117) and (118) for various particle numbers and parameters. As this requires a rather large numerical effort we will limit our particle numbers to 1000 and 1D motion and present the results only for some typical values. It can be seen from the equations quite easily that in a 1D plane wave situation the cases of red and blue detuning are equivalent, if one neglects the contribution of spontaneous emission. In practice this assumption would be more easily fulfilled in the blue detuned case, where the atoms are trapped near the nodes of the field, while in a focused red detuned field one would have the advantage of a builtin transverse confinement. As we are mainly interested in the general performance of the cooling as a function of various parameters as atom number N, pump strength η and detuning Δ_c, we will restrict ourselves to the simplest case of counterpropagating plane waves with symmetric pumping.

Let us start with a cold atomic ensemble in a blue detuned light field. The pump field is assumed almost resonant with the two counterpropagating cavity modes of the empty cavity. In Fig. 44 we show the time evolution of the positions and momenta of N=1000 particles according to the full equations (117) and (118). We start with a cold cloud of particles initially located near antinodes of field (potential maximum)(see crosses). After a surprisingly short time ($t = 10/\kappa$) the center of mass position and momentum of the cloud has damped out and the particles are located around the antinodes of the field (potential minima) (see dots). The cooling now proceeds on a much slower timescale. At time $t = 300/\kappa$ the cloud has again compressed in position and momentum space (circles). For better visibility we have only plotted 250 randomly chosen particles out of the ensemble. Note that only very few particles are not cooled.

The time evolution of the average kinetic energy as well as the intracavity field are shown in Fig. 45. We find a rather faster exponential decrease of the average kinetic energy, while the particles get more and more localised near the nodes and the average intracavity field increases. At the same time the relative field phase

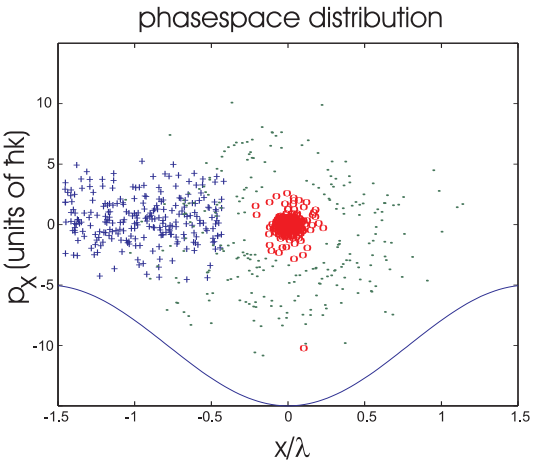

FIGURE 44. Numerical solution of the particle momenta and positions for N=1000 atoms for $U_0 = 0.001\kappa$, $\Delta_c = -0.5\kappa$ and $\eta = 150\kappa$ at $\kappa t = 0$ (crosses), $\kappa t = 10$ (small dots) and $\kappa t = 300$ (circles). In this figure 250 randomly chosen atoms are displayed. The solid line denotes the unperturbed optical potential.

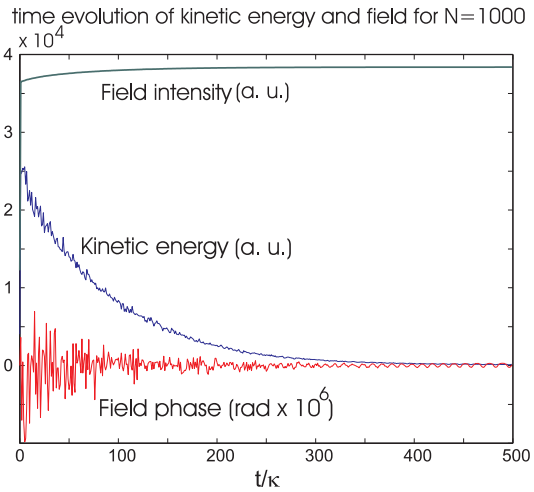

FIGURE 45. Time evolution of the total kinetic energy, as well as the field intensity and phase for N=1000 atoms for $U_0 = 0.001\kappa$, $\Delta_c = -0.5\kappa$ and $\eta = 150\kappa$.

between the two running waves fluctuates, which leads to fluctuations of the field nodes. This behaviour is quite different from the standing wave cavity case and leads to strong additional damping.

An important factor concerning the usefullness of this approach is the time scale of the cooling. Fortunately it is possible to speed up cooling by stronger pumping. This is demonstrated in Fig. 46, where we compare the time evolution of the kinetic energy of 300 particles for the same operating parameters and initial conditions except for three different pump strengths $\eta = (50, 80, 110)\kappa$. We see that the time

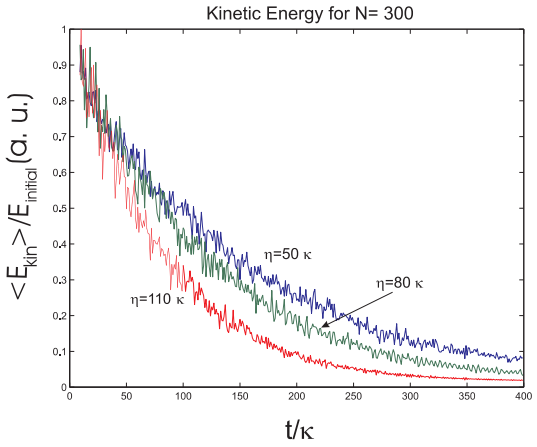

FIGURE 46. Time evolution of the total kinetic energy for N=300 atoms for $U_0 = 0.003\kappa$, $\Delta_c = -0.5\kappa$ and three different pump strengths $\eta = (50, 80, 110)\kappa$.

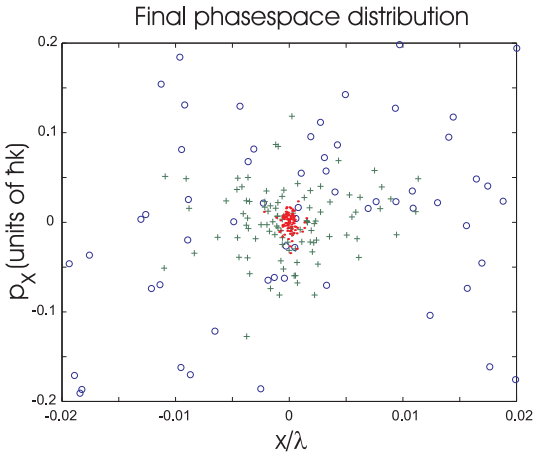

FIGURE 47. Position and momenta of N=300 atoms for $U_0 = 0.003\kappa$, $\Delta_c = -0.5\kappa$ and three different pump strengths $\eta = 50\kappa$ (circles), 80κ (crosses), 110κ (dots) at time $\kappa t = 500$ for the same initial conditions. In this figure 50 randomly chosen atoms are displayed.

after which the particles have lost half of their kinetic energy is approximately inversely proportional to the pump strength. The corresponding final phase space distributions at time $\kappa t = 500$ are shown in Fig. 47.

In the next graph we show the dependence of the cooling time on the particle number. For this we choose N=300 and N=100 particles with the same value of the collective coupling $U_0 N$ and again compare the time evolution of the mean kinetic energy. Clearly a significant slowing of the cooling process with particle number gets visible. Of course this effect can be compensated by choosing more suitable operating conditions.

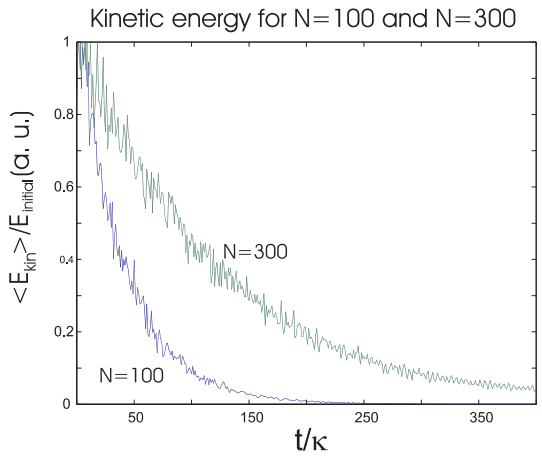

FIGURE 48. Time evolution of the total kinetic energy for N=300 atoms and N=100 atoms for the same value of $U_0 N = \kappa$, $\Delta_c = -0.5\kappa$ and strength $\eta = 80\kappa$.

4.5.5. Conclusions

In general we have shown that collective dynamic cooling provides an alternative method to enlarge the phase space density of a cold atomic sample without particle loss and avoiding the spontaneous emission reabsorption problem. In principle one does not require a closed transition but a sufficient optical dipole moment and a high-Q optical cavity. Using a multimode setup as e.g. a running wave cavity, we can considerably speed up the cooling process and lower the stringent requirements on cavity technology and cooling time. Hence the method seems to work sufficiently well in principle to provide an alternative cooling scheme for particles, where conventional methods are not applicable. In principle the final temperatures predicted by the semiclassical model are very low and are not limited by the recoil. The corresponding approximative quantum results for very cold particles seem to agree reasonably well with these predictions. Using more refined setups as quasiconfocal or quasispherical cavities or even microsphere resonators should provide further enhancements of the cooling and allow for generalisations to full 3D setups.

Acknowledgments

This work was supported by the Austrian Fonds zur Förderung der wissenschaftlichen Forschung under project no. P13435 and F1512.

Part II

Multilevel atoms in optical resonators

CHAPTER 5

Polarization gradient cooling inside optical resonators

5.1. Introduction

We have already discussed in chapter 2 how the existence of an internal atomic time-scale $\tau_P = 1/(\gamma_0 I)$ in an atom with a degenerate groundstate that can be much larger than the radiative time-scale $\tau_R = 1/\Gamma$ can lead to cooling effects at very low velocities $kv \ll \Gamma$ and laser power $sI \ll 1$.
On the other hand in chapter 3 we showed that even without relying on spontaneous emission one can achieve cooling of a two-level atom at such low velocities by the use of an optical resonator which introduces the cavity reaction time $\tau_\kappa = 1/\kappa$. In a high-Q cavity, where $\kappa \ll g$ it was shown that cooling times

$$\tau_{C,Cav} = \frac{\omega_{Rec}^{-1}}{4s}\left(\frac{\kappa}{2g}\right)^2 \tag{133}$$

much lower than in free space where

$$\tau_{C,Dopp} = \frac{\omega_{Rec}^{-1}}{4s} \tag{134}$$

and steady-state temperatures $k_B T = \hbar\kappa$ below the Doppler limit $k_B T = \hbar\Gamma$ can be reached.

In the present and the following chapter we will investigate how the mechanical light effects on a multilevel atom ($J_g = N \to J_e = N+1$ and $J_g = N \to J_e = N$, respectively) are modified inside a ring resonator that is prepared in a σ^+-σ^- laser setup. For a $J_g = N \to J_e = N+1$ atomic transition we will show that free-space polarization gradient cooling is dramatically changed due to the backreaction of the induced atomic dipole on the cavity field.
A $J_g = N \to J_e = N$ atomic transition is known to show the phenomenon of velocity selective coherent population trapping (VSCPT) that together with momentum diffusion leads to cooling of atoms well below the recoil limit $k_B T_{Rec} = (\hbar k)^2/(2m)$. We will show in section 6 that by generalizing this cooling scheme to the interaction of an

atom with the laser modes of a ringcavity most of the problems of free space VSCPT

- long cooling times,
- need of closed optical transition and
- final atomic density limited by photon reabsorption

can be solved.

Let us give a short mathematical account how to describe the interaction of a $J_g = N_g \rightarrow J_e = N_e$ atomic transition with the laser field of a ring cavity given by

$$\vec{E} = \vec{E}^+ e^{-i\omega_P t} + \vec{E}^- e^{i\omega_P t} \tag{135}$$

where

$$\vec{E}^+ = \mathcal{E}\left(A\vec{e}_+ + B\vec{e}_-\right) \tag{136}$$

and

$$\begin{aligned} A &= \alpha_+ e^{ikz} + \alpha_- e^{-ikz} \\ B &= \beta_+ e^{ikz} + \beta_- e^{-ikz}. \end{aligned} \tag{137}$$

Here we have used the right and left circular unit vectors $\vec{e}_\pm = \mp 1/\sqrt{2}(\vec{e}_x \pm i\vec{e}_y)$. By defining the projectors on the groundstate and the excited state

$$\begin{aligned} P_g &= \sum_{m=-J_g}^{J_g} |g_m\rangle\langle g_m| \\ P_e &= \sum_{m=-J_e}^{J_e} |e_m\rangle\langle e_m| \end{aligned} \tag{138}$$

we can write the atomic density operator as

$$\rho = \rho_{gg} + \rho_{eg} + \rho_{ge} + \rho_{ee} \tag{139}$$

where $\rho_{ij} = P_i \rho P_j$ $(i, j = e, g)$. The atomic dipole operator can be written as

$$\begin{aligned} \vec{D} &= \vec{D}^+ + \vec{D}^- \\ \vec{D}^+ &= d\left(S_+\vec{e}_+ + S_-\vec{e}_-\right), \end{aligned} \tag{140}$$

where $S_\pm$ and S_0 are the atomic lowering operators for $\sigma^\pm$ and π polarized light, respectively. In a $J_g = 1 \rightarrow J_e = 2$ atomic transition they read

$$
\begin{aligned}
S_+ &= \frac{1}{\sqrt{6}}|g_{-1}\rangle\langle e_0| + \frac{1}{\sqrt{2}}|g_0\rangle\langle e_1| + |g_1\rangle\langle e_2| \\
S_- &= \frac{1}{\sqrt{6}}|g_1\rangle\langle e_0| + \frac{1}{\sqrt{2}}|g_0\rangle\langle e_{-1}| + |g_{-1}\rangle\langle e_{-2}| \\
S_0 &= \frac{1}{\sqrt{2}}|g_{-1}\rangle\langle e_{-1}| + \sqrt{\frac{2}{3}}|g_0\rangle\langle e_0| + \frac{1}{\sqrt{2}}|g_1\rangle\langle e_1|. \qquad (141)
\end{aligned}
$$

In the rotating wave approximation valid for optical frequencies the dipole-interaction Hamiltonian

$$
\begin{aligned}
H_I &= -\vec{D}\cdot\vec{E} \\
&= -\vec{D}^-\cdot\vec{E}^+ - \vec{D}^+\cdot\vec{E}^- \qquad (142)
\end{aligned}
$$

reads

$$
H_I = g\left(A^*S_+ + B^*S_-\right) + g\left(AS_+^\dagger + BS_-^\dagger\right) \qquad (143)
$$

where $g = -d\mathcal{E}$ is the Rabifrequency per photon for an atomic transition with unity Clebsch-Gordan coefficient.
Thus the system Hamiltonian can be written as

$$
H = -\Delta_a P_e + gG^- + gG^+, \qquad (144)
$$

where we have defined $G^- = A^*S_+ + B^*S_-$, $G^+ = (G^-)^\dagger$. Dissipation via spontaneous atomic decay is included by using the standard master equation approach

$$
\begin{aligned}
\dot{\rho} &= -\frac{i}{\hbar}[H,\rho]\mathcal{L}\rho \\
\mathcal{L}\rho &= -\Gamma(P_e\rho + \rho P_e - 2S_+\rho S_+^\dagger - 2S_-\rho S_-^\dagger - 2S_0\rho S_0^\dagger). \qquad (145)
\end{aligned}
$$

As we are only interested in the low laser power $sI \ll 1$ and low velocity $kv \ll \Gamma$ regime the excited atomic states can be adiabatically eliminated yielding

$$
\rho_{eg} = -\frac{ig}{\Gamma - i\Delta_a}G^+\rho_{gg} \qquad (146)
$$

$$
\rho_{ee} = \frac{g^2}{\Gamma^2 + \Delta_a^2}G^+\rho_{gg}G^- \qquad (147)
$$

$$
\dot{\rho}_{gg} = -\gamma_0\{G^-G^+, \rho_{gg}\}_+ - iU_0[G^-G^+, \rho_{gg}] + 2\gamma_0\sum_{l=0,-,+} S_l G^+\rho_{gg}G^-S_l^\dagger \qquad (148)
$$

The cavity field is pumped from one side by σ^+ polarized light only and from the other side by σ^- polarized light with pump strength η. In a cavity Maxwell's equations show that we have to take into account the backaction of the induced

atomic dipole moment on the cavity field as a source term in the equation of motion for $\vec{E}^+$

$$\dot{\vec{E}}^+ = (-\kappa + i\Delta_C)\,\vec{E}^+ - 2ig\cos k(z - z_a)\vec{d}^+ + \eta\left(e^{ikz}\vec{e}_+ + e^{-ikz}\vec{e}_-\right) \qquad (149)$$

where $\vec{d}^+ \equiv \langle\vec{D}^+\rangle$. For the four cavity field amplitudes we get the following equations

$$\begin{aligned}
\dot{\alpha}_+ &= (-\kappa + i\Delta_C)\alpha_+ - ige^{-ikz_a}\langle S_+\rangle + \eta \\
\dot{\alpha}_- &= (-\kappa + i\Delta_C)\alpha_- - ige^{ikz_a}\langle S_+\rangle \\
\dot{\beta}_+ &= (-\kappa + i\Delta_C)\beta_+ - ige^{-ikz_a}\langle S_-\rangle \\
\dot{\beta}_- &= (-\kappa + i\Delta_C)\beta_- - ige^{ikz_a}\langle S_-\rangle + \eta
\end{aligned} \qquad (150)$$

Note that the σ^+ polarized cavity modes $\alpha_\pm$ couple to $\langle S_+\rangle$ and the σ^- polarized cavity modes $\beta_\pm$ couple to $\langle S_-\rangle$ only.

In the next section we will use these equations to calculate the evolution of cavity and atomic variables for a $J_g = 1/2 \rightarrow J_e = 3/2$ and a $J_g = 1 \rightarrow J_e = 2$ atomic transition.

In the remainder of this section we want to give a more physical description of the changes that arise inside a cavity compared to free space for a $J_g = 1 \rightarrow J_e = 2$ atomic transition.

First let us calculate the expectation value of the induced dipole moment for a slowly moving atom.

Starting from eq. 140 we see that we have to calculate $\langle S_\pm\rangle$ by using

$$\begin{aligned}
\langle S_\pm +\rangle &= Tr(S_\pm\rho_{eg}) \\
&= -\frac{ig}{\Gamma - i\Delta_a}Tr(S_\pm G^+\rho_{gg})
\end{aligned} \qquad (151)$$

and noting that

$$\begin{aligned}
\langle S_+S_+^\dagger\rangle &= 1/6\Pi_- + 1/2\Pi_0 + \Pi_+, \\
\langle S_-S_-^\dagger\rangle &= 1/6\Pi_+ + 1/2\Pi_0 + \Pi_-, \\
\langle S_+S_-^\dagger\rangle &= 1/6\rho_{+-} \quad \text{and} \\
\langle S_-S_+^\dagger\rangle &= 1/6\rho_{-+}
\end{aligned} \qquad (152)$$

we get

$$\langle S_+\rangle = -\frac{ig}{\Gamma - i\Delta_a}\left[A\left(1/6\Pi_- + 1/2\Pi_0 + \Pi_+\right) + 1/6B\rho_{+-}\right]$$
$$\langle S_-\rangle = -\frac{ig}{\Gamma - i\Delta_a}\left[B\left(1/6\Pi_+ + 1/2\Pi_0 + \Pi_-\right) + 1/6A\rho_{-+}\right] \quad (153)$$

For an atom at rest we can insert the steady-state values for the atomic ground-state populations and Zeeman coherences

$$\begin{aligned}\Pi_+ &= 13/34\\ \Pi_- &= 13/34\\ \Pi_0 &= 4/17\\ \rho_{+-} &= 5/34e^{2ikz_a}\end{aligned} \quad (154)$$

defined by $\Pi_\pm = \langle g_{\pm1}|\rho_{gg}|g_{\pm1}\rangle$, $\Pi_0 = \langle g_0|\rho_{gg}|g_0\rangle$, $\rho_{+-} = \langle g_1|\rho_{gg}|g_{-1}\rangle$ and noting that

$$\begin{aligned}\vec{E}_0^+(z_a) &= A(z_a)\vec{e}_+ + B(z_a)\vec{e}_-\\ &= \frac{\eta}{\kappa + 20/17\gamma_0 - i(\Delta_C - 20/17U_0)}\left(e^{ikz_a}\vec{e}_+ + e^{-ikz_a}\vec{e}_-\right)\end{aligned} \quad (155)$$

we get the expected result of an induced atomic dipole moment oriented along the local pump field polarization

$$\vec{d}_0^+ = p\vec{E}_0^+(z_a) \quad (156)$$

where we have defined the complex atomic polarization p by

$$p = -\frac{10/17ig}{\Gamma - i\Delta_a}.$$

For a slowly moving atom $kv \ll min(\gamma_0|A^0|^2, \kappa)$ we make the ansatz

$$\begin{aligned}A &\approx A^0 + vA^1\\ B &\approx B^0 + vB^1\end{aligned} \quad (157)$$

and

$$\begin{aligned}\Pi_\pm &\approx \Pi_\pm^0 + v\Pi_\pm^1\\ \rho_{+-} &\approx (C_r^0 + iC_i^0)e^{2ikz_a} + v(C_r^1 + iC_i^1)e^{2ikz_a}\\ \vec{d}^+ &= \vec{d}_0^+ + v\vec{d}_1^+.\end{aligned} \quad (158)$$

This gives the correction of the induced atomic dipole moment to first order in v

$$\vec{d}_1^+ = p\vec{E}_1^+(z_a) + i\frac{p}{2}\langle J_z^1\rangle\vec{e}_z \times \vec{E}_0^+(z_a), \quad (159)$$

where $\langle J_z^1 \rangle = \Pi_+^1 - \Pi_-^1$. Interestingly $\vec{d}_1^+$ has a component perpendicular to the polarization of the local pump field and proportional to the difference in the population of the two Zeeman groundstate sublevels $\Pi_\pm^1$ to first order in v. Analytical expressions for the first order corrections of the field amplitudes and atomic variables are given in section 5.6.4.

A simple physical picture for the unequally populated groundstate sublevels can be given by first order perturbation theory in the limit where $\Gamma \ll \Delta_a$.

Using the effective Hamiltonian defined by

$$\begin{aligned} H_{\text{eff}} &= \hbar U_0 G^- G^+ \\ &= \hbar U_0 \left(|A|^2 S_+ S_+^\dagger + |B|^2 S_- S_-^\dagger + AB^* S_- S_+^\dagger + A^* B S_+ S_-^\dagger \right) \end{aligned} \tag{160}$$

and using again eqs. 157 for the first order corrections in v of the cavity fields we can define the unperturbed Hamiltonian H_0 for an atom at rest and the Hamiltonian H_1 caused by the perturbation by

$$\begin{aligned} H_0 &= \hbar U_0 \big[\left(|A^0|^2 + |B^0|^2 \right) /2 |g_0\rangle\langle g_0| + \\ &\quad \left(|A^0|^2/6 + |B^0|^2 \right) |g_{-1}\rangle\langle g_{-1}| + \left(|A^0|^2 + |B^0|^2/6 \right) |g_1\rangle\langle g_1| + \\ &\quad 1/6 \left(A^0 (B^0)^* |g_1\rangle\langle g_{-1}| + (A^0)^* B^0 |g_{-1}\rangle\langle g_1| \right) \big] \\ H_1 &= 5/6 \hbar U_0 \left[(A^1)^* A^0 + A^1 (A^0)^* \right] J_z + \\ &\quad 1/6 \hbar U_0 \left[(A^1)^* A^0 - A^1 (A^0)^* \right] \left(e^{-2ikz_a} |g_{-1}\rangle\langle g_1| - e^{2ikz_a} |g_1\rangle\langle g_{-1}| \right) \\ H &= H_0 + H_1 \end{aligned} \tag{161}$$

where $J_z = |g_1\rangle\langle g_1| - |g_{-1}\rangle\langle g_{-1}|$ and $z_a = vt$. Transforming into a comoving coordinate system by $T(t) = e^{-ikvtJ_z}$ we get the time-independent transformed Hamiltonian $\tilde{H} = T(t) H T^\dagger(t) + kvJ_z$ which reads

$$\begin{aligned} \tilde{H}_0 &= \hbar U_0 |A^0|^2 \big[|g_0\rangle\langle g_0| + 7/6 \left(|g_{-1}\rangle\langle g_{-1}| + |g_1\rangle\langle g_1| \right) + \\ &\quad 1/6 \left(|g_1\rangle\langle g_{-1}| + |g_{-1}\rangle\langle g_1| \right) \big] \\ \tilde{H}_1 &= \left\{ \hbar k + 5/6 \hbar U_0 \left[(A^1)^* A^0 + A^1 (A^0)^* \right] \right\} J_z + \\ &\quad 1/6 \hbar U_0 \left[(A^1)^* A^0 - A^1 (A^0)^* \right] \left(|g_{-1}\rangle\langle g_1| - |g_1\rangle\langle g_{-1}| \right). \end{aligned} \tag{162}$$

where we have used $B^0(z_a) = A^0(z_a) e^{-2ikz_a}$ and $B^1(z_a) = -A^1(z_a) e^{-2ikz_a}$ to replace all B's by A's. It is easy to see that the eigenstates of $\tilde{H}_0$ are

$$\begin{aligned} |\tilde{\psi}_S^0\rangle &= \frac{1}{\sqrt{2}} \left(|g_1\rangle + |g_{-1}\rangle \right) \\ |\tilde{\psi}_A^0\rangle &= \frac{1}{\sqrt{2}} \left(|g_1\rangle - |g_{-1}\rangle \right) \end{aligned} \tag{163}$$

with eigenvalues $\tilde{E}_S^0 = 4/3 U_0 |A^0|^2$ and $\tilde{E}_A^0 = U_0 |A^0|^2$.

In the comoving coordinate system the perturbation caused by the atomic motion is time-independent and perturbation theory gives the first order corrections for the eigenstates

$$\begin{aligned}|\tilde{\psi}_S^1\rangle = &\frac{1}{U_0|A^0|^2/3}\Big\{k + 5/6U_0\left[(A^1)^*A^0 + A^1(A^0)^*\right] - \\ &1/6U_0\left[(A^1)^*A^0 - A^1(A^0)^*\right]\Big\}|\tilde{\psi}_A^0\rangle \\ |\tilde{\psi}_A^1\rangle = &-\frac{1}{U_0|A^0|^2/3}\Big\{k + 5/6U_0\left[(A^1)^*A^0 + A^1(A^0)^*\right] - \\ &1/6U_0\left[(A^1)^*A^0 - A^1(A^0)^*\right]\Big\}|\tilde{\psi}_S^0\rangle \end{aligned} \tag{164}$$

and eigenvalues $\tilde{E}_S^1 = 0$ and $\tilde{E}_A^1 = 0$. One can see that the wavefunctions are perturbed while the eigenenergies are not modified to first order in v. It is now obvious that contrary to the eigenstates for the atom at rest $|\tilde{\psi}_S^0\rangle$ and $|\tilde{\psi}_A^0\rangle$, $|\tilde{\psi}_S\rangle$ and $|\tilde{\psi}_A\rangle$ contain different proportions of $|g_{\pm 1}\rangle$ which explains the imbalance in groundstate sublevel population $\Pi_{\pm 1}$ for a moving atom. The perturbed symmetric eigenstate reads e. g.

$$\begin{aligned}|\tilde{\psi}_S\rangle = \frac{1}{\sqrt{2}}\Big\{ &\Big[1 + \frac{3kv}{U_0|A^0|^2} + \\ &\frac{v}{2|A^0|^2}\left(5((A^1)^*A^0 + A^1(A^0)^*) - ((A^1)^*A^0 - A^1(A^0)^*)\right)\Big]|g_1\rangle + \\ &\Big[1 - \frac{3kv}{U_0|A^0|^2} - \\ &\frac{v}{2|A^0|^2}\left(5((A^1)^*A^0 + A^1(A^0)^*) - ((A^1)^*A^0 - A^1(A^0)^*)\right)\Big]|g_{-1}\rangle\Big\} \end{aligned} \tag{165}$$

This shows that new physical effects not present in two-level atoms arise inside a cavity for atoms with degenerate groundstates. The free-space results found by Cohen-Tannoudji et al. [21] can be recovered by neglecting cavity dynamics, i. e. setting $A^1 = 0$.

5.2. Publication 5: Cavity-assisted polarization gradient cooling

Cavity-assisted polarization gradient cooling

Markus Gangl and Helmut Ritsch

Institut für Theoretische Physik, Universität Innsbruck,
Technikerstr. 25, A-6020 Innsbruck, Austria.

Abstract:
We show that light forces acting on atoms with degenerate groundstates are dramatically increased by the use of an optical ring resonator in a σ^+-σ^- setup. We generalize our previous results obtained for two-level atoms inside optical cavities to atoms with degenerate ground and excited states. It is shown that well-known free space polarization gradient cooling is modified by the backaction of the induced atomic dipole on the laser field. We present a detailed model that allows the calculation of the friction coefficient and shows the existence of a cooling force even for very far detuned lasers which makes this mechanism a candidate for the cooling of molecules. PACS number(s): 32.80.Pj, 42.50.Vk, 42.50.Lc

to be submitted

5.3. Introduction

The preparation of ultra-cold atoms for use in fundamental experiments that probe the quantum nature of matter [62, 63, 64] has become a field with ever growing importance, as can be seen in the light of the 1997 and 2001 Nobel prizes. A variety of cooling schemes to reach the low temperature regime has been investigated theoretically [1, 8, 9, 14, 22] and experimentally [4, 5, 6]. Each of these schemes however has problematic aspects that limit the reachable final temperature and atomic density in the trap. Doppler cooling, the very first mechanism exploited to cool atoms is limited by the random direction of the spontaneously emitted photons that are used to dissipate the kinetic energy of the atoms. This limit can be overcome by a more sophisticated laser setup together with the utilization of the existence of a very long internal time-scale for atoms with several degenerate Zeeman levels in their groundstate. A detailed investigation shows a spatially varying laser polarization to be essential for this cooling scheme leading to the denomination polarization gradient cooling. With this scheme temperatures lower than the Doppler limit by two orders of magnitude can be reached. Here the inherent heating process is connected to the recoil momentum of a single photon absorption-emission cycle. Going beyond this so called recoil limit is possible for certain atomic transitions [22, 70] but connected to serious practical problems such as long cooling times in three dimensions. A joint problem of all of the above cooling schemes even above the recoil limit is their dependence on spontaneous emission for dissipation which requires a closed optical transition. Hence none of these cooling schemes can be used to cool and trap molecules where no such closed transition exists due to vibrational and rotational couplings. Also the achievable final atomic density in the trap is limited by photon reabsorption. In some previous work [65] we have shown how these two problems can be overcome by the use of one or several degenerate resonator eigenmodes to dissipate the atomic energy. We found that in the strong coupling regime a significant reduction of cooling times as well as temperatures well below the Doppler limit are possible for any polarizable particle including molecules and Bose-Einstein-condensates. In this work we generalize our cavity cooling scheme for a two-level atom to atoms with several degenerate Zeeman sublevels in their ground and excited states moving in a σ^+-σ^- laser setup. We investigate how the well known free space polarization gradient cooling mechanism is modified by taking into account the backaction of the atom on the cavity field.

This work is organized as follows: In section 5.4 we introduce the model of an atom with a degenerate ground- and excited state interacting with the radiation modes of a high-Q ring cavity. In section 5.5 we study the equations of motion for the combined dynamics of the cavity modes and an atom with a $J_g = 1/2 \rightarrow J_e = 3/2$ and a $J_g = 1 \rightarrow J_e = 2$ transition, respectively. In section 5.6 the friction force is calculated analytically and the physical origin of its various contributions is discussed in the two limiting cases of an adiabatically following atom and cavity, respectively. Finally numerical results for the force for arbitrary velocities of the atom are discussed.

5.4. Model

In this section we develop the equations of motion for the combined dynamics of an atomic transition connecting two level manifolds $|g\rangle$ and $|e\rangle$ with angular momentum J_g and J_e respectively, coupled to the modes of a high-Q ring cavity. For simplicity we will approximate the modes by plane running waves and consider only the motion in one dimension. Generalization to three dimensions is, however, straightforward. The intracavity field can be decomposed in two counterpropagating modes for each polarization yielding $\vec{E}^+ = \mathcal{E}(\alpha_+ e^{ikz} + \alpha_- e^{-ikz})\vec{e}_+ + \mathcal{E}(\beta_+ e^{ikz} + \beta_- e^{-ikz})\vec{e}_-$ or in shorthand $\vec{E}^+ = A\vec{e}_+ + B\vec{e}_-$, where $\vec{e}_+ = -\frac{1}{\sqrt{2}}(\vec{e}_x + i\vec{e}_y)$, $\vec{e}_- = \frac{1}{\sqrt{2}}(\vec{e}_x - i\vec{e}_y)$, and $\mathcal{E} = \sqrt{\hbar\omega_P/(2\epsilon_0 V)}$ is the electric field that one would associate with a photon in a quantum mechanical description of the light field. Here $\alpha_\pm$, $\beta_\pm$ are the classical cavity mode amplitudes.

The system Hamiltonian for the internal atomic dynamics coupled to these fields in the rotating wave approximation can be written as

$$H = -\Delta_a P_e + g(A^* S_+ + B^* S_-) + g(S_+^\dagger A + S_-^\dagger B) \tag{166}$$

or in shorthand $H = -\Delta_a P_e + gG^- + gG^+$, with $g \equiv -d\mathcal{E}$ denoting the Rabifrequency for atomic transition with unit Clebsch-Gordon coefficient per photon and atomic dipole moment d, $\Delta_a = \omega_P - \omega_a$ being the detuning between pump and atom and $P_e = \sum_{m=-J_e}^{J_e} |e_m\rangle\langle e_m|$ being the projector on the excited atomic states and $P_g = \sum_{m=-J_g}^{J_g} |g_m\rangle\langle g_m|$ being the projector on the atomic ground states.

To include dissipation via atomic decay we use a standard master equation approach

$$\begin{aligned} \dot{\rho} &= -\frac{i}{\hbar}[H, \rho] + \mathcal{L}\rho \\ \mathcal{L}\rho &= -\Gamma(P_e\rho + \rho P_e - 2S_+\rho S_+^\dagger - 2S_-\rho S_-^\dagger - 2S_0\rho S_0^\dagger). \end{aligned} \tag{167}$$

where 2Γ is the atomic linewidth. Decomposing the density operator as $\rho = \rho_{gg} + \rho_{eg} + \rho_{ge} + \rho_{ee}$, with $\rho_{ij} = P_i\rho P_j$, where $i, j = e, g$ we get the equations of motion for the ground state manifold and the excited state manifold respectively as well as for the optical coherences between them

$$\begin{aligned} \dot{\rho}_{gg} &= -igG^-\rho_{eg} + ig\rho_{ge}G^+ + 2\Gamma(S_0\rho_{ee}S_0^\dagger + S_-\rho_{ee}S_-^\dagger + S_+\rho_{ee}S_+^\dagger) \\ \dot{\rho}_{ee} &= ig\rho_{eg}G^- - igG^+\rho_{ge} - 2\Gamma\rho_{ee} \\ \dot{\rho}_{eg} &= -igG^+\rho_{gg} + ig\rho_{ee}G^+ + (i\Delta_a - \Gamma)\rho_{eg} \end{aligned} \tag{168}$$

Adiabatic elimination of the excited atomic states in eq. 168 yields

$$\rho_{eg} = -\frac{ig}{\Gamma - i\Delta_a} G^+ \rho_{gg} \tag{169}$$

$$\rho_{ee} = \frac{g^2}{\Gamma^2 + \Delta_a^2} G^+ \rho_{gg} G^- \tag{170}$$

$$\dot{\rho}_{gg} = -\gamma_0 \{G^- G^+, \rho_{gg}\}_+ - iU_0 [G^- G^+, \rho_{gg}] + 2\gamma_0 \sum_{l=0,-,+} S_l G^+ \rho_{gg} G^- S_l^\dagger \tag{171}$$

where $\gamma_0 = \Gamma s$ is the spontaneous emission rate per photon and $U_0 = \Delta_a s$ is the optical potential per photon. For the adiabatic elimination to be valid the saturation parameter $s = g^2/(\Delta_a^2 + \Gamma^2)$ times the photon number has to be much smaller than one. In section 5.6 we will have to demand additionally that $kv \ll \Gamma$ where v is the velocity of the atom.

The fields are treated classically and hence described by a c-number amplitude α for each mode. Incorporating the slowly varying envelope approximation and the rotating wave approximation, Maxwell's equations provide

$$\begin{aligned}
\dot{\alpha}_+ &= (-\kappa + i\Delta_C)\alpha_+ - ige^{-ikz_a}\langle S_+ \rangle + \eta \\
\dot{\alpha}_- &= (-\kappa + i\Delta_C)\alpha_- - ige^{ikz_a}\langle S_+ \rangle \\
\dot{\beta}_+ &= (-\kappa + i\Delta_C)\beta_+ - ige^{-ikz_a}\langle S_- \rangle \\
\dot{\beta}_- &= (-\kappa + i\Delta_C)\beta_- - ige^{ikz_a}\langle S_- \rangle + \eta
\end{aligned} \tag{172}$$

for the amplitudes of the 4 cavity modes. η denotes the pump rate of the cavity, 2κ is the cavity linewidth, $\Delta_C = \omega_P - \omega_C$ the detuning between pump field and cavity field and z_a is the position of the atom. Analogous to the fields we describe the center-of-mass motion of the atom by a classical variable z_a. This description is adequate for not too cold atoms ($\hbar\omega_{Recoil} \ll k_B T$).

5.5. System Dynamics

Let us now turn to specific examples. Instead of using a general $J \to J+1$ transition, we will consider the two generic examples $1/2 \to 3/2$ and $1 \to 2$. This contains all the relevant physics and reduces the size of the equations.

5.5.1. $J_g = 1/2 \to J_e = 3/2$

Choosing $J_g = 1/2$ and $J_e = 3/2$ (fig. 1) we can specialize our results of section 5.4

with the generalized atomic lowering operators for right-, left- and linear polarized light (with respect to the cavity axis z)

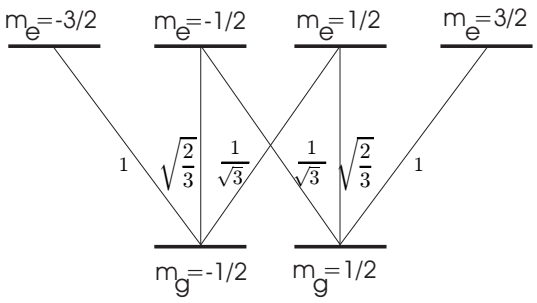

FIGURE 1. Level scheme for a $J_g = 1/2 \rightarrow J_e = 3/2$-transition.

$$
\begin{aligned}
S_+ &= \frac{1}{\sqrt{3}}|g_{-1/2}\rangle\langle e_{1/2}| + |g_{1/2}\rangle\langle e_{3/2}| \\
S_- &= |g_{-1/2}\rangle\langle e_{-3/2}| + \frac{1}{\sqrt{3}}|g_{1/2}\rangle\langle e_{-1/2}| \\
S_0 &= \sqrt{\frac{2}{3}}|g_{-1/2}\rangle\langle e_{-1/2}| + \sqrt{\frac{2}{3}}|g_{1/2}\rangle\langle e_{1/2}|
\end{aligned} \tag{173}
$$

and eqs. 171 we can calculate the equations of motion for the expectation values of the populations of the eigenstates of J_z, $\Pi_- = \langle g_{-1/2}|\rho_{gg}|g_{-1/2}\rangle$ and $\Pi_+ = \langle g_{1/2}|\rho_{gg}|g_{1/2}\rangle$

$$
\begin{aligned}
\dot{\Pi}_- &= -4/9\gamma_0(|A|^2 + |B|^2)\Pi_- + 4/9\gamma_0|B|^2 \\
\dot{\Pi}_+ &= -4/9\gamma_0(|A|^2 + |B|^2)\Pi_+ + 4/9\gamma_0|A|^2
\end{aligned} \tag{174}
$$

Note that any initial ground state coherence between $|g_{-1/2}\rangle$ and $|g_{1/2}\rangle$ decays to zero as there is no coherent coupling between these two states because of angular momentum conservation. Therefor incoherent one-photon processes are the only mechanism for population redistribution.

Inserting the steady state atomic populations

$$
\begin{aligned}
\langle S_+\rangle &= -\frac{ig}{\Gamma - i\Delta_a}A(1/3\Pi_- + \Pi_+) \\
\langle S_-\rangle &= -\frac{ig}{\Gamma - i\Delta_a}B(\Pi_- + 1/3\Pi_+)
\end{aligned} \tag{175}
$$

in eqs. 172 we get

$$
\begin{aligned}
\dot{\alpha}_+ &= (-\kappa + i\Delta_C)\alpha_+ - (\gamma_0 + iU_0)(\alpha_+ + \alpha_- e^{-2ikz_a})(1/3\Pi_- + \Pi_+) + \eta \\
\dot{\alpha}_- &= (-\kappa + i\Delta_C)\alpha_- - (\gamma_0 + iU_0)(\alpha_- + \alpha_+ e^{2ikz_a})(1/3\Pi_- + \Pi_+) \\
\dot{\beta}_+ &= (-\kappa + i\Delta_C)\beta_+ - (\gamma_0 + iU_0)(\beta_+ + \beta_- e^{-2ikz_a})(\Pi_- + 1/3\Pi_+) \\
\dot{\beta}_- &= (-\kappa + i\Delta_C)\beta_- - (\gamma_0 + iU_0)(\beta_- + \beta_+ e^{2ikz_a})(\Pi_- + 1/3\Pi_+) + \eta
\end{aligned} \tag{176}
$$

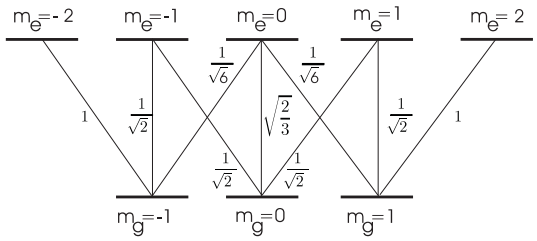

FIGURE 2. Level scheme for a $J_g = 1 \to J_e = 2$-transition.

which shows that changes in the groundstate sub-level populations affect the phase and amplitude of the cavity modes.

Note that the differently polarized field modes $\alpha_\pm$ and $\beta_\pm$ do not couple to each other. This can be seen clearly by calculating the steady state of eqs. 174 and eqs. 176 for the atom at rest at position z_a

$$\begin{aligned}
\Pi_+^0 &= 1/2 \\
\Pi_-^0 &= 1/2 \\
\alpha_+^0 &= \frac{\eta}{-\kappa + i\Delta_C} \frac{-\kappa - 2/3\gamma_0 + i(\Delta_C - 2/3U_0)}{\kappa + 4/3\gamma_0 - i(\Delta_C - 4/3U_0)} \\
\alpha_-^0 &= \frac{\eta}{-\kappa + i\Delta_C} \frac{2/3(\gamma_0 + iU_0)e^{2ikz_a}}{\kappa + 4/3\gamma_0 - i(\Delta_C - 4/3U_0)} \\
\beta_+^0 &= \frac{\eta}{-\kappa + i\Delta_C} \frac{2/3(\gamma_0 + iU_0)e^{-2ikz_a}}{\kappa + 4/3\gamma_0 - i(\Delta_C - 4/3U_0)} \\
\beta_-^0 &= \frac{\eta}{-\kappa + i\Delta_C} \frac{-\kappa - 2/3\gamma_0 + i(\Delta_C - 2/3U_0)}{\kappa + 4/3\gamma_0 - i(\Delta_C - 4/3U_0)}
\end{aligned} \tag{177}$$

Due to translational symmetry we find equal populations independent of z_a. Similar to the two state case for strong coupling $\kappa, \gamma_0 \ll U_0$ we find a standing wave field with a node at the atomic position. Note that the σ^+-polarized field at the position of an atom at rest $A^0(z_a) = \alpha_+^0 e^{ikz_a} + \alpha_-^0 e^{-ikz_a} = \eta e^{ikz_a}/(\kappa + 4/3\gamma_0 - i(\Delta_C - U_0))$ relates to the σ^--polarized field $B^0(z_a) = \beta_+^0 e^{ikz_a} + \beta_-^0 e^{-ikz_a} = \eta e^{-ikz_a}/(\kappa + 4/3\gamma_0 - i(\Delta_C - U_0))$ by $A^0(z_a)e^{-ikz_a} = B^0(z_a)e^{ikz_a}$.

5.5.2. $J_g = 1 \to J_e = 2$

Let us now turn to the next example $1 \to 2$. Here coherent coupling decouples the system into a V and a W subsystem, allowing ground state coherences to build up. For this transition (fig. 2) the atomic lowering operators read

$$
\begin{aligned}
S_+ &= \frac{1}{\sqrt{6}}|g_{-1}\rangle\langle e_0| + \frac{1}{\sqrt{2}}|g_0\rangle\langle e_1| + |g_1\rangle\langle e_2| \\
S_- &= \frac{1}{\sqrt{6}}|g_1\rangle\langle e_0| + \frac{1}{\sqrt{2}}|g_0\rangle\langle e_{-1}| + |g_{-1}\rangle\langle e_{-2}| \\
S_0 &= \frac{1}{\sqrt{2}}|g_{-1}\rangle\langle e_{-1}| + \sqrt{\frac{2}{3}}|g_0\rangle\langle e_0| + \frac{1}{\sqrt{2}}|g_1\rangle\langle e_1|
\end{aligned} \tag{178}
$$

The population equations then are

$$
\begin{aligned}
\dot{\Pi}_- &= -5/18\gamma_0|A|^2\Pi_- + 1/18\gamma_0|B|^2\Pi_+ + 1/2\gamma_0|B|^2\Pi_0 - \\
&\quad (1/9\gamma_0 + 1/6iU_0)A^*B\rho_{+-} + cc. \\
\dot{\Pi}_+ &= -5/18\gamma_0|B|^2\Pi_+ + 1/18\gamma_0|A|^2\Pi_- + 1/2\gamma_0|A|^2\Pi_0 - \\
&\quad (1/9\gamma_0 - 1/6iU_0)A^*B\rho_{+-} + cc. \\
\dot{\Pi}_0 &= -1/2\gamma_0(|A|^2 + |B|^2)\Pi_0 + 2/9\gamma_0|A|^2\Pi_- + 2/9\gamma_0|B|^2\Pi_+ + \\
&\quad 2/9\gamma_0 A^*B\rho_{+-} + cc. \\
\dot{\rho}_{+-} &= -5/6\gamma_0(|A|^2 + |B|^2)\rho_{+-} - i5/6U_0(|A|^2 - |B|^2)\rho_{+-} + 1/2\gamma_0 B^*A\Pi_0 + \\
&\quad 1/6(\gamma_0 + iU_0)B^*A\Pi_+ + 1/6(\gamma_0 - iU_0)B^*A\Pi_-
\end{aligned} \tag{179}
$$

where $\Pi_- = \langle g_{-1}|\rho_{gg}|g_{-1}\rangle$, $\Pi_0 = \langle g_0|\rho_{gg}|g_0\rangle$, $\Pi_+ = \langle g_1|\rho_{gg}|g_1\rangle$, $\rho_{-+} = \langle g_{-1}|\rho_{gg}|g_1\rangle$ while for the field amplitudes we now find

$$
\begin{aligned}
\dot{\alpha}_+ &= (-\kappa + i\Delta_C)\alpha_+ - (\gamma_0 + iU_0)[(\alpha_+ + \alpha_- e^{-2ikz_a})(1/6\Pi_- + 1/2\Pi_0 + \Pi_+) + \\
&\quad 1/6(\beta_+ + \beta_- e^{-2ikz_a})\rho_{+-}] + \eta \\
\dot{\alpha}_- &= (-\kappa + i\Delta_C)\alpha_- - (\gamma_0 + iU_0)[(\alpha_- + \alpha_+ e^{2ikz_a})(1/6\Pi_- + 1/2\Pi_0 + \Pi_+) + \\
&\quad 1/6(\beta_- + \beta_+ e^{2ikz_a})\rho_{+-}] \\
\dot{\beta}_+ &= (-\kappa + i\Delta_C)\beta_+ - (\gamma_0 + iU_0)[(\beta_+ + \beta_- e^{-2ikz_a})(1/6\Pi_+ + 1/2\Pi_0 + \Pi_-) + \\
&\quad 1/6(\alpha_+ + \alpha_- e^{-2ikz_a})\rho_{-+}] \\
\dot{\beta}_- &= (-\kappa + i\Delta_C)\beta_- - (\gamma_0 + iU_0)[(\beta_- + \beta_+ e^{2ikz_a})(1/6\Pi_+ + 1/2\Pi_0 + \Pi_-) + \\
&\quad 1/6(\alpha_- + \alpha_+ e^{2ikz_a})\rho_{-+}] + \eta
\end{aligned} \tag{180}
$$

The amplitudes of the differently polarized modes are now connected by the atomic groundstate coherence ρ_{+-}. Obviously there is a mechanism for atomic population transfer via a stimulated two-photon process even for the $\gamma_0 \to 0$ case in the $J_g = 1 \to J_e = 2$-transition. Later we will show that this allows for a new mechanism to cool atoms in an efficient way even for large atomic detunings Δ_a, where only cavity dissipation is present.

We can again calculate the steady-state for the combined system atom and cavity to find

$$
\begin{aligned}
\Pi_+ &= 13/34 \\
\Pi_- &= 13/34 \\
\Pi_0 &= 4/17 \\
\rho_{+-} &= 5/34 e^{2ikz_a} \\
\alpha_+^0 &= \frac{\eta}{-\kappa + i\Delta_C} \frac{-\kappa - 10/17\gamma_0 + i(\Delta_C - 10/17U_0)}{\kappa + 20/17\gamma_0 - i(\Delta_C - 20/17U_0)} \\
\alpha_-^0 &= \frac{\eta}{-\kappa + i\Delta_C} \frac{10/17(\gamma_0 + iU_0)e^{2ikz_a}}{\kappa + 20/17\gamma_0 - i(\Delta_C - 20/17U_0)} \\
\beta_+^0 &= \frac{\eta}{-\kappa + i\Delta_C} \frac{10/17(\gamma_0 + iU_0)e^{-2ikz_a}}{\kappa + 20/17\gamma_0 - i(\Delta_C - 20/17U_0)} \\
\beta_-^0 &= \frac{\eta}{-\kappa + i\Delta_C} \frac{-\kappa - 10/17\gamma_0 + i(\Delta_C - 10/17U_0)}{\kappa + 20/17\gamma_0 - i(\Delta_C - 20/17U_0)}
\end{aligned} \tag{181}
$$

Again the populations are position independent and also independent of γ_0 and U_0. We see that eqs. 177 and 181 yield the same results for the fields, if we take account of the different Clebsch-Gordon coefficients.

5.5.3. Forces

Let us now turn to the light forces induced by the field. Following the standard semiclassical treatment [14] the expectation value of the force operator reads

$$
f = -g(Tr(\nabla G^+ \rho) + Tr(\nabla G^- \rho)) \tag{182}
$$

For an atom at rest we simply insert the steady state value for the optical coherences to find for a $J_g = 1/2 \rightarrow J_e = 3/2$-transition

$$
\begin{aligned}
f &= f_{rp} + f_{dip} \\
f_{rp} &= 2\hbar k\gamma_0(|\alpha_+|^2 - |\alpha_-|^2)(1/3\Pi_- + \Pi_+) + 2\hbar k\gamma_0(|\beta_+|^2 - |\beta_-|^2)(\Pi_- + 1/3\Pi_+) \\
f_{dip} &= 2\hbar k i U_0(\alpha_+^* \alpha_- e^{-2ikz_a} - \alpha_-^* \alpha_+ e^{2ikz_a})(1/3\Pi_- + \Pi_+) + \\
&\quad 2\hbar k i U_0(\beta_+^* \beta_- e^{-2ikz_a} - \beta_-^* \beta_+ e^{2ikz_a})(\Pi_- + 1/3\Pi_+)
\end{aligned} \tag{183}
$$

Here f_{rp} denote contributions stemming from incoherent photon scattering out of the cavity proportional to γ_0. f_{dip} denote contributions from coherent photon redistribution between the modes proportional to U_0. Clearly although we have a standing wave formation all forces vanish for an atom at rest and symmetric pump as one would expect from translational symmetry. Hence the atoms are not drawn to a specific position and see a constant adiabatic potential. However this symmetry will be broken for a moving atom and forces will appear, which depending on parameters can accelerate or decelerate a moving particle. This is similar to the free-space case, which can of course be recovered by setting $\alpha_- = \beta_+ = 0$ and neglecting any time-dependence of α_+, β_-.

For a $J_g = 1 \rightarrow J_e = 2$-transition we find

$$\begin{aligned}
f_{rp} = & 2\hbar k\gamma_0(|\alpha_+|^2 - |\alpha_-|^2)(1/6\Pi_- + 1/2\Pi_0 + \Pi_+) + \\
& 2\hbar k\gamma_0(|\beta_+|^2 - |\beta_-|^2)(\Pi_- + 1/2\Pi_0 + 1/6\Pi_+) + \\
& 1/3\rho_{-+}\hbar k\gamma_0(\beta_+^*\alpha_+ - \beta_-^*\alpha_-) + \\
& 1/3\rho_{+-}\hbar k\gamma_0(\alpha_+^*\beta_+ - \alpha_-^*\beta_-) \\
f_{dip} = & 2\hbar kiU_0(\alpha_+^*\alpha_- e^{-2ikz_a} - \alpha_-^*\alpha_+ e^{2ikz_a})(1/6\Pi_- + 1/2\Pi_0 + \Pi_+) + \\
& 2\hbar kiU_0(\beta_+^*\beta_- e^{-2ikz_a} - \beta_-^*\beta_+ e^{2ikz_a})(\Pi_- + 1/2\Pi_0 + 1/6\Pi_+) + \\
& 1/3\rho_{+-}i\hbar kU_0(\alpha_+^*\beta_- e^{-2ikz_a} - \alpha_-^*\beta_+ e^{2ikz_a}) - \\
& 1/3\rho_{-+}i\hbar kU_0(\alpha_+\beta_-^* e^{2ikz_a} - \alpha_-\beta_+^* e^{-2ikz_a})
\end{aligned} \tag{184}$$

Comparing eqs. 183 and 184 we see that the additional terms in eqs. 184 are caused by two-photon transitions between modes of different polarization mediated by the groundstate coherences ρ_{+-} and ρ_{-+}. In free space only the first and the third term on the last line in eqs. 184 would be present since all other terms contain unpumped modes of radiation (α_-,β_+).

5.6. Moving atom

In this section we will turn to the more interesting aspect of the influence of the cavity on the cooling properties.

For the coupled system atom and cavity there are 3 different time-scales: $T_\kappa = 1/\kappa$, $T_\Gamma = 1/\Gamma$ and $T_\gamma = 1/(\gamma_0|A^0|^2)$.

$T_\kappa = 1/\kappa$ is the cavity time-lag, $T_\Gamma = 1/\Gamma$ is the radiative life-time of the excited atomic state and $T_\gamma = 1/(\gamma_0|A^0|^2)$ is the optical pumping time (atomic time-lag).

For adiabatic elimination of the atomic excited state manifold and low cavity photon number $|A^0|^2$ the inequality $\kappa, \gamma_0|A^0|^2 \ll \Gamma$ must be fullfilled. Due to the three time-scales there are several different parameter regimes to be studied depending on their relative size.

5.6.1. Adiabatic following of cavity dynamics

Let us first look at the case of large atom-pump detuning and a slow atom with a $1 \rightarrow 2$ transition. If $\gamma_0|A^0|^2 \ll \kappa$ and $kv \ll \kappa$ the cavity field will follow the atom adiabatically, in this regime we can neglect any time lag of the field modes as long as $kv \ll \kappa$. Inserting steady-state values 181 we obtain for the force on the atom

$$f_{dip} = -2/3\hbar k U_0 |A^0|^2 C_i \left[1 + \frac{20/17(\kappa\gamma_0 - \Delta_C U_0)}{\kappa^2 + \Delta_C^2}\right] + 5/3\hbar k U_0 |A^0|^2 \langle J_z\rangle \frac{20/17(U_0\kappa + \gamma_0\Delta_C)}{\kappa^2 + \Delta_C^2}$$
$$f_{rp} = 5/3\hbar k \gamma_0 |A^0|^2 \langle J_z\rangle \left[1 + \frac{20/17(\kappa\gamma_0 - \Delta_C U_0)}{\kappa^2 + \Delta_C^2}\right] + 2/3\hbar k \gamma_0 |A^0|^2 C_i \frac{20/17(U_0\kappa + \gamma_0\Delta_C)}{\kappa^2 + \Delta_C^2} \quad (185)$$

which gives as a total force of

$$f = 2\hbar k \gamma_0 \langle J_z\rangle |A^0|^2 \left[1 + \frac{20/17(\kappa\gamma_0 - \Delta_C U_0)}{\kappa^2 + \Delta_C^2}\right] + \hbar k \frac{5U_0^2 - \gamma_0^2}{3U_0} \langle J_z\rangle |A^0|^2 \frac{20/17(U_0\kappa + \Delta_C\gamma_0)}{\kappa^2 + \Delta_C^2} \quad (186)$$

Note that the part that is multiplied by 1 in the first term of the expression for the force is just the result obtained in the original work by Cohen-Tannoudji et al. [14] in the free-space regime. Noting that $\alpha_+ = \beta_-$ and $\alpha_- e^{-2ikz_a} = \beta_+ e^{2ikz_a}$ we see that the bracket in the first term is just $|\alpha_+|^2 - |\alpha_-|^2$, which results from a modification of radiation pressure in a ring resonator. The second term is proportional to $i(\alpha_+\alpha_-^* e^{-2ikz_a} - \alpha_+^*\alpha_- e^{2ikz_a})$ and does not appear at all in free space (lack of counterpropagating modes of equal polarization). It describes the dipole force exerted by the co-moving standing wave created by the atom. This term becomes dominant for $\gamma_0 \ll U_0$. As $\langle J_z\rangle$ depends on $|A^0|^2$ like $1/|A^0|^2$ and $C_i = -\gamma_0/(2U_0)\langle J_z\rangle$ it can be seen, that in this limit the total force $f_{dip} + f_{rp}$ is independent of the intensity. Obviously $f_{rp} \ll f_{dip}$ if $\gamma_0 \ll U_0$ as opposed to the situation in free-space, where radiation pressure is stronger than the dipole force even in this case. The explanation is of course that in free-space the stimulated redistribution processes that are the origin of the dipole force are limited to a finite number of steps in the case of a σ^+-σ^--configuration [14]. In a cavity this argument is no longer correct. There can be an unlimited number of redistribution events due to the existence of a counterpropagating beam for each of the two polarizations.

For a very slow atom ($kv \ll |A^0|^2\gamma_0$) eq. 186 specializes to

$$f = 2\hbar k \gamma_0 \frac{kv}{\gamma_0}\frac{30}{17}\frac{U_0\gamma_0}{(U_0^2 + 5\gamma_0^2)}\left[1 + \frac{20/17(\kappa\gamma_0 - \Delta_C U_0)}{\kappa^2 + \Delta_C^2}\right] + \hbar k \frac{5U_0^2 - \gamma_0^2}{3U_0}\frac{kv}{\gamma_0}\frac{30}{17}\frac{U_0\gamma_0}{(U_0^2 + 5\gamma_0^2)}\frac{20/17(U_0\kappa + \Delta_C\gamma_0)}{\kappa^2 + \Delta_C^2} \quad (187)$$

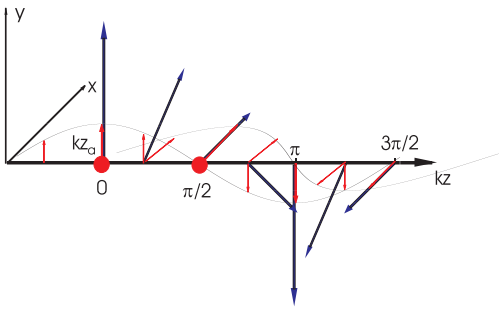

FIGURE 3. Cavity electric field in a σ^+-σ^- setup, modified by an atom at position $kz_a = 0$ and $kz_a = \pi/2$ respectively. The field scattered by the atom has a cosine envelope and a polarization along the local pump field.

which is clearly independent of the intensity $|A^0|^2$.
Here we have used

$$\langle J_z \rangle = \frac{30}{17} \frac{U_0 \gamma_0}{(U_0^2 + 5\gamma_0^2)} \frac{kv}{|A^0|^2 \gamma_0} \tag{188}$$

In the case of a $1/2 \to 3/2$-transition we will show later (section 5.6.3) that in this limit there is no force on an atom.

The effect of the atom on the cavity field is easy to see (eq. 189 and fig. 3). The first term is the pump field which is of linear polarization rotating around the z-axis. The atom creates a standing wave field with polarization parallel to the field at its position and a phase dependent on its location. This scattered field is dragged by the atom as it moves along the z-axis. E. g. for the atom at position $kz_a = 0$ the scattered field is polarized along the y-axis while it has a polarization along the x-axis if the atom sits at $kz_a = \pi/2$. The total field inside the cavity is the sum of the pump and scattered field.

$$\begin{aligned} \vec{E}^+ = & \frac{\eta}{\kappa - i\Delta_C}(\sin kz\vec{e}_x + \cos kz\vec{e}_y) - \\ & \frac{20}{17}\frac{\gamma_0 + iU_0}{\kappa - i\Delta_C}\frac{\eta \cos k(z - z_a)}{\kappa + 20/17\gamma_0 - i(\Delta_C - 20/17U_0)}(\sin kz_a\vec{e}_x + \cos kz_a\vec{e}_y) \end{aligned} \tag{189}$$

5.6.2. Adiabatic following of the atomic dynamics

In the good cavity limit where $\kappa \ll \gamma_0$ the atomic variables will follow adiabatically the evolution of the cavity fields as long as $kv \ll \gamma_0|A^0|^2$. Hence we cannot expect any atom mediated force terms for either transition. Consequently eqs. 183 for a $1/2 \to 3/2$-transition simplify to

$$\begin{aligned} f_{rp} &= \hbar k \gamma_0 4/3(|\alpha_+|^2 - |\alpha_-|^2 + |\beta_+|^2 - |\beta_-|^2) \\ f_{dip} &= \hbar k i U_0 4/3 \left[(\alpha_+^* \alpha_- + \beta_+^* \beta_-)e^{-2ikz_a} - (\alpha_-^* \alpha_+ + \beta_-^* \beta_+)e^{2ikz_a}\right] \end{aligned} \tag{190}$$

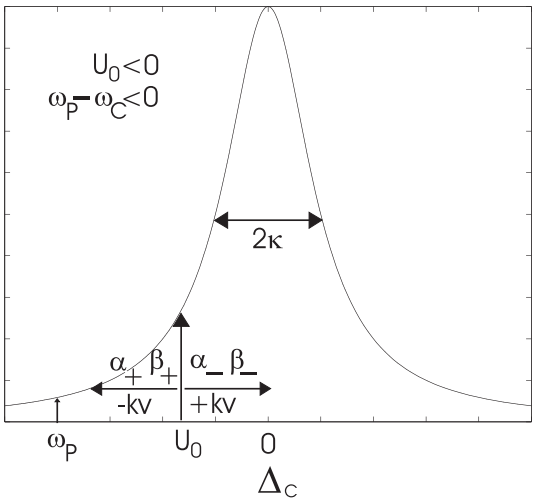

FIGURE 4. Cavity line profile. A moving atom can shift the counter-propagating pumped cavity mode in resonance.

Obviously all modes are weighted by the same combination of steady-state atomic populations and Clebsch-Gordon coefficients. Differing photon numbers can only be expected for a moving atom which produces a velocity-dependent index of refraction. Copropagating modes will experience a refraction index different from counterpropagating ones due to the Doppler-shifted cavity frequencies. This will result in non-zero cavity-mediated dipole- and radiation pressure forces on the atom in either transition.

Eqs. 184 simplify to

$$\begin{aligned} f_{rp} =& \hbar k\gamma_0 115/102(|\alpha_+|^2 - |\alpha_-|^2 + |\beta_+|^2 - |\beta_-|^2) + \\ & 5/102 e^{-2ikz_a}\hbar k\gamma_0(\beta_+^*\alpha_+ - \beta_-^*\alpha_-) + 5/102 e^{2ikz_a}\hbar k\gamma_0(\alpha_+^*\beta_+ - \alpha_-^*\beta_-) \\ f_{dip} =& \hbar k i U_0 115/102 \left[(\alpha_+^*\alpha_- + \beta_+^*\beta_-)e^{-2ikz_a} - (\alpha_-^*\alpha_+ + \beta_-^*\beta_+)e^{2ikz_a}\right] \\ & 5/102 e^{2ikz_a} i\hbar k U_0(\alpha_+^*\beta_- e^{-2ikz_a} - \alpha_-^*\beta_+ e^{2ikz_a}) - \\ & 5/102 e^{-2ikz_a} i\hbar k U_0(\alpha_+\beta_-^* e^{2ikz_a} - \alpha_-\beta_+^* e^{-2ikz_a}) \end{aligned} \tag{191}$$

We get additional force terms due to the steady-state atomic ground state coherences in both f_{rp} and f_{dip}. While we have photon redistribution between modes of equal polarization only for a $1/2 \rightarrow 3/2$-transition, stimulated Raman transitions between $|g_{-1}\rangle$ and $|g_1\rangle$ can transfer photons between σ^+ and σ^- polarized modes.

5.6.3. Full dynamics

In the intermediate regime between the two previous limiting cases ($\kappa \approx \gamma_0$ or $\gamma_0 \ll \kappa$ and $kv \approx \kappa$) we have to deal with the combined time-dependence of cavity and atomic expressions. For this one can still get analytical results in the limit of a slow atom ($kv \ll min(\gamma_0|A^0|^2, \kappa)$). This allows one to find a qualitative picture

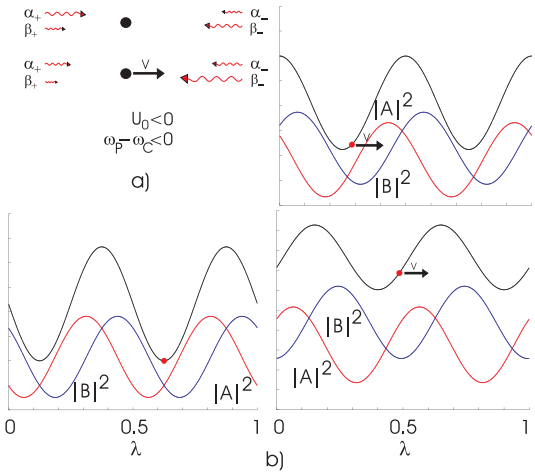

FIGURE 5. a) Copropagating modes are shifted out of resonance and counterpropagating modes are shifted into resonance by a moving atom. b) Cavity fields for an atom at rest (top), $kv = \gamma_0$ (middle) and $kv = \kappa$ (bottom). $\Delta_C = -1.2\Gamma$, $U_0 = -0.1\Gamma$, $\gamma_0 = 0.1\Gamma$, $\kappa = 0.3\Gamma$.

of the interaction between a multilevel atom and the cavity modes (choose $\Delta_C < 0$, $U_0 < 0$):

An atom at rest with equally populated ground state levels shifts all cavity modes closer towards resonance, but still the pump is red detuned with respect to the cavity. An atom moving in positive z-direction shifts the counterpropagating modes β_-, α_- into resonance while the copropagating modes α_+, β_+ are shifted out of resonance even further (fig. 4). Hence the σ^--polarized light intensity gets larger than the σ^+-polarized and the atom is optically pumped into Π_-. If the population was completely pumped into this state, the coupling between atom and σ^+-polarized cavity modes gets weaker, leading to an increase in σ^+-polarized light intensity and increased redistribution to Π_+. Therefore the combined system atom and cavity reaches a steady state with a non-zero population difference and different intensities for both polarizations of the intracavity field. The force on the atom in this steady state is exerted mostly by the σ^--polarized light (fig. 5). For the $1/2 \to 3/2$ transition this forces are caused by one-photon transitions only, for a $1 \to 2$ transition there are additional two-photon processes at very low velocities, even for $\gamma_0 = 0$. In free space these two-photon effects lead to a time-lag between the induced atomic dipole vector and the local electric field leading to the well known polarization gradient cooling effects described by Cohen-Tannoudji [14]. Equivalently an atom with very small γ_0 moving in a cavity experiences a non-aligned cavity field due to the non-zero cavity reaction time if κ is not too large.

5.6.4. Friction forces

Let us now study the limit where $T_{int} \ll T_{ext}$ where $T_{ext} = 1/(kv)$, that is a slowly moving atom, more carefully. To this end we expand the cavity fields in the form $A \approx A^0 + vA^1$, $B \approx B^0 + vB^1$ and the atomic groundstate populations

as $\Pi_\pm \approx \Pi^0_\pm + v\Pi^1_\pm$. For a $J_g = 1 \to J_e = 2$ transition we have additionally $\rho_{+-} \approx (C^0_r + iC^0_i)e^{2ikz_a} + v(C^1_r + iC^1_i)e^{2ikz_a}$ In this subsection we will set $\Delta_C = 0$ in order to increase readability of our results.

We note that the population imbalance $\langle J_z\rangle = \Pi_+ - \Pi_-$ can be written as $\langle J_z\rangle = -2\Pi_- v$ for a slowly moving atom. Using symmetry considerations we see that $B^0(z_a)e^{ikz_a} = A^0(z_a)e^{-ikz_a}$ and $B^1(z_a)e^{ikz_a} = -A^1(z_a)e^{-ikz_a}$. Furthermore we note that $C^0_i = 0$ and $C^1_r = 0$.

Hence we have the following two algebraic equations for the first order corrections in v for a $J_g = 1/2 \to J_e = 3/2$ transition

$$\begin{aligned}\Pi^1_- &= -\frac{1}{2|A^0|^2}\left[(A^1)^* A^0 + A^1(A^0)^*\right]\\ A^1 &= \frac{A^0(\gamma_0 + iU_0)}{\kappa\left[\kappa + 4/3(\gamma_0 + iU_0)\right]}\left(4/3\kappa\Pi^1_- + i\frac{4}{3}k\right),\end{aligned} \tag{192}$$

where $A^0 = \eta e^{ikz_a}/(\kappa + 4/3\gamma_0 + i4/3U_0)$. Note that an unbalanced groundstate population is only due to a time-lag in the cavity response for a $1/2 \to 3/2$-transition. Hence one cannot expect any non-trivial kinetic effects in the limit where the cavity fields follow the atom adiabatically. This explains our previous result of section 5.6.1. We get the following three equations for a $J_g = 1 \to J_e = 2$ transition

$$\begin{aligned}\Pi^1_- &= \frac{U_0}{\gamma_0}C^1_i - \frac{15}{102\gamma_0|A^0|^2}\left[5\gamma_0(A^{1*}A^0 + c.c.) + iU_0(A^{1*}A^0 - c.c.)\right]\\ C^1_i &= -\frac{U_0}{5\gamma_0}\Pi^1_- - \frac{6}{34}\frac{k}{\gamma_0|A^0|^2} - \frac{5}{3|A^0|^2 102}\left[\frac{U_0}{\gamma_0}(A^{1*}A^0 + c.c.) - i(A^{1*}A^0 - c.c.)\right]\\ A^1 &= \frac{2A^0(\gamma_0 + iU_0)}{\kappa\left[\kappa + 55/51(\gamma_0 + iU_0)\right]}\left(5/6\kappa\Pi^1_- - i\kappa/6C^1_i + i\frac{10}{17}k\right)\end{aligned} \tag{193}$$

with corresponding $A^0 = \eta e^{ikz_a}/(\kappa + 20/17\gamma_0 + i20/17U_0)$.

Note that we recover the equations found by Cohen-Tannoudji by setting $A^1 = 0$, i. e. neglecting any atomic influence on the cavity field.

a. $J_g = 1/2 \to J_e = 3/2$**.**

$$\begin{aligned}f_{rp} &= \frac{8/3\hbar k^2 v|A^0|^2}{\kappa^2|b|^2}\frac{4\gamma_0}{3k}\Pi^1_-\\ &\quad\left[4U_0^2\kappa^2 + 28/3\gamma_0^2\kappa^2 - 3/4\kappa^4 + 160/9\kappa\gamma_0(\gamma_0^2 + U_0^2) + 256/27(\gamma_0^2 + U_0^2)^2\right]\\ f_{dip} &= \frac{-8/3\hbar k^2 v|A^0|^2}{\kappa^2|b|^2}\left\{\frac{8}{3k}\Pi^1_- U_0^2\kappa^2(\kappa + 4/3\gamma_0) + \right.\\ &\quad\left. 16/9U_0\left[(\gamma_0^2 + U_0^2)(\kappa + 8/3\gamma_0) + \kappa(U_0^2 + 3/2\gamma_0\kappa + 3\gamma_0^2)\right]\right\}\end{aligned} \tag{194}$$

where

$$
\begin{aligned}
b &= \kappa + 4/3(\gamma_0 + iU_0) \\
A^0 &= \frac{\eta}{b} e^{ikz_a} \\
\Pi^1_- &= \frac{4/3kU_0}{(\kappa + 4/3\gamma_0)(\kappa + 8/3\gamma_0) + 32/9U_0^2}
\end{aligned} \tag{195}
$$

for $\gamma_0 > 0$.

Obviously radiation pressure f_{rp} is caused solely by the cavity-induced Π^1_-, while there is a second term in the expression for the dipole force f_{dip} that is the cavity-induced force, as for a two-level atom in a ring cavity.

In the strong coupling regime where $\kappa, \gamma_0 \ll U_0$, we get $\Pi_- = 3k/(8U_0)$ and we receive for the friction forces

$$f_{rp} = \frac{64}{9} \frac{\hbar k^2 \gamma_0 U_0 |A^0|^2}{\kappa^2} v \tag{196}$$

$$f_{dip} = \frac{48}{9} \frac{\hbar k^2 U_0 |A^0|^2}{\kappa} v - \frac{64}{9} \frac{\hbar k^2 \gamma_0 U_0 |A^0|^2}{\kappa^2} v \tag{197}$$

$$f_{tot} = \frac{48}{9} \frac{\hbar k^2 U_0 |A^0|^2}{\kappa} v \tag{198}$$

The total force f_{tot} is just the result we obtained in the corresponding limit for a two-level atom in a symmetrically pumped ring cavity if we replace $4/3U_0$ by U_0. This means that in the limit where $\kappa, \gamma_0 \ll U_0$, the radiation pressure force that is caused by the motion-induced population difference and the corresponding part of the dipole force cancel each other.

b. $J_g = 1 \to J_e = 2$**.** In the limit of a slowly moving atom, the general friction force can be thought of as a contribution of cavity mediated terms (proportional to $|A^0|^2$) and atomic mediated terms (independent of $|A^0|^2$). Thus for high intensity $|A^0|^2$ the cavity mediated force terms (eqs. 198) will dominate, while for small intensity the cavity-modified terms in eqs. 186 will prevail.

$$
\begin{aligned}
f_{rp} = & \frac{2\hbar k\gamma_0 v|A^0|^2}{\kappa^2|b|^2}\Big\{5/6\kappa^2\Pi_-^1\Big[6600/51^2(\gamma_0^2+U_0^2) - 230/51\gamma_0\kappa - \\
& 2\kappa^2 - 13200/51^2\gamma_0^2\Big] + \\
& \kappa^2/6C_i^1U_0\Big(230/51\kappa + 13200/51^2\gamma_0\Big) + \\
& \frac{55}{51}\frac{10}{17}kU_0\Big[10/55\kappa^2 + 240/51\kappa\gamma_0 + 13200/51^2(\gamma_0^2+U_0^2)\Big]\Big\} \\
f_{dip} = & -\frac{2\hbar kU_0 v|A^0|^2}{\kappa^2|b|^2}\Big\{5/6\kappa^2\Pi_-^1U_0\Big(230/51\kappa + 13200/51^2\gamma_0\Big) - \\
& \kappa^2/6C_i^1\Big[6600/51^2(\gamma_0^2+U_0^2) - 230/51\gamma_0\kappa - 2\kappa^2 - 13200/51^2\gamma_0^2\Big] + \\
& \frac{55}{51}\frac{10}{17}k\Big[(24055/51^2\gamma_0 + 350/51\kappa)(\gamma_0^2+U_0^2) + \\
& 120/51\kappa(\gamma_0^2-U_0^2) + 230/55\kappa^2\gamma_0\Big]\Big\}
\end{aligned}
\tag{199}
$$

where

$$
\begin{aligned}
|A^0|^2 &= \frac{\eta^2}{(\kappa+20/17\gamma_0)^2 + (20/17U_0)^2} \\
|b|^2 &= (\kappa+55/51\gamma_0)^2 + (55/51U_0)^2
\end{aligned}
$$

We did not insert our result for C_i^1

$$
\begin{aligned}
C_i^1 = & \frac{-1}{\frac{5}{3}\left[\gamma_0 + \frac{10}{102|b|^2}(\gamma_0^2+U_0^2)(\kappa+55/51\gamma_0)\right]} \\
& \left\{\frac{10k}{34|A^0|^2} - \frac{1500k}{51^2\kappa|b|^2}(\gamma_0^2+U_0^2)\left(\kappa+\frac{55}{51}\gamma_0\right) + \right. \\
& \left.\Pi_-^1\frac{U_0}{3}\left[1+\frac{6875}{51^2|b|^2(\gamma_0^2+U_0^2)}\right]\right\}
\end{aligned}
\tag{200}
$$

and Π_-

$$\Pi^1_- = \frac{\frac{5kU_0}{51^2|b|^2}\left\{100(5\gamma_0^2+U_0^2)-\frac{1}{|A^0|^2}\left[90\kappa\gamma_0+51\kappa^2+60\frac{55}{51}(\gamma_0^2+U_0^2)\right]\right\}}{u1+u2} \tag{201}$$
$$u1 = \frac{5}{9}\left[\gamma_0+\frac{50}{102|b|^2}(5\gamma_0 w+\kappa U_0^2)\right]\left[\gamma_0+\frac{10}{102|b|^2}(\gamma_0^2+U_0^2)(\kappa+55/51\gamma_0)\right]$$
$$u2 = \frac{U_0^2}{18}\left[1+\frac{10}{102|b|^2}(w-5\gamma_0\kappa)\right]\left[2+10\frac{25}{51|b|^2}55/51(\gamma_0^2+U_0^2)\right]$$
$$w = \kappa\gamma_0+55/51(\gamma_0^2+U_0^2)$$

as the expressions for the forces are already complicated enough.

In the regime where $\kappa, \gamma_0 \ll U_0$, the expressions for the forces again reduce to the corresponding ones for a two-level atom.

5.6.5. Far off resonance force

a. $J_g = 1/2 \rightarrow J_e = 3/2$**.** Expanding eqs. 174 to first order in velocity shows that $\Pi^1_- = 0$ for $\gamma_0 = 0$, hence we get only the second term in the expression for the dipole force (eq. 183)

$$f_{dip} = \frac{-8/3\hbar k^2 v|A^0|^2}{\kappa|b|^2}32/9U_0^3 \tag{202}$$

which again is a similar result to the one we received for a two-level atom in a symmetrically pumped ring cavity [3]. Hence in the strong coupling limit, cavity enhanced cooling should work also for high detuning.

b. $J_g = 1 \rightarrow J_e = 2$**.** For this transition we get a non-zero population imbalance for $\gamma_0 = 0$. Setting $|A^0|^2 = 1$ eqs. 199 specialize to

$$\Pi^1_- = \frac{30k}{34U_0}q$$
$$C_i^1 = -\frac{4k}{34^2U_0^2 5\kappa}(51^2\kappa^2-2075U_0^2+(51^2\kappa^2+180U_0^2 55)q)$$
$$(A^1)^*A^0+c.c. = -\frac{12k}{10U_0}(1+q)$$
$$(A^1)^*A^0-c.c. = -\frac{2ik}{17\kappa}(11+36q) \tag{203}$$

where we have defined the dimensionless parameter

$$q = \frac{-51^2\kappa^4-1225U_0^2\kappa^2+1800\frac{55^2}{51^2}U_0^4}{51^2\kappa^4+13825U_0^2\kappa^2+1800\frac{55^2}{51^2}6U_0^4}$$

to simplify the notation of our results.

For the force up to first order in velocity we get

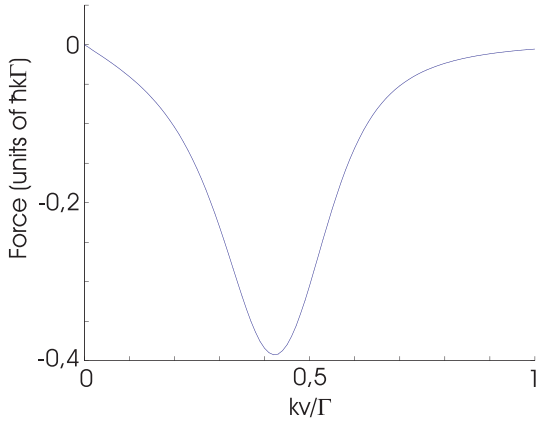

FIGURE 6. Total force plotted against the velocity for a $1/2 \rightarrow 3/2$-transition. $\kappa = 0.3\Gamma$, $U_0 = -0.3\Gamma$, $\gamma_0 = 0.01\Gamma$, $\Delta_C = -1.2\Gamma$.

$$f_{dip} = -\frac{16k^2 v}{30 \cdot 34^2 U_0 \kappa(\kappa^2 + (55/51U_0)^2)} \cdot \left[q(-51^2\kappa^4 + 7775U_0^2\kappa^2 + 55^2/51^2 U_0^4 6 \cdot 1800) + (-51^2\kappa^4 + 5375U_0^2\kappa^2 + 55^2/51^2 U_0^4 8400) \right] \quad (204)$$

which is clearly different from the corresponding expression eq. 202 for a $1/2 \rightarrow 3/2$-transition. For $\kappa \ll U_0$ we see that $q = 1/6$ which leads to the result eq. 202 which we obtained already for a $1/2 \rightarrow 3/2$-transition with the corresponding Clebsch-Gordon coefficients. For $U_0 \ll \kappa$ (bad cavity limit) we get $q = -1$ and consequently $f_{dip} = 0$. In the absence of any atom-mediated force terms there is no force on the atom as the cavity-mediated ones vanish in the bad cavity limit.

5.6.6. Velocity dependence

Solving eqs. 183 for a $J_g = 1/2 \rightarrow J_e = 3/2$-transition or eqs. 184 for a $J_g = 1 \rightarrow J_e = 2$-transition numerically for a moving atom we can study the variation of the forces with the velocity v. An intensity $|A^0|^2 = 1$ and mass $m = 10\hbar k^2/\Gamma$ (Rb^{85} would have a mass of 6.2 in these units) has been chosen in all of the plots. A lower photon number would stress the force terms independent of the intensity while a higher photon number would lead to dominating cavity mediated terms that are linear in intensity.

Note that in all of the subsequent plots the conventional free-space Doppler cooling, situated at $kv \approx \Gamma$ has been neglected. For $U_0 < 0$ it would add a decelerating force in this high-velocity regime.

Fig. 6 shows the total (radiation pressure and dipole) force acting on an atom that is blue detuned with respect to the pump field ($\Delta_a < 0$) but red detuned with respect to the cavity modes ($\Delta_a - \Delta_C > 0$) for a $1/2 \rightarrow 3/2$-transition.

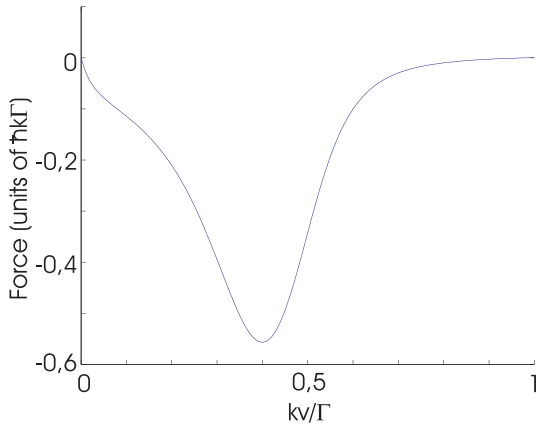

FIGURE 7. Total force plotted against the velocity for a $1 \rightarrow 2$-transition. $\kappa = 0.3\Gamma$, $U_0 = -0.3\Gamma$, $\gamma_0 = 0.01\Gamma$, $\Delta_C = -1.2\Gamma$.

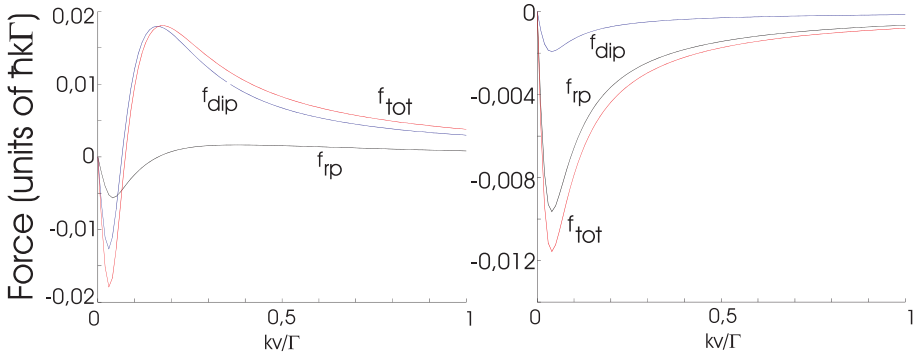

FIGURE 8. Dipole-, radiationpressure-, and total Force plotted against the velocity for a $1 \rightarrow 2$-transition inside a ring resonator (left) and in free space (right) respectively. $\kappa = 0.3\Gamma$, $U_0 = -0.1\Gamma$, $\gamma_0 = 0.02\Gamma$, $\Delta_C = 0\Gamma$.

Comparing this with fig. 7 we see that there is an additional structure at $kv \approx \gamma_0$ for a $1 \rightarrow 2$-transition. This is exactly the atomic mediated part (cavity-modified polarization gradient force) which we found in section 5.6.1. Fig. 8 (left hand side) shows essentially the same plot but with $U_0 > 0$ and $\Delta_C = 0$. The dipole force f_{dip} and the radiation pressure force f_{rp} are shown additionally to the total force f_{tot}. It can be clearly seen, that the atomic mediated force at $kv \approx \gamma_0$ still leads to deceleration while the cavity mediated force at $kv \approx \kappa$ accelerates the atom. The right hand side of fig. 7 was obtained by modifying eqs. 184 to recover the free-space situation of [14]. Our results are in accordance with the the ones in this previous work. Furthermore as we have chosen $|U_0| = 5\gamma_0$ the dipole force in the cavity setup is always larger than radiation pressure. Due to the lack of counterpropagating modes of equal polarization allowing unlimited stimulated photon transitions, f_{rp} is always larger than f_{dip} in free space. Additionally the force in the cavity is always larger than the force in free-space for corresponding velocities which shows the enhancement of kinetic light effects in resonators.

5.7. Conclusions

We have shown that the induced dipole of an atom with a degenerate groundstate moving in a σ^+-σ^- cavity laser field leads to significant changes in the mechanical friction coefficient even in the bad-cavity regime where cavity dynamics is negligible. Although we have included spontaneous atomic emission in our model it was shown that even for a very far detuned laser field considerable mechanical light effects still exist. Hence this cooling scheme is in principle suitable for any polarizable particle including molecules and Bose-Einstein condensates. It can also be expected that interesting multi-particle effects arise which could be used to implement quantum computational schemes.

Acknowledgments

This work was supported by the Austrian Fonds zur Förderung der wissenschaftlichen Forschung under project no. P13435 and F1512 as part of the Spezialforschungsbereich Quantenoptik.

CHAPTER 6

VSCPT inside a ring cavity

6.1. Introduction

As we have already mentioned in section 2.2.4 velocity selective coherent population trapping in free space has some serious problems: The achievable cooling times are relatively long due to the lack of a cooling force and VSCPT needs a closed optical transition and spontaneous atomic emission to reach the final dark states which also limits the final density and temperature. In the next section 6.2 we will show that a generalized dark state cooling scheme involving high-Q cavity fields can overcome these disadvantages of free space VSCPT.

6.1.1. Cooling phases

In principle a full treatment of VSCPT has to be based on a quantum description of atomic motion.

For practical calculations however the atom-field dynamics can be split into two phases:

1. Precooling towards temperatures somewhat above the recoil temperature (needing a large number ($> 10^3$) of photons to be scattered).

2. The final VSCPT step which requires only one (or very few) spontaneous jumps to reach the velocity selective dark state.

While phase 2 definitely requires a quantum description, a semiclassical description is adequate in phase 1. The validity of a semiclassical treatment for cavity induced cooling above the recoil limit (but even much below the Doppler limit) has been shown in some earlier work by us by direct comparison of semiclassical calculations and full quantum Monte Carlo wavefunction simulations (see e. g. section 4.5). These methods could in principle be also applied here.

The central goal of the the next section 6.2 is to show that a strongly improved precooling phase going far below the Doppler limit without spontaneous emission should be feasible using high-Q ring cavities. As cooling time is a central bottleneck of VSCPT, this makes it an ideal basis for the final VSCPT step and should greatly enhance the overall performance. For this part a semiclassical treatment is sufficient.

6.1.2. Role of the cavity for the final VSCPT cooling phase

It is rather obvious at least for quasi 1D cavity geometry, that the periodicity of the cavity field limits cavity induced cooling to the recoil temperature. However, one could argue, that the cavity would negatively influence the final VSCPT step and prevent the system from reaching sub-recoil temperatures.
In order to clarify this objection and put our arguments on firmer ground, we have used a quantum description of the atomic motion with the following results:
In general it turns out that the cavity only plays a significant role and leads to dissipation when the relevant time scales are comparable with the cavity photon lifetime. However, for a realistic setup one always has $kv_{Rec} \ll \kappa$, so that one can adiabatically eliminate the cavity dynamics in the VSCPT regime and the field always adjusts to the momentary atomic state. Hence no further cooling can be expected.

This argument can also be made more explicit. Expanding the atomic wavefunction in terms of plane waves

$$|\psi(p)\rangle = \sum_{n=-\infty}^{\infty} (c_n|g_{-1}, p + n\hbar k\rangle + d_n|g_1, p - n\hbar k\rangle) \tag{205}$$

one finds, that the backward scattering term for the cavity field amplitude vanishes, if the momentum width of the wavepacket is smaller than the recoil momentum (i. e. a delocalised wavepacket larger than a wavelength will not coherently backscatter the light). Hence in the subrecoil regime only the pumped fields persist as in free space. This is true for any internal atomic state (dark and bright state). The final cooling step hence involves only the usual σ^+-σ^- field configuration. The situation then is largely identical to the free space situation, which is fairly well understood and has been treated extensively in literature [22], so that we do not need to include it again in this work in detail.

Nevertheless, in the next section we included some more explicit considerations and calculations to substantiate this point. Following the lines of the original VSCPT treatment by C. Cohen-Tannoudji [22], we present the equations for a moving atom with a velocity distribution narrower than a single recoil momentum $\delta p < \hbar k$. Atomic motion still couples the dark and bright internal states with respect to the momentary fields so that the standard VSCPT mechanism is still present. Nevertheless, our calculation shows one small difference to the free space case. While an atom in the VSCPT dark state completely decouples from the field and stays in this dark state an atom in the bright state will phase shift the intracavity field and induce some dynamics, which will transfer it slowly to the dark state. In principle this enhances the effective dark volume in phase space and speeds up cooling. However, in practical situations $kv_{Rec} \ll \kappa$ this process is too slow to be significant.

In addition, the cavity still enhances the effective field present, which simply rescales the light intensity and increases the number of spontaneous emission events.

In this sense the cavity will also lead to enhanced effective cooling rates in this ultracold limit.

Nevertheless, the final step in the VSCPT process can only occur via spontaneous populations of $v = 0$ dark state.

Note that the situation should be different in a high-Q wide angle spherical cavity setup which, however, seems to be hard to realize in practise.

6.1.3. The role of many atoms

As we have shown in some earlier work [3] and in chapter 4 cavity induced cooling can be extended to several atoms. In general they will influence each other via the field, which gives limitations on the number of atoms and cooling time scale. Of course such a behaviour must also be expected in this model. However, the existence of a dark state strongly reduces these limitations, as an atom in the dark state does not see the field any more and hence should not contribute in the dynamics. In addition it should stay in the dark state as long as the field changes adiabatically with respect to the internal time scale given by the atom field coupling, which requires sufficiently strong cooling fields.

Unfortunately we have to admit, that a full N-atom quantum calculation for multilevel atoms required to clearly prove this claim, seems impossible at the moment. Nevertheless even using the scaling properties for the two-level case to get some estimates gives encouraging results.

6.2. Publication 6: Cavity-mediated dark-state cooling without spontaneous emission

Cavity mediated dark state cooling without spontaneous emission

Markus Gangl and Helmut Ritsch

Institut für Theoretische Physik, Universität Innsbruck,
Technikerstr. 25, A-6020 Innsbruck, Austria.

Abstract:
We extend the concept of dark state cooling to enclose the fields in a high-Q resonator. Choosing a sufficiently large detuning between the atomic transition and the driving fields, spontaneous emission during the cooling process is largely suppressed and the energy dissipation occurs dominantly via cavity decay. For a ring cavity with two degenerate counterpropagating waves of opposite circular polarization the final dark state is identical as in free space. However, we find a strong cavity mediated force with a large capture range as a precooling mechanism. In this scheme spontaneous emission is only important for the final jump to the dark state in the dynamics and the reabsorption problem is strongly reduced. In principle the scheme could also be applied to molecules with a suitable transition.
PACS number(s): 32.80.Pj, 42.50.Vk, 42.50.Lc

Published as Physical Review A **64**, 063414 (2001).

Laser cooling of atoms has been a very active field of research for many years culminating in the 1997 Nobel prize. A variety of cooling schemes has been proposed to get to lower and lower temperatures. Nevertheless there are processes inherent to optical cooling schemes that limit the reachable steady-state temperature and density. Quite generally, spontaneous emission from the excited atomic states is used as a dissipation channel to get rid of the motional energy of the atom. This directly introduces momentum diffusion via the random number and direction of the spontaneous emission events involving atomic recoil. In addition, the scattered photons can be reabsorbed to further increase the diffusion.

Some more sophisticated cooling schemes making use of the internal structure of the atom, as e. g. polarization gradient cooling [21], lead to stronger friction forces. Temperatures below the Doppler limit $k_B T \approx \hbar\Gamma$, where 2Γ is the atomic linewidth, can be achieved. As an alternative it has been suggested [1, 2, 29, 30, 3, 66] and partly experimentally confirmed [67, 68] that instead of a Sisyphus effect using the internal atomic structure the dissipative dynamics of a cavity field can be exploited to get cooling to a temperature $k_B T \approx \hbar\kappa$, where 2κ is the cavity linewidth, which can be below the Doppler limit as well.

All of these schemes mentioned so far are limited by the recoil energy connected with the spontaneous emission of a single photon. Apart from reaching BEC by subsequent evaporative cooling only the utilization of so called dark atomic states as in the VSCPT scheme proposed and demonstrated by Cohen-Tannoudji et. al allowed temperatures well below this recoil limit. This is one of the most promising approaches to reach all optical BEC. Nevertheless the scheme has limitations, which prevented success so far. In particular dark states are quite fragile with respect to perturbation and the cooling time in 3D is rather long. VSCPT needs a closed optical transition and spontaneous atomic relaxation to reach the final dark states [69]. Hence the reabsorption problem strongly limits the final density and temperature.

In this work we theoretically investigate a generalized dark state cooling scheme implying high-Q cavity fields, which strongly diminuish these disadvantages of free-space VSCPT. In particular we find an efficient sub Doppler precooling mechanism, where the system evolves towards the zero-momentum eigenstate via cavity induced dissipation and the reabsorption problem is cured by strongly reducing spontaneous emission. Of course there is some price to pay in form of a more complex setup and a limited cooling volume.

We study an atom with a $J_g = 1$ to $J_e = 1$ transition as depicted in Fig.1 coupled to the counterpropagating modes of a high-Q ring cavity. It is well known that it has a dark eigenstate for any spatial light field configuration with a fixed frequency ω_l[70]. Using the Clebsch-Gordon-coefficients for this levelscheme we can write the generalized atomic lowering operators for σ_+, σ_- and linear polarized light as $S_+ = -1/\sqrt{2}(|g_{-1}\rangle\langle e_0| + |g_0\rangle\langle e_1|)$, $S_- = 1/\sqrt{2}(|g_1\rangle\langle e_0| + |g_0\rangle\langle e_{-1}|)$ and $S_0 = 1/\sqrt{2}(|g_1\rangle\langle e_1| - |g_{-1}\rangle\langle e_{-1}|)$.

The intracavity field can be decomposed in two counterpropagating modes for each polarization yielding $\vec{E}^+ = \mathcal{E}(\alpha_+ e^{ikz} + \alpha_- e^{-ikz})\vec{e}_+ + \mathcal{E}(\beta_+ e^{ikz} + \beta_- e^{-ikz})\vec{e}_-$ or

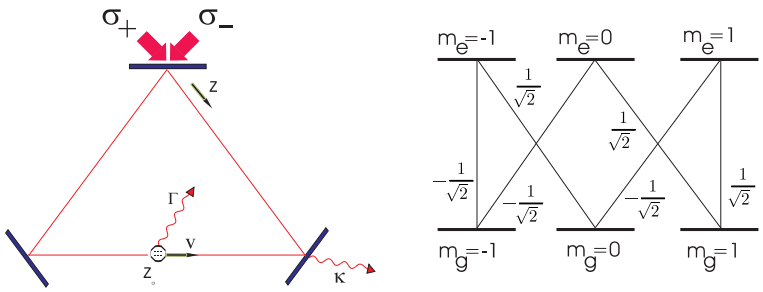

FIGURE 9. Cavity setup and level scheme for a $J_g = 1 \rightarrow J_e = 1$-transition.

in shorthand $\vec{E}^+ = A\vec{e}_+ + B\vec{e}_-$, so that the system Hamiltonian for the internal atomic dynamics and the fields can be written as

$$H = -\Delta_a P_e + g(A^* S_+ + B^* S_-) + g(S_+^\dagger A + S_-^\dagger B) \tag{206}$$

with $g \equiv -d\mathcal{E}$ denoting the Rabifrequency for atomic transition with unit Clebsch-Gordon coefficient per photon, $\Delta_a = \omega_P - \omega_a$ being the detuning between pump and atom and P_e being the projector on the excited atomic states. To include dissipation via atomic and cavity decay we use a standard master equation approach

$$\begin{aligned} \dot{\rho} &= -\frac{i}{\hbar}[H, \rho] + \mathcal{L}\rho \\ \mathcal{L}\rho &= -\Gamma(P_e\rho + \rho P_e - 2S_+\rho S_+^\dagger - 2S_-\rho S_-^\dagger - 2S_0\rho S_0^\dagger). \end{aligned} \tag{207}$$

Adiabatic elimination of the excited states in eq. 207 yields the following equations for the populations of the ground-state levels Π_-, Π_0, Π_+ and the ground-state coherence $\rho_{g-1,g1}$

$$\begin{aligned} \dot{\Pi}_- &= -\gamma_0/2|A|^2\Pi_- + \gamma_0/2|B|^2\Pi_+ + \gamma_0/2|B|^2\Pi_0 + \\ &\quad iU_0/2(A^*B\rho_{g1,g-1} - AB^*\rho_{g-1,g1}) \\ \dot{\Pi}_+ &= -\gamma_0/2|B|^2\Pi_+ + \gamma_0/2|A|^2\Pi_- + \gamma_0/2|A|^2\Pi_0 - \\ &\quad iU_0/2(A^*B\rho_{g1,g-1} - AB^*\rho_{g-1,g1}) \\ \dot{\Pi}_0 &= -\gamma_0/2(|A|^2 + |B|^2)\Pi_0 \\ \dot{\rho}_{g-1,g1} &= -\gamma_0/2(|A|^2 + |B|^2)\rho_{g-1,g1} - \\ &\quad iU_0/2(|A|^2 - |B|^2)\rho_{g-1,g1} + \\ &\quad iU_0/2A^*B(\Pi_+ - \Pi_-) + 1/2\gamma_0 A^*B \end{aligned} \tag{208}$$

where $U_0 = \Delta_a g^2/(\Gamma^2 + \Delta_a^2)$ is the optical potential and $\gamma_0 = \Gamma g^2/(\Gamma^2 + \Delta_a^2)$ is the incoherent photon scattering rate into non-cavity modes. Similarily the equations for the cavity-modes read [3]

$$\begin{aligned}
\dot{\alpha}_+ =& (-\kappa + i\Delta_c)\alpha_+ - (\gamma_0 + iU_0)/2 \\
& [(\alpha_+ + \alpha_- e^{-2ikz_a})(\Pi_- + \Pi_0) - \\
& (\beta_+ + \beta_- e^{-2ikz_a})\rho_{g1,g-1}] + \eta \\
\dot{\alpha}_- =& (-\kappa + i\Delta_c)\alpha_- - (\gamma_0 + iU_0)/2 \\
& [(\alpha_- + \alpha_+ e^{2ikz_a})(\Pi_- + \Pi_0) - \\
& (\beta_- + \beta_+ e^{2ikz_a})\rho_{g1,g-1}] \\
\dot{\beta}_+ =& (-\kappa + i\Delta_c)\beta_+ - (\gamma_0 + iU_0)/2 \\
& [(\beta_+ + \beta_- e^{-2ikz_a})(\Pi_+ + \Pi_0) - \\
& (\alpha_+ + \alpha_- e^{-2ikz_a})\rho_{g-1,g1}] \\
\dot{\beta}_- =& (-\kappa + i\Delta_c)\beta_- - (\gamma_0 + iU_0)/2 \\
& [(\beta_- + \beta_+ e^{2ikz_a})(\Pi_+ + \Pi_0) - \\
& (\alpha_- + \alpha_+ e^{2ikz_a})\rho_{g-1,g1}] + \eta,
\end{aligned} \tag{209}$$

where we haven chosen to pump only one polarization for each propagation direction with amplitude η. z_a denotes the atomic position, $\Delta_C = \omega_P - \omega_C$ is the detuning between pump and cavity modes and κ is the cavity decay rate. Note that modes of different polarizations are coupled by stimulated Raman processes via the coherence between the two ground state sublevels $|g_{-1}\rangle$ and $|g_1\rangle$. So far these equations do not contain atomic motion and the atomic position enters only as a parameter in these equations. As long as one deals with not too cold atoms such a semiclassical treatment [21, 2, 14] has proven rather successfull. In our case the applicability is, however, limited to the initial CPT precooling phase. As outlined in the last paragraph in the ultracold VSCPT regime the model has to be refined and a quantum description of the external atomic motion is mandatory [71].

Let us first calculate the combined atom field eigenstates. Assuming large detuning and weak saturation we can now adiabatically eliminate the upper atomic states and drop the $m = 0$ ground state to arrive at a simplified Hamiltonian reading

$$\begin{aligned}
H_{el} =& U_0/2[|A|^2|g_{-1}\rangle\langle g_{-1}| + |B|^2|g_1\rangle\langle g_1| - \\
& A^*B|g_{-1}\rangle\langle g_1| - AB^*|g_1\rangle\langle g_{-1}|]
\end{aligned}$$

For any given pump amplitude η this Hamiltonian has two eigenstates, namely the dark state with eigenvalue $\lambda_{DS} = 0$

$$|\psi_{DS}\rangle = \frac{1}{\sqrt{|A|^2 + |B|^2}} \left(B|g_{-1}\rangle + A|g_1\rangle\right) \tag{210}$$

$\alpha_+ = \beta_- = \eta/(\kappa - i\Delta_c)$, $\alpha_- = \beta_+ = 0$,

and the maximally coupled bright state with eigenvalue $\lambda_{BS} = U_0(|A|^2 + |B|^2)/2$

$$
\begin{aligned}
|\psi_{BS}\rangle &= \frac{1}{\sqrt{|A|^2+|B|^2}}\left(A^*|g_{-1}\rangle - B^*|g_1\rangle\right) \\
\alpha_+ &= \beta_- = \frac{\kappa - i\Delta_c + (\gamma_0 + iU_0)/2}{(\kappa - i\Delta_c)(\kappa + \gamma_0 + i(U_0 - \Delta_c))}\eta \\
\alpha_- &= -\frac{(\gamma_0 + iU_0)e^{2ikz_a}}{2(\kappa - i\Delta_c)(\kappa + \gamma_0 + i(U_0 - \Delta_c))}\eta \\
\beta_+ &= -\frac{(\gamma_0 + iU_0)e^{-2ikz_a}}{2(\kappa - i\Delta_c)(\kappa + \gamma_0 + i(U_0 - \Delta_c))}\eta
\end{aligned} \tag{211}
$$

As could be expected the field dynamics decouples from the atom in a dark state and the reflected components (α_-, β_+) are zero, while they are nonvanishing for the atom in a bright state. This opens a new dissipation channel for the bright state besides spontaneous emission, as the reflected components decay. It is very interesting to notice that for any prescribed field configuration (even with non-zero (α_-, β_+)) an internally dark atomic state exists. However, as no new photons are scattered into (α_-, β_+) by the atom in this case, this state is not stable with respect to cavity decay. Hence the reflected amplitudes decay and the atom is slowly transferred to the dark eigenstate of the total Hamiltonian. This process strongly enhances the effective filling rate of the stable dark state and can also be expected to diminish the perturbation between different atoms in the cavity.

Let us now turn to an atom in its bright state and calculate the intracavity steady state field explicitly

$$
\begin{aligned}
\vec{E} = \frac{\eta}{\kappa + iU_0}&(\sin kz\vec{e}_x + \cos kz\vec{e}_y + \\
& i\frac{U_0}{\kappa}\sin k(z - z_a)(\cos kz_a\vec{e}_x - \sin kz_a\vec{e}_y)).
\end{aligned} \tag{212}
$$

The induced atomic dipole moment is orthogonal to the polarization of the pump field at the position of the atom as can be understood easily. Choosing the polarization of the pump field at the position of the atom as the quantization axis, the dark state becomes $|g_0\rangle$ with a polarization parallel to that of the pump field. An atom in the orthogonal bright state possesses a dipole moment orthogonal to this, which determines the scattered field polarization. Note that the phase as well as the polarization of the scattered field depend on the position of the atom and that the atom always sits at a node of the scattered field. This is a generalization of the situation of a two-level atom in a ring-cavity, where the light is scattered always with a polarization parallel to that of the pump field and creates long range intensity modulations [3].

In a free space (σ^+, σ^-) setup the expectation value of the force on an atom in a bright or dark state is zero. One finds only momentum diffusion induced by spontaneous emission. Including cavity dynamics this is not true and we calculate the following expressions for the force on an atom at rest within the cavity

$$
\begin{aligned}
f_{total} &= f_{pol} + f_{inter-pol} \\
f_{pol} &= \hbar k \gamma_0 (|\alpha_+|^2 - |\alpha_-|^2)(\Pi_- + \Pi_0) + \\
&\quad \hbar k \gamma_0 (|\beta_+|^2 - |\beta_-|^2)(\Pi_+ + \Pi_0) + \\
&\quad i\hbar k U_0 (\alpha_+^* \alpha_- e^{-2ikz_a} - \alpha_-^* \alpha_+ e^{2ikz_a})(\Pi_- + \Pi_0) + \\
&\quad i\hbar k U_0 (\beta_+^* \beta_- e^{-2ikz_a} - \beta_-^* \beta_+ e^{2ikz_a})(\Pi_+ + \Pi_0) \\
f_{inter-pol} &= -\rho_{g1,g-1} [\hbar k \gamma_0 (\alpha_+^* \beta_+ - \alpha_-^* \beta_-) + \\
&\quad i\hbar k U_0 (\alpha_+^* \beta_- e^{-2ikz_a} - \alpha_-^* \beta_+ e^{2ikz_a})] - \\
&\quad \rho_{g-1,g1} [\hbar k \gamma_0 (\alpha_+ \beta_+^* - \alpha_- \beta_-^*) - \\
&\quad i\hbar k U_0 (\alpha_+ \beta_-^* e^{2ikz_a} - \alpha_- \beta_+^* e^{-2ikz_a}))]
\end{aligned} \tag{213}
$$

Here f_{pol} is just the usual combination of radiation pressure and dipole force weighted by the respective populations that appeared already for a two-level atom inside a ring-cavity [3] for each pump polarization individually. In addition $f_{inter-pol}$ describes these forces for processes connecting the two modes of different polarizations. These are driven by the ground-state coherence. Naturally, no force is found for an atom in its dark state at rest completely decoupled from the light. However, in analogy to VSCPT in free space a moving atom in an internal dark state now couples to the bright state and hence starts to redistribute photons between the different cavity modes and also scatters light spontaneously into non-cavity modes. The relative contribution of these two contributions can be changed by choosing an appropriate atom-field detuning. Depending on the choice of parameters this will lead to cooling or heating of the atomic center of mass motion, which is still present without spontaneous emission ($\gamma_0 = 0$). In general the kinetic energy loss is very fast as we will see in the numerical calculations below. Interestingly, for an initially dark atom the lowest order momentum dissipation term is quadratic in velocity, so that we have no cavity induced friction linear in velocity. Note, however, that the validity of the semiclassical formulas is limited to the regime above the recoil temperature.

Let us now turn to the dynamic semiclassical model and demonstrate the cooling properties of the system by numerical solution of Eqs 208 and 209 together with the semiclassical kinetic equations for atomic motion.

Fig. 10 shows the deceleration of a moving atom from an initial momentum of $60\hbar k$ to the vicinity of zero momentum without spontaneous emission, where the semiclassical theory breaks down. Fig. 11 shows how an atom that is initially in its dark eigenstate at rest evolves back into it after receiving a momentum kick. To be more realistic we have included a small spontaneous emission rate $\gamma_0 = 0.1\Gamma$ but the number of incoherent emission events for the whole process N_{Counts} can be calculated by

$$
N_{Counts}(T) = \int_0^T dt R_F(t) \tag{214}
$$

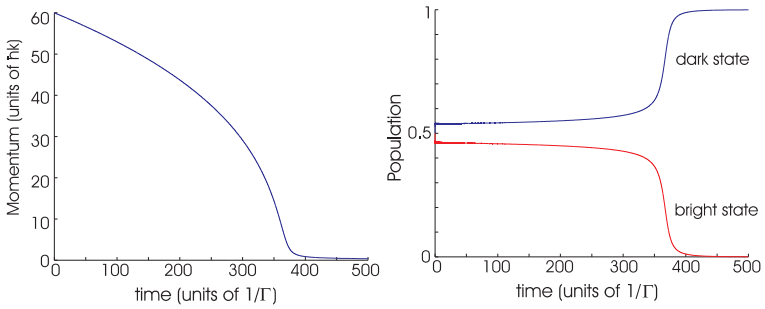

FIGURE 10. Cooling of a multilevel atom. Momentum (left) and population of dark and bright state (right). $\gamma_0 = 0$, $\kappa = 30\Gamma$, $\eta = 30\Gamma$, $U_0 = -6\Gamma$, $\Delta_c = 0$.

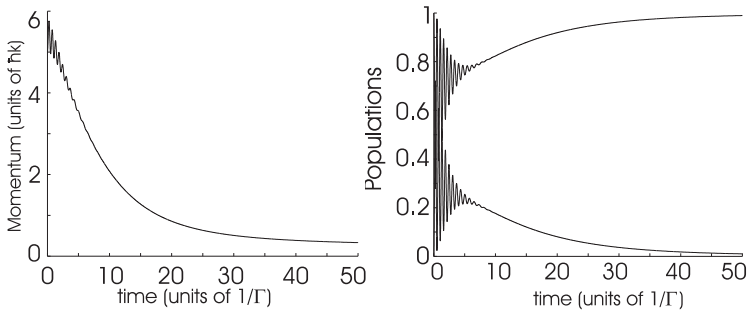

FIGURE 11. Cooling of a kicked dark atom with $\kappa = 30\Gamma$, $\gamma_0 = 0.1\Gamma$, $\eta = 30\Gamma$, $U_0 = -6\Gamma$, $\Delta_c = 0$ (left). Evolution of the dark state (upper) and bright state (lower) population of the atom (right).

where $R_F = \gamma_0(|A|^2 + |B|^2)\Pi_{BS}$ denotes the fluorescence rate of the atom. For the chosen parameters we find $N_{Counts}(50) = 0.91$. Hence we have less than a single spontaneous emission event, while the momentum has been reduced by several tens of recoils.

As mentioned before, the semiclassical theory breaks down close to the recoil limit. For atoms with a momentum spread of $\delta p \approx \hbar k$ one has to go to a quantum description of the external atomic motion. As the cavity fields couple only momentum eigenstates with a momentum difference of 0 or of $2\hbar k$, we generalize the standard VSCPT ansatz and set $|\psi(p)\rangle = \sum_{n=-\infty}^{\infty}(c_n|g_{-1}, p + n\hbar k\rangle + d_n|g_1, p - n\hbar k\rangle)$ for the wavefunction with given momentum p. The cavity induced dynamics will then only couple different coefficients c_n, d_n for the same p. Assuming that in the initial state only the the coefficients (c_{-1} and d_{-1} corresponding to the states $|g_{-1}, p - \hbar k\rangle$ and $|g_1, p + \hbar k\rangle$ are nonzero, the Schrödinger equations for the atomic amplitudes together with the equations for the cavity fields (eqs. 215) read:

$$
\begin{aligned}
\dot{\alpha}_+ &= (-\kappa + i(\Delta_c - U_0|c_{-1}|^2/2))\alpha_+ + \\
&\quad iU_0/2c^*_{-1}d_{-1}\beta_- + \eta \\
\dot{\alpha}_- &= (-\kappa + i(\Delta_c - U_0|c_{-1}|^2/2))\alpha_- \\
\dot{\beta}_+ &= (-\kappa + i(\Delta_c - U_0|d_{-1}|^2/2))\beta_+ \\
\dot{\beta}_- &= (-\kappa + i(\Delta_c - U_0|d_{-1}|^2/2))\beta_- + \\
&\quad iU_0/2d^*_{-1}c_{-1}\alpha_+ + \eta \\
\dot{c}_{-1} &= -i((p-k)^2/(2m) + U_0/2|\alpha_+|^2)c_{-1} + \\
&\quad iU_0/2d_{-1}\alpha^*_+\beta_- \\
\dot{d}_{-1} &= -i((p+k)^2/(2m) + U_0/2|\beta_-|^2)d_{-1} + \\
&\quad iU_0/2c_{-1}\beta^*_-\alpha_+
\end{aligned}
\tag{215}
$$

We see that in this regime only the externally pumped fields (α_+,β_-) are coupled by the atom, while we have no backscattering to the counterpropagating modes α_-, β_+, which will simply decay to zero. At the same time for zero (α_-,β_+) also the other coefficients (c_n, d_n) decouple and remain zero. This can be easily understood by noting that the coupling between counterpropagating fields of the same polarization (eqs. 209) averages to zero for an atom delocalized over a wavelength. Hence once the atom has reached the subrecoil regime, we get the well known motion induced bright-dark coupling as for the free space case and cavity induced cooling will stop. For very slow atoms $kp/m \ll \kappa$ and a realistic cavity decay rate $\omega_{recoil} \ll \kappa$ the cavity field will adiabatically follow the atomic dynamics[21] and one cannot expect any cavity induced momentum dissipation. Hence the final cooling step can only be achieved by spontaneous emission. However, as in the semiclassical regime, an atom jumping to a bright state with $p \approx .0$ can be adiabatically transfered to the corresponding dark state without spontaneous emission. This leads to some enhancement of the capture volume even in the ultracold limit. The situation could be substantially improved for a 3D cavity geometry, but such a setup seems rather unrealistic.

In summary we have found that applying a high-Q optical cavity for the cooling fields two central limitations of dark state cooling, namely photon reabsorption and unefficient precooling, can be strongly reduced. As the final dark state of the atom in the cavity field is the same as for free space VSCPT state, comparably low temperatures at higher densities are expected using this scheme. This renders this setup as a possible candidate for all optical BEC or a CW atom laser. In addition due to the strongly reduced number of spontaneous emission events necessary to reach a state close to the final dark state, the method could also be applied to systems with some leakage out of the closed CPT cycle. Even if one does not aim for the quantum regime of cooling the setup could be helpful for efficient cooling of molecules where vibrational and rotational redistribution of population has to be avoided and one needs a significant velocity capture range. Let us finally remark, that an interesting but yet open question in this respect is the appearance and possible usefulness of

correlated long range multiatom dark states, which could be efficiently populated in this setup.

Acknowledgments

We thank P. Horak for many helpful discussions. This work was supported by the Austrian Fonds zur Förderung der wissenschaftlichen Forschung under project no. P13435 and F1512 as part of the Spezialforschungsbereich Quantenoptik.

Bibliography

[1] P. Horak *et. al.*, Phys. Rev. Lett. **79**, 4974 (1997)

[2] G. Hechenblaikner *et. al.*, Phys. Rev. A **58**, 3030 (1998).

[3] M. Gangl and H. Ritsch, Phys. Rev. A **61** (2000) 043405.

[4] G. Rempe, Appl. Phys. B **60**, 233 (1995).

[5] P. Münstermann *et. al.*, Opt. Comm., **159**, 63 (1999).

[6] H. Mabuchi, Q. A. Turchette, M. S. Chapman, and H. J. Kimble, Optics Lett. **21**, 1393 (1996).

[7] W. D. Phillips and H. Metcalf, Phys. Rev. Lett. **48**, 596 (1982).

[8] J. P. Gordon and A. Ashkin, Phys. Rev. A **21**, 1606 (1980).

[9] J. Dalibard and C. Cohen-Tannoudji, J. Opt. Soc. Am. B **2**, 1707 (1985).

[10] A. Ashkin, Science **210**, 1081 (1980).

[11] V. S. Letokhov and V. G. Minogin, Phys. Rep. **73**, 1 (1981).

[12] S. Stenholm, Rev. Mod. Phys. **58**, 699 (1986).

[13] D. Phillips, P. L. Gould and P. D. Lett, Science **239**, 878 (1991).

[14] C. Cohen-Tannoudji, in *Fundamental Systems in Quantum Optics*, Proceedings of the Les Houches Summer School, Session LIII, edited by J. Dalibard, J.-M. Raimond, and J. Zinn-Justin (North-Holland, Amsterdam, 1992), pp.1-164.

[15] V. G. Minogin and V. S. Letokhov, *Laser Light Pressure on Atoms*, New York: Gordon and Breach (1987).

[16] H. J. Metcalf and P. van der Straten, *Laser cooling and trapping*, New York, Berlin, Heidelberg: Springer (1999).

[17] F. Bardou, J.-P. Bouchaud, A. Aspect and C. Cohen-Tannoudji, *Levy Statistics and Laser Cooling*, Cambridge: Cambridge University Press (2001)

[18] P. Lett *et. al.*, Phys. Rev. Lett. **61**, 169 (1988).

[19] J. Dalibard *et. al.*, in *Proceedings of the 11th Conference on Atomic Physics*, edited by S. Harsche, J. C. Gay, and G. Grynberg (World Scientific, Singapore, 1989).

[20] S. Chu *et. al.*, , in *Proceedings of the 11th Conference on Atomic Physics*, edited by S. Harsche, J. C. Gay, and G. Grynberg (World Scientific, Singapore, 1989).

[21] J. Dalibard and C. Cohen-Tannoudji, J. Opt. Soc. Am. B **6**, 2023 (1989).

[22] A. Aspect *et. al.*, Phys. Rev. Lett. **61**, 826 (1988).

[23] E. M. Pourcel, Phys. Rev. **69**, 681 (1946).

[24] A. Hemmerich, Phys. Rev. A **60**, 943 (1999).

[25] J. I. Cirac and P. Zoller, Phys. Rev. Lett. **74**, 4091 (1995)

[26] A. C. Doherty, A. S. Parkins, S.M. Tan, and D. F. Walls, Phys. Rev. A **56**, 833 (1997)

[27] K. S. Wong, M. J.Collett, and D. F. Walls, Opt. Comm. **137**, 269 (1997)

[28] A. C. Doherty, A. S. Parkins, S. M. Tan, and D. F. Walls, Phys. Rev. A **57**, 4804 (1998).

[29] M. Gangl and H. Ritsch, Eur. Phys. J. D **8**, 29-40 (2000).

[30] M. Gangl and H. Ritsch, Phys. Rev. A **61**, 011402(R) (2000).

[31] P. Münstermann *et. al.*, Phys. Rev. Lett. **82**, 3791 (1999)

[32] Jun. Ye *et. al.*, IEEE Trans. on instr. and meas., **48**, 608 (1999)

[33] G. Hechenblaikner, Master Thesis, University of Innsbruck (1997).

[34] M. G. Moore, O. Zobay, and P. Meystre, Phys. Rev. A **60**, 1491 (1999).

[35] J. Denschlag, D. Cassettari, A. Chenet, S. Schneider, J. Schmiedmayer, Appl. Phys. B **69** (1999) 291.

[36] R. Folman, P. Krüger, D. Cassettari, B. Hessmo, T. Maier and J. Schmiedmayer, Phys. Rev. Lett. **84** (2000) 4749.

[37] M. Brune, S. Haroche, V. Lefèvre, J. M. Raimond, and N. Zagury, Phys. Rev. Lett. **65** (1990) 976.

[38] V. Savalli, G. Zs. Horvath, P. D. Featonby, L. Cognet, N. Westbrook, C. I. Westbrook, and A. Aspect, Opt. Lett. **24** (1999) 1552.

[39] H. Mabuchi, Q. A. Turchette, M. S. Chapman, and H. J. Kimble, Opt. Lett. **23** (1996) 247.

[40] C. J. Hood, M. S. Chapman, T. W. Lynn, and H. J. Kimble, Phys. Rev. Lett. **80** (1998) 4157.

[41] D. W. Vernooy, A. Furusawa, N. Ph. Georgiades, V. S. Ilchenko, and H. J. Kimble, Phys. Rev. A **57** (1998) R2293.

[42] R. Quadt, M. Collett, and D. Walls, Phys. Rev. Lett. **74** (1995) 351.

[43] J. Michaelis, C. Hettich, J. Mlynek, and V. Sandoghdar, Nature, **405** (2000) 325.

[44] H. Mabuchi and H. J. Kimble, Opt. Lett. **19** (1994) 749.

[45] F. Treussart, J. Hare, L. Collot, V. Lefèvre, D. S. Weiss, V. Sandoghdar, J. M. Raimond, and S. Haroche, Opt. Lett. **19** (1995) 1651.

[46] D. S. Weiss, V. Sandoghdar, J. Hare, V. Lefèvre, J. M. Raimond, and S. Haroche, Opt. Lett. **20** (1995) 1935.

[47] N. Dubreuil, J. C. Knight, D. K. Leventhal, V. Sandoghdar, J. Hare, and V. Lefèvre, Opt. Lett. **20** (1995) 813.

[48] P. Horak and H. Ritsch, Phys. Rev. A **64**, 033422 (2001).

[49] A. Hemmerich, private communication.

[50] M.G. Raizen *et al.*, Phys. Rev. A **58**, 4757 (1998)

[51] W. Ketterle *et al.*, Phys. Rev. A **46**, 4760 (1992)

[52] A. S. Parkins and D. F. Walls, Phys. Rep. **303**, 1 (1998).

[53] S. Kuppens *et al.*, Phys. Rev. A **58**, 3068 (1998)

[54] Yu.B. Ovchinnikov *et al.*, Eurphys. Lett. **43**, 510 (1998).

[55] M. Morinaga, I. Bouchoule, J.-C. Karam, and C. Salomon, Phys. Rev. Lett. **83**, 4037 (1999).

[56] A. J. Kerman, V. Vuletic, C. Chin, and S. Chu, Phys. Rev. Lett. **84**, 439 (2000).

[57] M. T. DePue, C. McCormick, S. Lukman Winoto, S. Oliver, and D. S. Weiss, Phys. Rev. Lett. **82**, 2262 (1999).

[58] G. Rempe *et al.* in "Laser Spectroscopy" edited by R. Blatt, J. Eschner, D. Leibfried, and F. Schmidt-Kaler (World Scientific, Singapore, 1999).

[59] J. Ye, D. W. Vernooy, and H. J. Kimble, Phys. Rev. Lett. **83**, 4987 (1999).

[60] P. Horak, S. M. Barnett, and H. Ritsch, Phys. Rev. A **61**, 033609 (2000); P. Horak and H. Ritsch, preprint: cond-mat/0002247.

[61] B. W. J. McNeil, G. R. M. Robb, R. Bonifacio, and N. Piovella, Eurphys. Lett. **49**, 316 (2000).

[62] M. Anderson *et al.*, Science **269**, 198 (1995).

[63] K. B. Davies *et al.*, Phys. Rev. Lett. **75**, 3969 (1995).

[64] A. Görlitz *et al.*, Phys. Rev. Lett. **87**, 130402 (2001).

[65] M. Gangl and H. Ritsch, Phys. Rev. A **64**, 063414 (2001).

[66] V. Vuletic and S. Chu, Phys. Rev. Lett. **84**, 3787, (1999).

[67] P. W. H. Pinkse, T. Fischer, P. Maunz, and G. Rempe, Nature (London) **404**, 365 (2000).

[68] A. C. Doherty, T. W. Lynn, C. J. Hood, and H. J. Kimble, Phys. Rev. A **63**, 013401 (2000).

[69] R. Dum, P. Marte, T. Pellizzari, and P. Zoller, Phys. Rev. Lett. **73**, 2829, (1994).

[70] M. A. Olshanii, Opt. Comm. **89**, 393, (1992).

[71] P. Horak and H. Ritsch, Phys. Rev. A **63**, 023603 (2001).

Dank

Am meisten Dank gebührt meinem Betreuer Prof. Helmut Ritsch, der sich ständig für Diskussionen und Fragen Zeit nahm und mir durch die Aufnahme in seine Forschungsgruppe in finanzieller Hinsicht die vorliegende Arbeit ermöglicht hat.

Danken möchte ich auch meinen Kollegen Dr. Peter Horak, Dr. Peter Domokos und Dr. Claus Lamprecht für viele hilfreiche Diskussionen und Ratschläge.

Meinen engen Freunden Mag. Herbert Crepaz, Mag. Gerald Hechenblaikner, Mag. Pavle Torbica, Mag. Andreas Pichler und Rupesh Ghelani danke ich für den Spaß jenseits der Physik.

Den zahlreichen Leidensgenossen, die mit mir das Schicksal eines Pendlers teilen und so wie ich der Unzuverlässigkeit und willkürlichen Preisgestaltung der Österreichen Bundesbahnen ausgeliefert sind, danke ich mit der Bemerkung: "Geteiltes Leid ist halbes Leid".

Besonders danken möchte ich auch den Studenten der drei Jahrgänge des Studienberechtigungsprüfungskurses am Berufsförderungsinstitut Tirol, die ich unterrichten durfte. Durch ihre Fragen habe ich mehr Physik gelernt als in so mancher Vorlesung.

Wenig Sinn macht es, meiner Verlobten Sonja Schrott Dank auszusprechen da es Dinge gibt, für die Worte allein nicht ausreichen. Dasselbe gilt für meine Familienmitglieder in Landeck und Innsbruck.

Lebenslauf

Mag. Markus Gangl

Geburtstag:	26-08-1973
Geburtsort:	Innsbruck, Österreich
Adresse:	Salurnerstr. 13 A-6500 Landeck

Ausbildung

1979 bis 1982	Volksschule Wilten/Innsbruck
1983 bis 1986	Hauptschule Rum
1987 bis 1992	Bundeshandelsakademie Hall i. Tirol, Abschluß mit ausgezeichnetem Erfolg
26-06-1992	Reifeprüfung mit ausgezeichnetem Erfolg
01-10-1992	Beginn des Studiums der Physik (Diplom) an der Leopold-Franzens-Universität Innsbruck
01-02-1993	Unterbrechung des Studiums um den Zivildienst bei der Rettung Innsbruck abzuleisten
01-03-1994	Fortsetzung des Studiums der Physik
29-09-1998	Abschluß des Studiums der Physik mit ausgezeichnetem Erfolg

Berufserfahrung

01-10-1998 bis jetzt	Forschungsassistent am Institut für Theoretische Physik, Doktorarbeit
1994 bis 2002	Tätigkeit als Tutor am Institut für Theoretische Physik
15-01-1999 bis 15-02-1999	Aufenthalt am Europischen Labor für Teilchenphysik (CERN) in Genf
Oktober 1999 bis März 2000	Trainer in der Erwachsenenbildung am Berufsförderungsinstitut Tirol
Oktober 2000 bis März 2001	Trainer in der Erwachsenenbildung am Berufsförderungsinstitut Tirol
Oktober 2001 bis März 2002	Trainer in der Erwachsenenbildung am Berufsförderungsinstitut Tirol

Publikationen in referierten Fachjournalen

G. Hechenblaikner, M. Gangl, P. Horak and H. Ritsch, Cooling an atom in a weakly driven high-Q cavity, Physical Review A **58**, 3030 (1998)

M. Gangl and H. Ritsch, Collective dynamical cooling of neutral particles in a high-Q optical cavity, Physical Review A **61**, 011402(R) (2000)

M. Gangl and H. Ritsch, 3D dissipative motion of atoms in a strongly coupled driven cavity, European Physical Journal D **8**, 29 (2000)

M. Gangl and H. Ritsch, Cold atoms in a high-Q ring cavity, Physical Review A **61**, 043405 (2000)

P. Domokos, M. Gangl, H. Ritsch, Single-atom detection in high-Q multimode cavities, Optical Communications **185**, 115 (2000)

M. Gangl, P. Horak and H. Ritsch, Cooling neutral particles in multimode cavities without spontaneous emission, Journal of Modern Optics **47**, 2741 (2000)

M. Gangl, P. Domokos and H. Ritsch, Collective cooling of neutral particles in cavities without spontaneous emission, Modern Problems of Laser Physics, Novosibirsk, 2000

M. Gangl and H. Ritsch, Cavity mediated dark state cooling without spontaneous emission, Physical Review A **64**, 063414 (2001)

M. Gangl and H. Ritsch, Cavity assisted polarization gradient cooling, to be submitted